Elettra Sincrotrone Trieste

Elettra
Sincrotrone
Trieste

Powder Diffraction with Synchrotron Radiation

Elettra
Sincrotrone
Trieste

Topics

- What is powder diffraction
- How do we measure powder diffraction and what do we have to be aware of
- Instrumentation at synchrotron beamlines for powder diffraction
- Why perform powder diffraction at synchrotrons
- Applications of SR-XRPD

Powder diffraction

Synchrotron Radiation: Basics, Methods and Applications

- Chapter 10:
  Powder Diffraction and synchrotron radiation

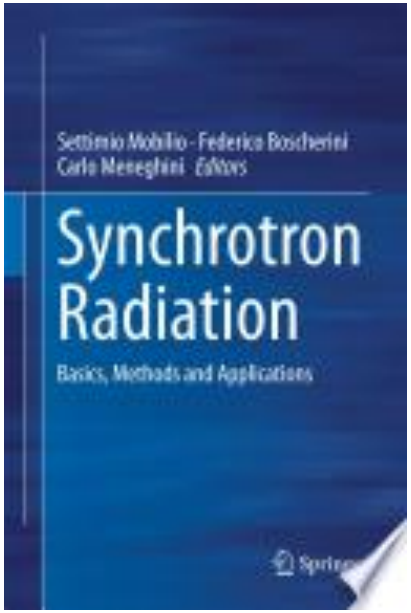

- Chapter 18:
  - Diffraction from nanocrystalline materials
- Chapter 24:
  - Synchrotron radiation and earth sciences
- Chapter 25:
  - Synchrotron radiation and environmental sciences
- Chapter 26:
  - Synchrotron radiation in art, archeology and cultural heritage
- Chapter 29:
  - Studies of matter at extreme conditions

Powder Diffraction

- Oxford Dictionary:

powder
Pronunciation: /ˈpaʊdə/
fine, dry particles produced by the grinding, crushing, or disintegration of a solid

solid
Pronunciation: /ˈsɒlɪd/
1 a substance or object that is solid rather than liquid or fluid.
2 *Geometry* a body or geometric figure having three dimensions.

Elettra
Sincrotrone
Trieste

Powder

Elettra
Sincrotrone
Trieste

A solid

Elettra
Sincrotrone
Trieste

A solid

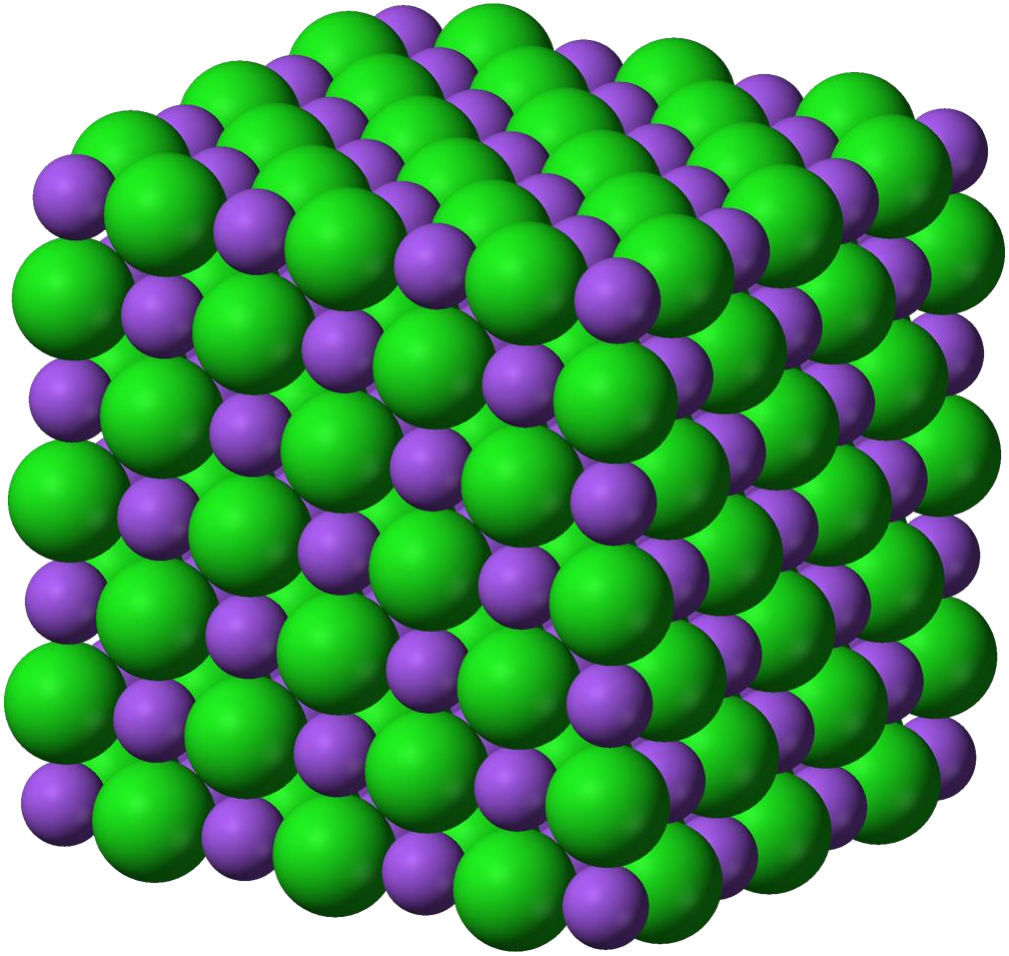

Elettra
Sincrotrone
Trieste

Unit cell

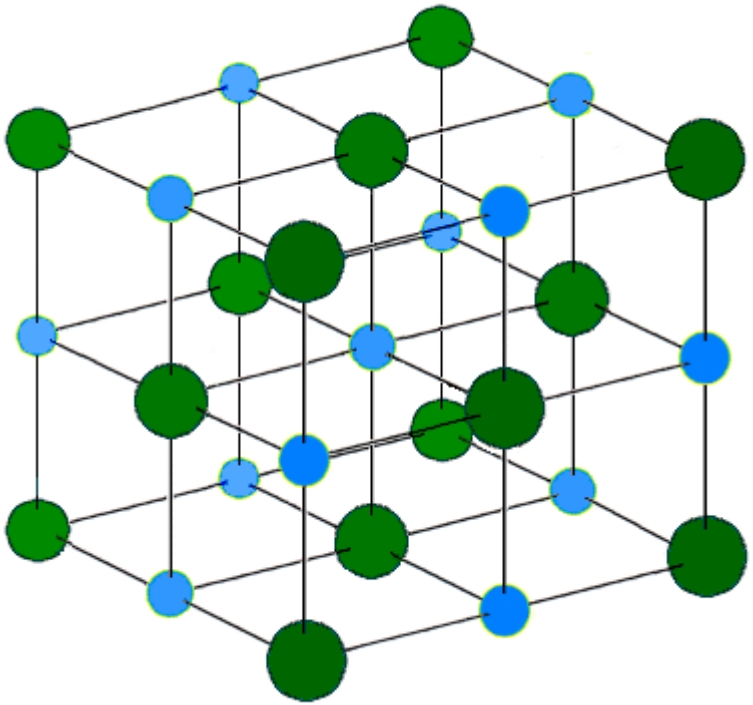

Elettra
Sincrotrone
Trieste

Solids

Crystalline

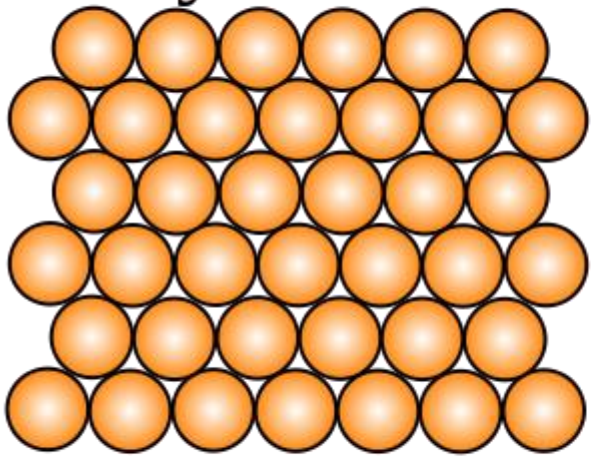

Polycrystalline

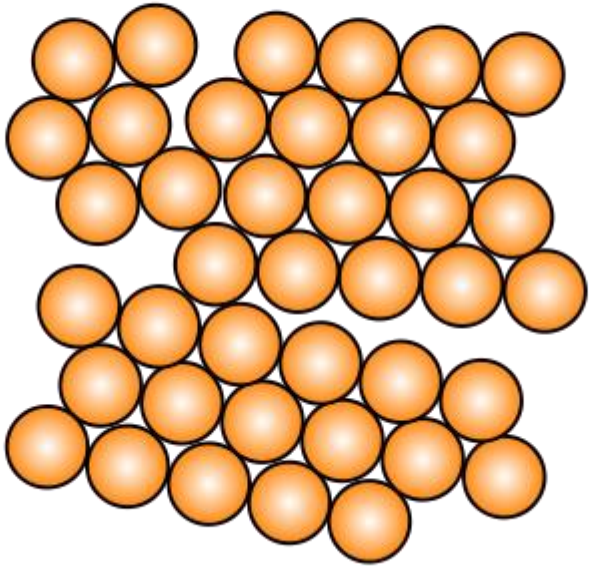

Amorphous

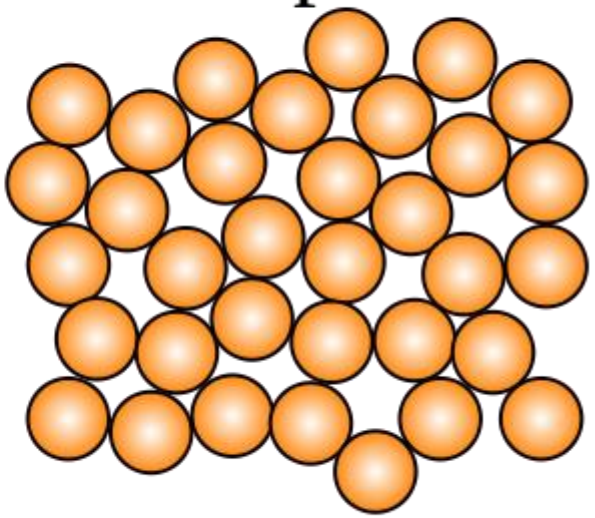

Elettra
Sincrotrone
Trieste

‘Powders’

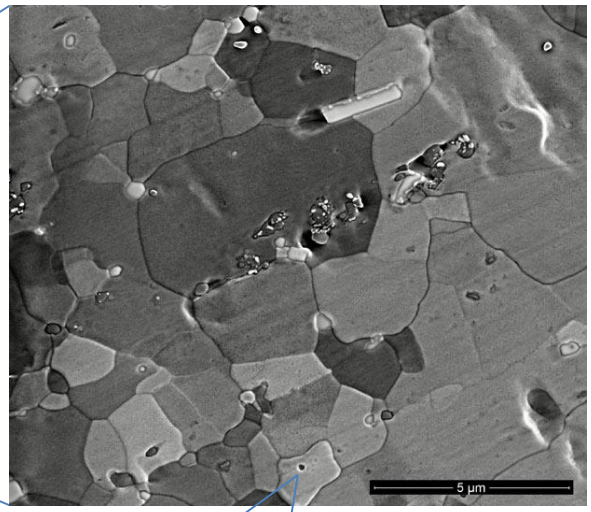

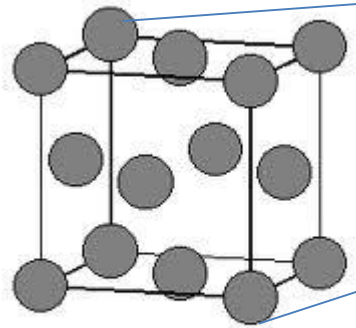

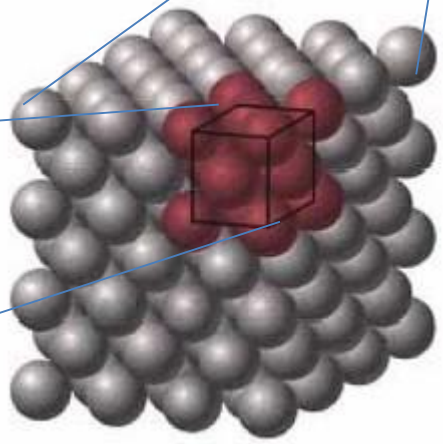

Elettra
Sincrotrone
Trieste

‘Powders’

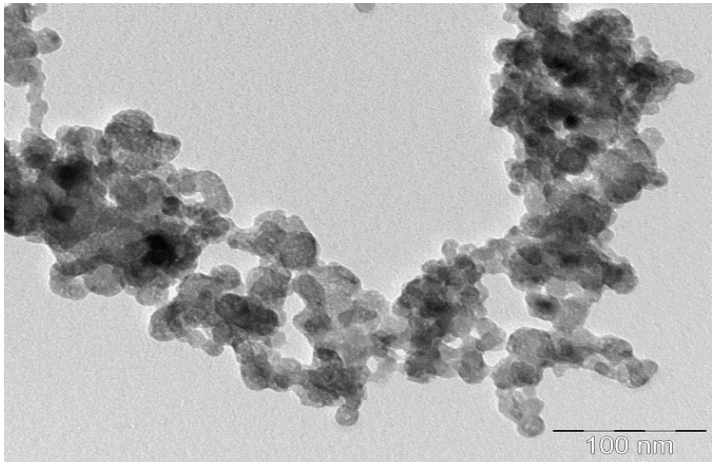

Elettra
Sincrotrone
Trieste

X-ray Diffraction

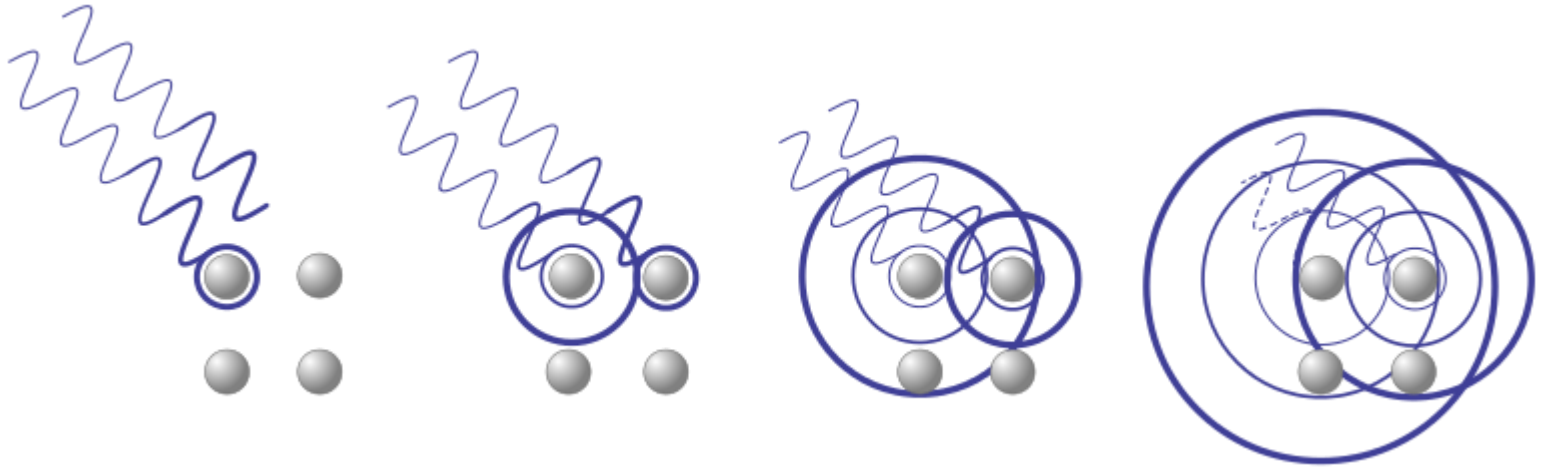

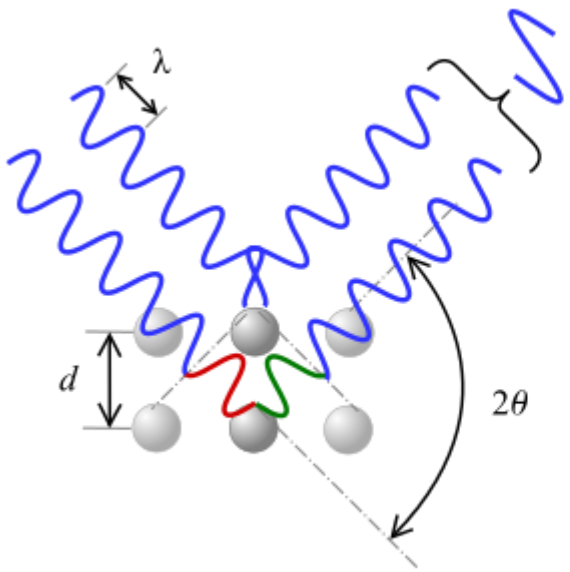

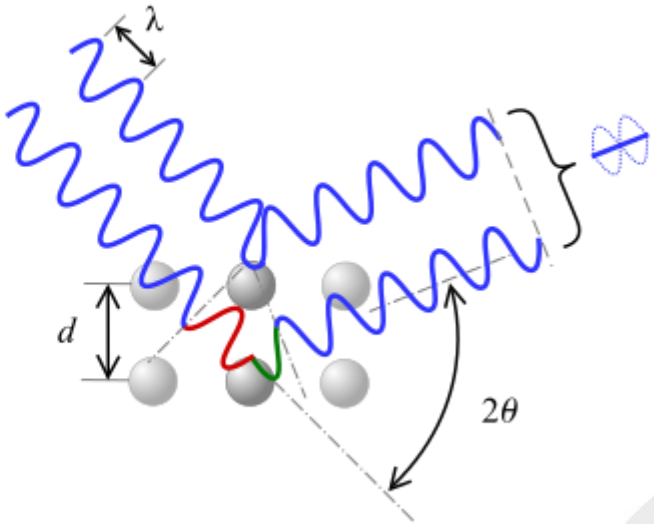

Bragg's law

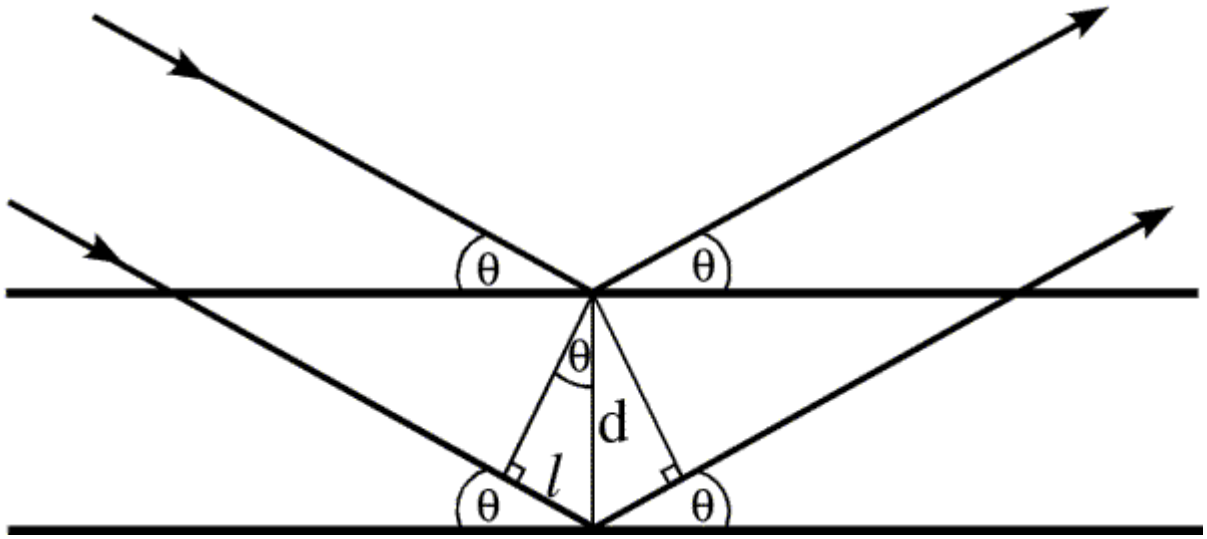

The two X-ray beams travel at different distances. This difference is related to the distance between parallel planes

$$2l = d \ \sin\Theta \qquad n\lambda = 2d \ \sin\Theta$$

Elettra
Sincrotrone
Trieste

Bragg's law

This condition is met when the distance equals an integer multiple of the wavelength, called order of diffraction, n. The final equation is the BRAGG'S LAW

$$n\lambda = 2d \sin\Theta$$

Data are collected by using X-rays of a known wavelength. The sample is rotated so that the angle of diffraction changes

When the angle is correct for diffraction a signal is recorded

Elettra
Sincrotrone
Trieste

Powder Diffraction

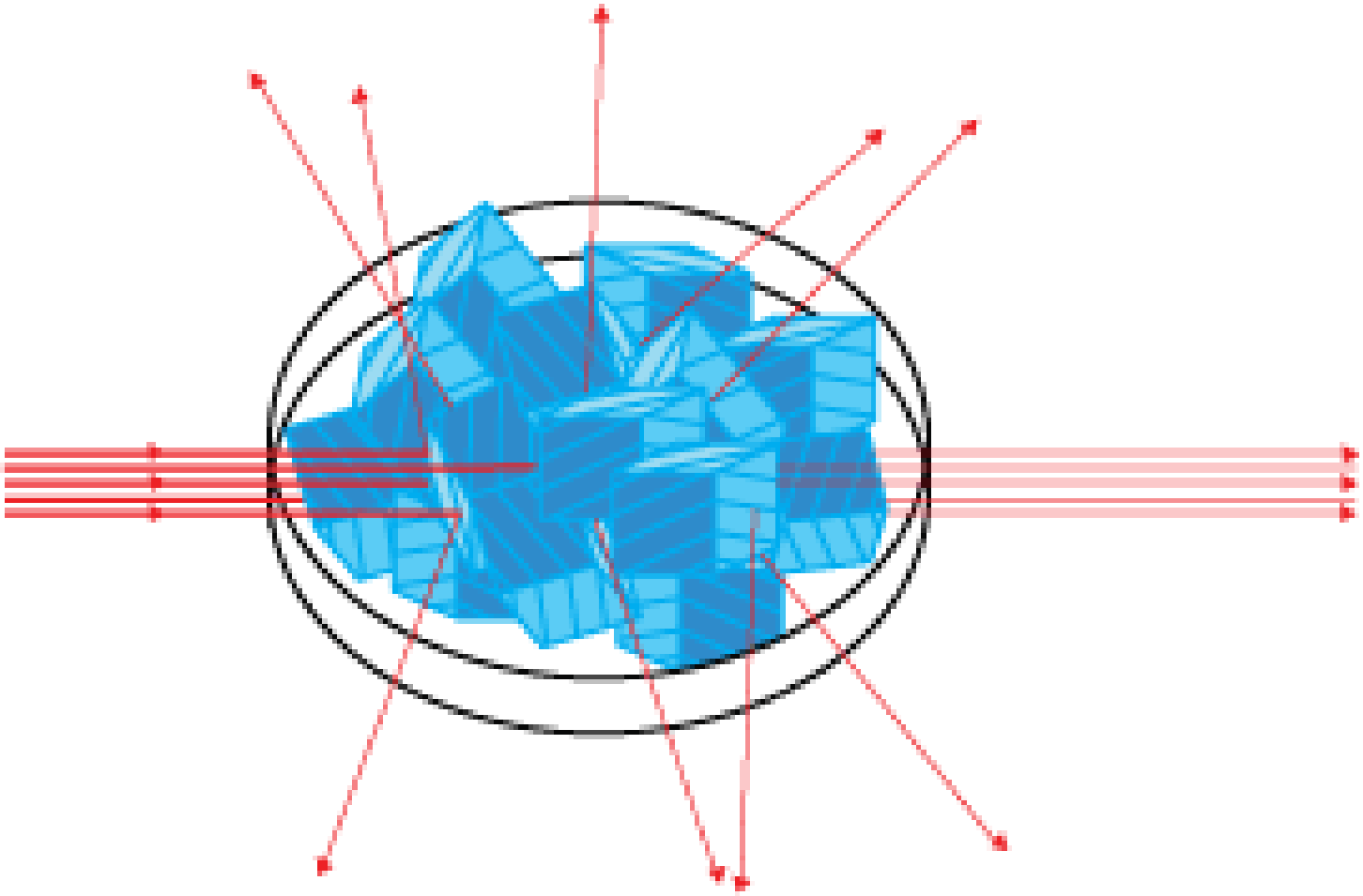

X

Elettra
Sincrotrone
Trieste

Powder Diffraction

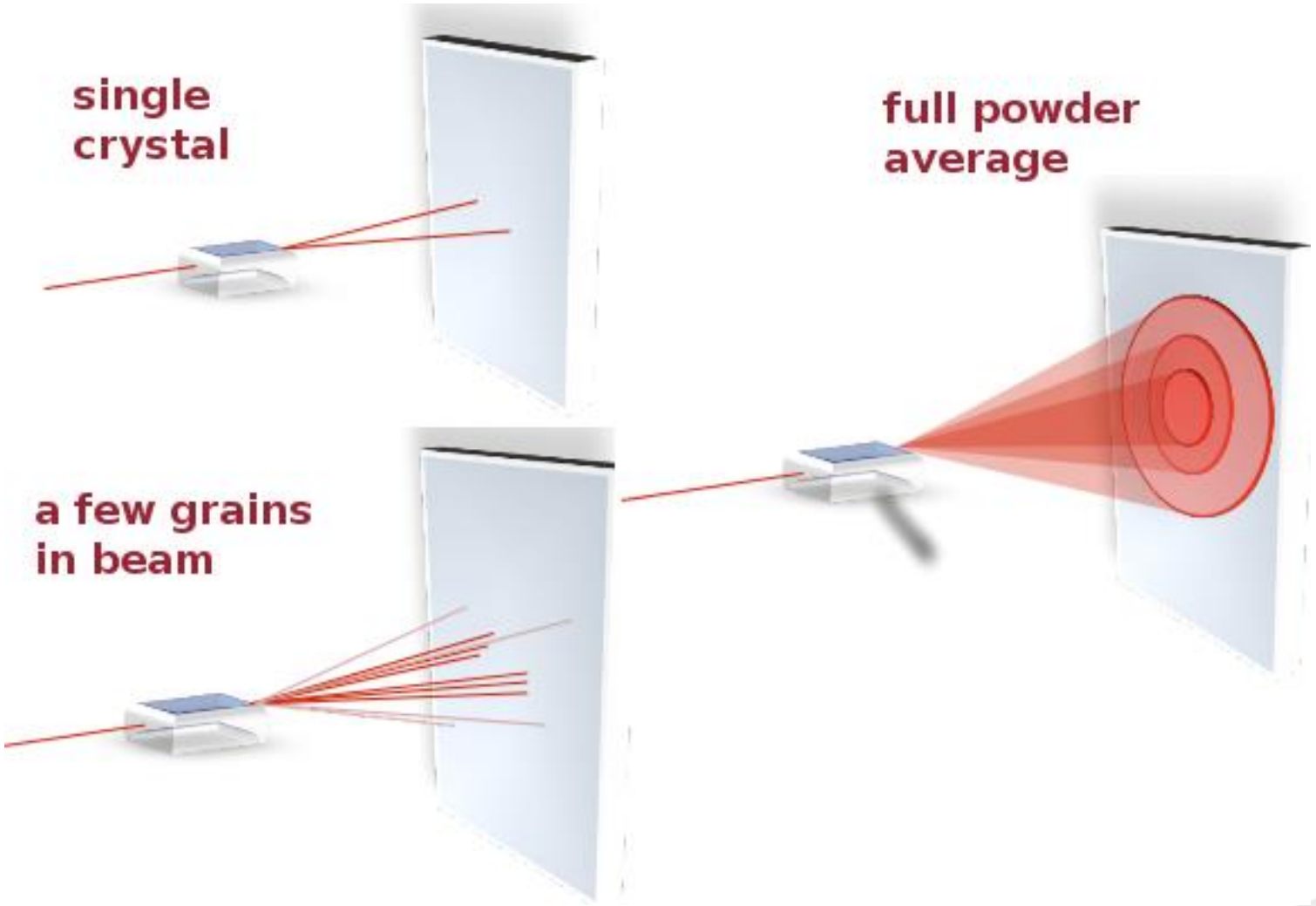

X

Elettra
Sincrotrone
Trieste

Powder diffraction

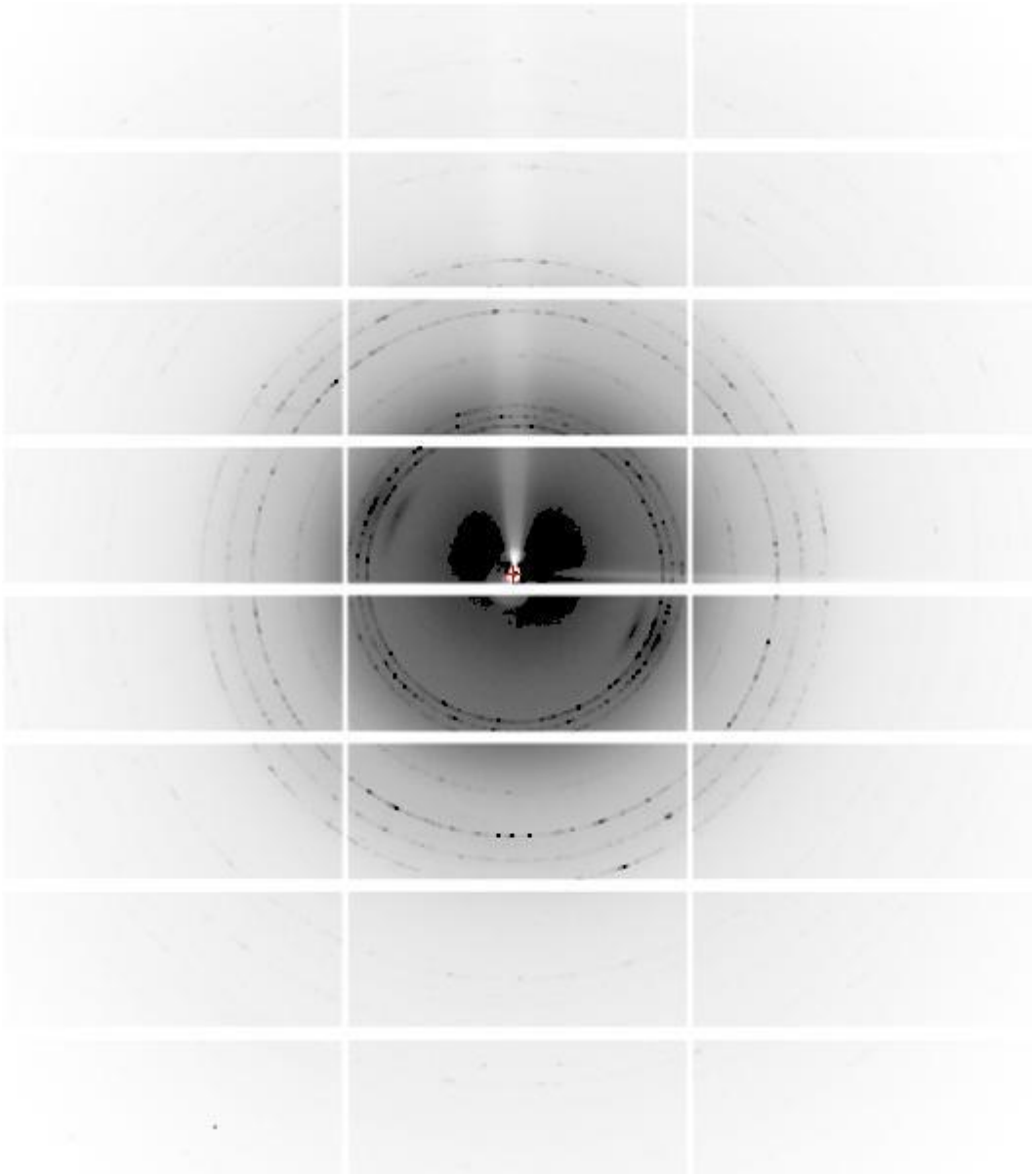

Elettra
Sincrotrone
Trieste

Powder diffraction

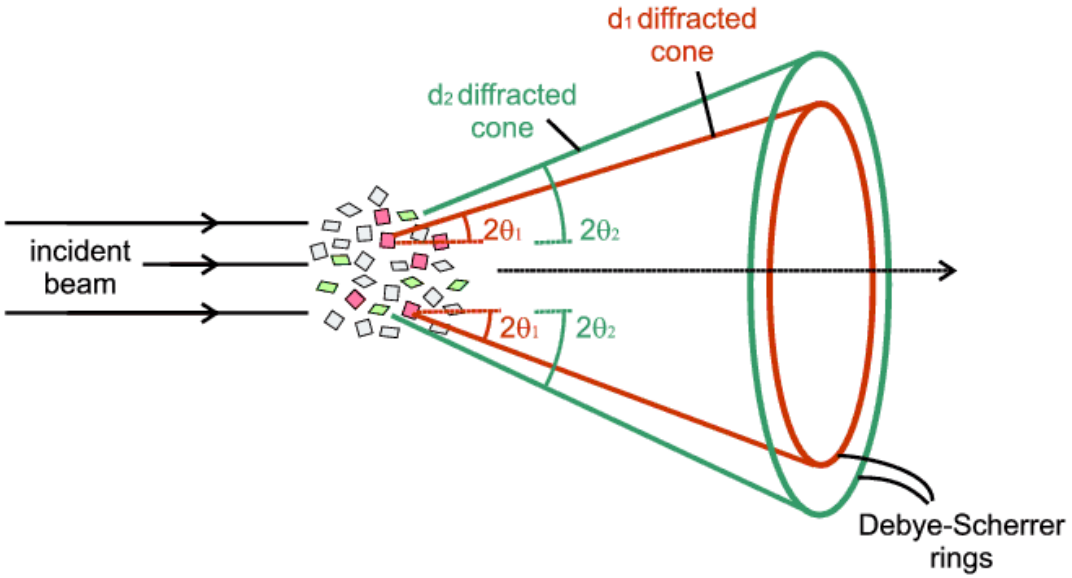

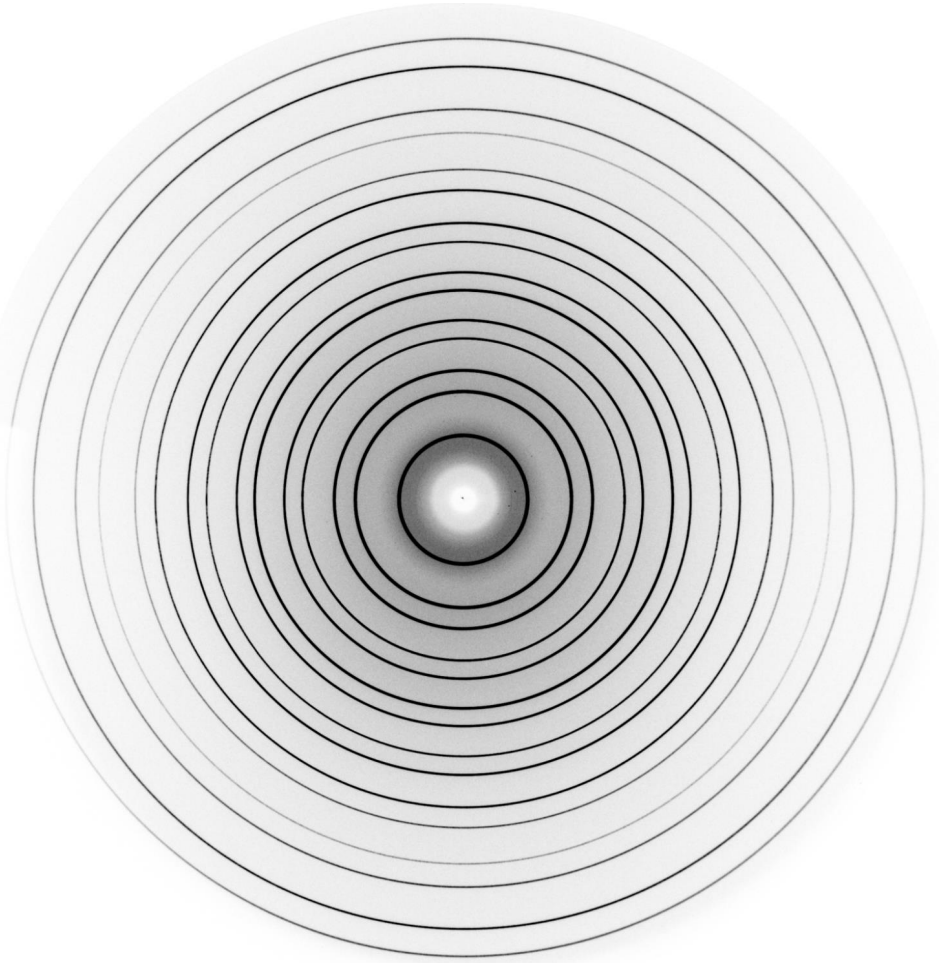

Elettra
Sincrotrone
Trieste

Powder diffraction

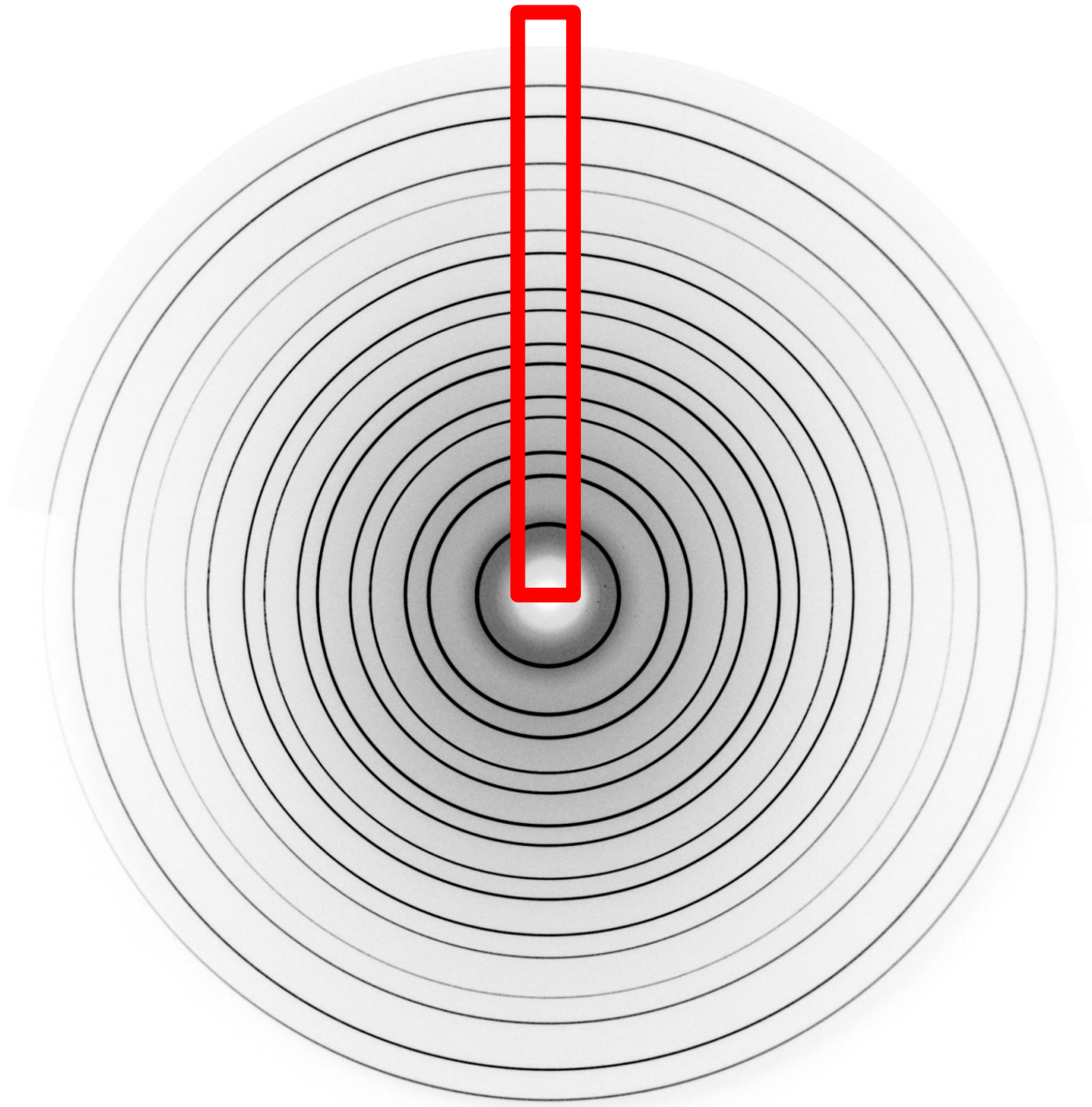

Elettra
Sincrotrone
Trieste

Powder diffraction

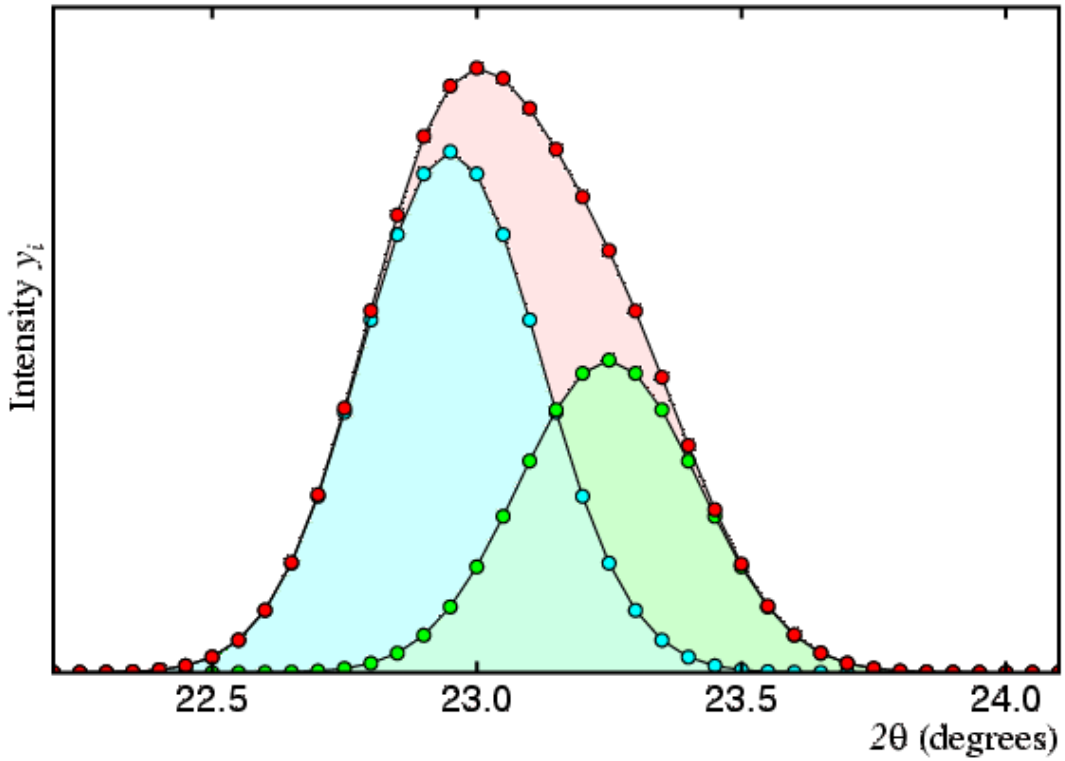

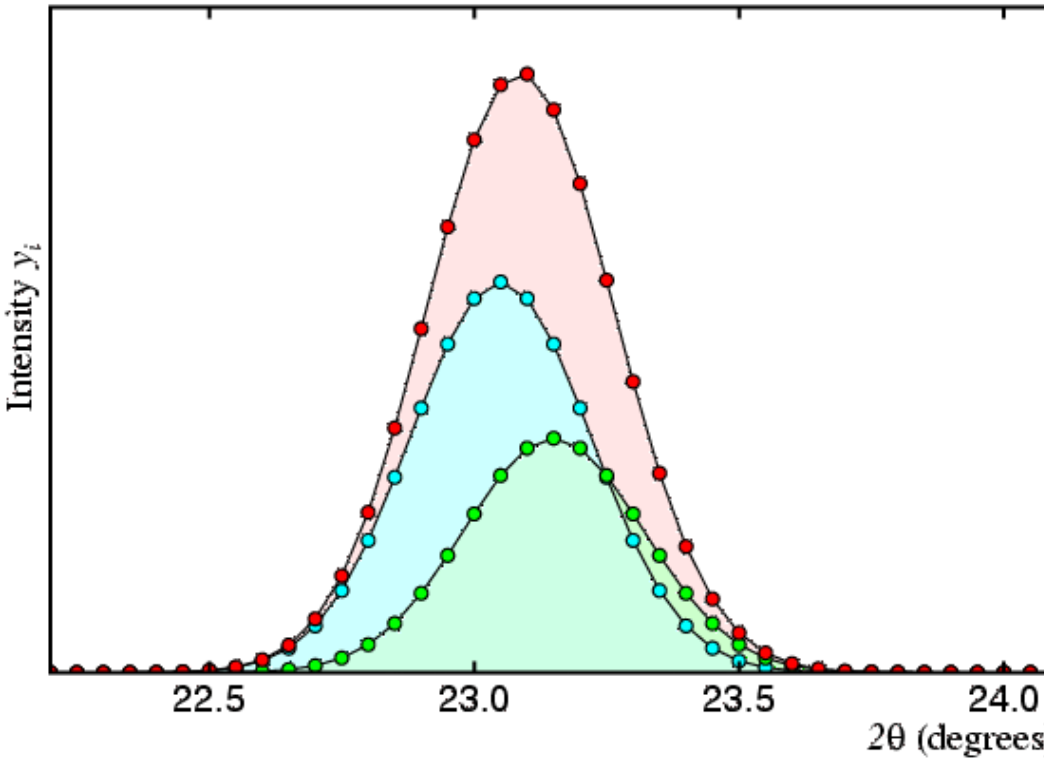

Elettra
Sincrotrone
Trieste

Diffraction geometries

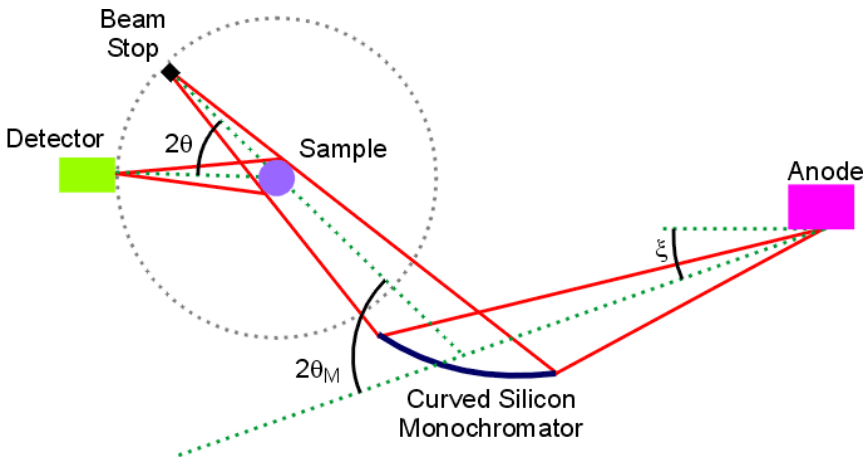

Debije-Scherrer
Transmission

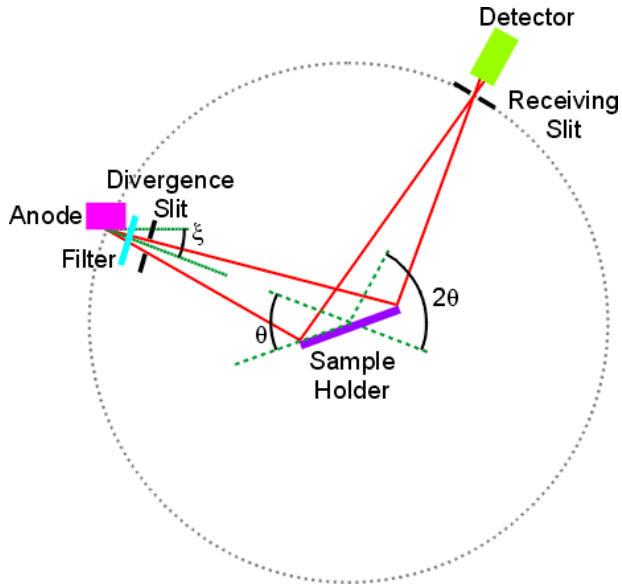

Bragg-Brentano
Reflection

Elettra
Sincrotrone
Trieste

Diffraction geometries

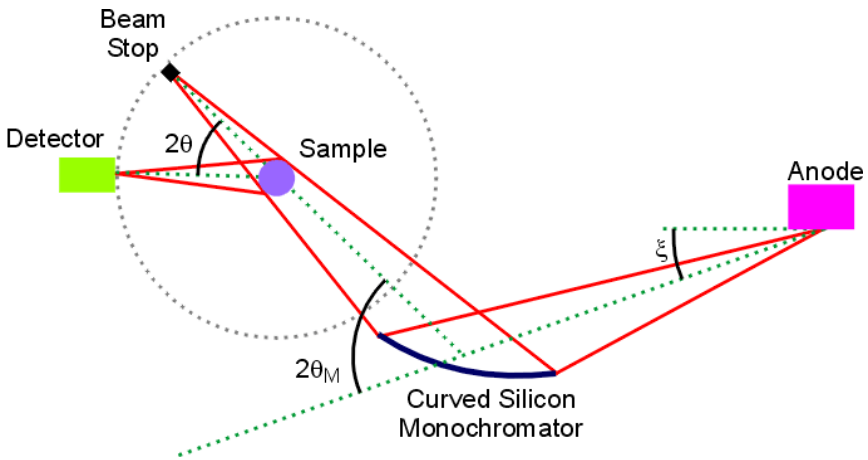

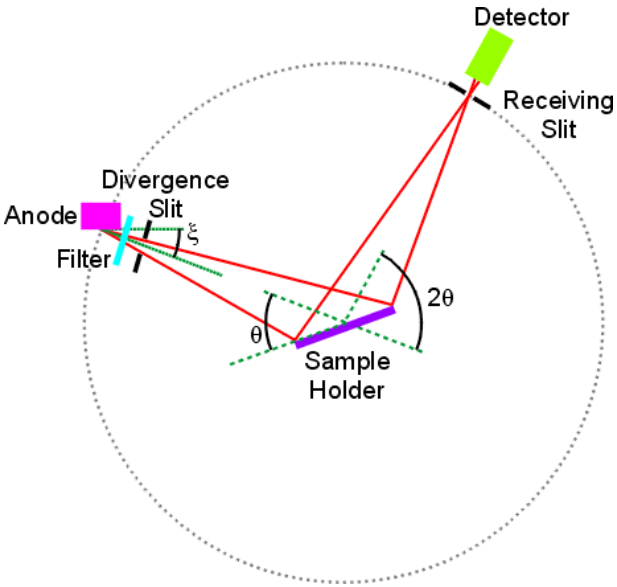

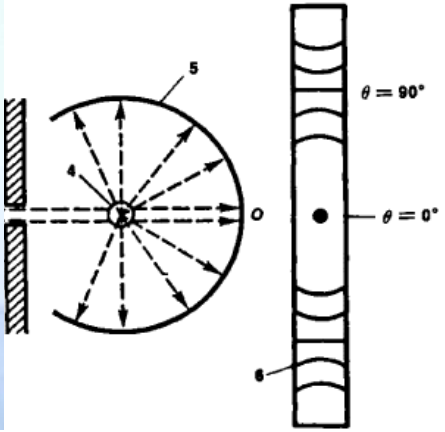

Elettra
Sincrotrone
Trieste

Diffraction geometries in synchrotrons

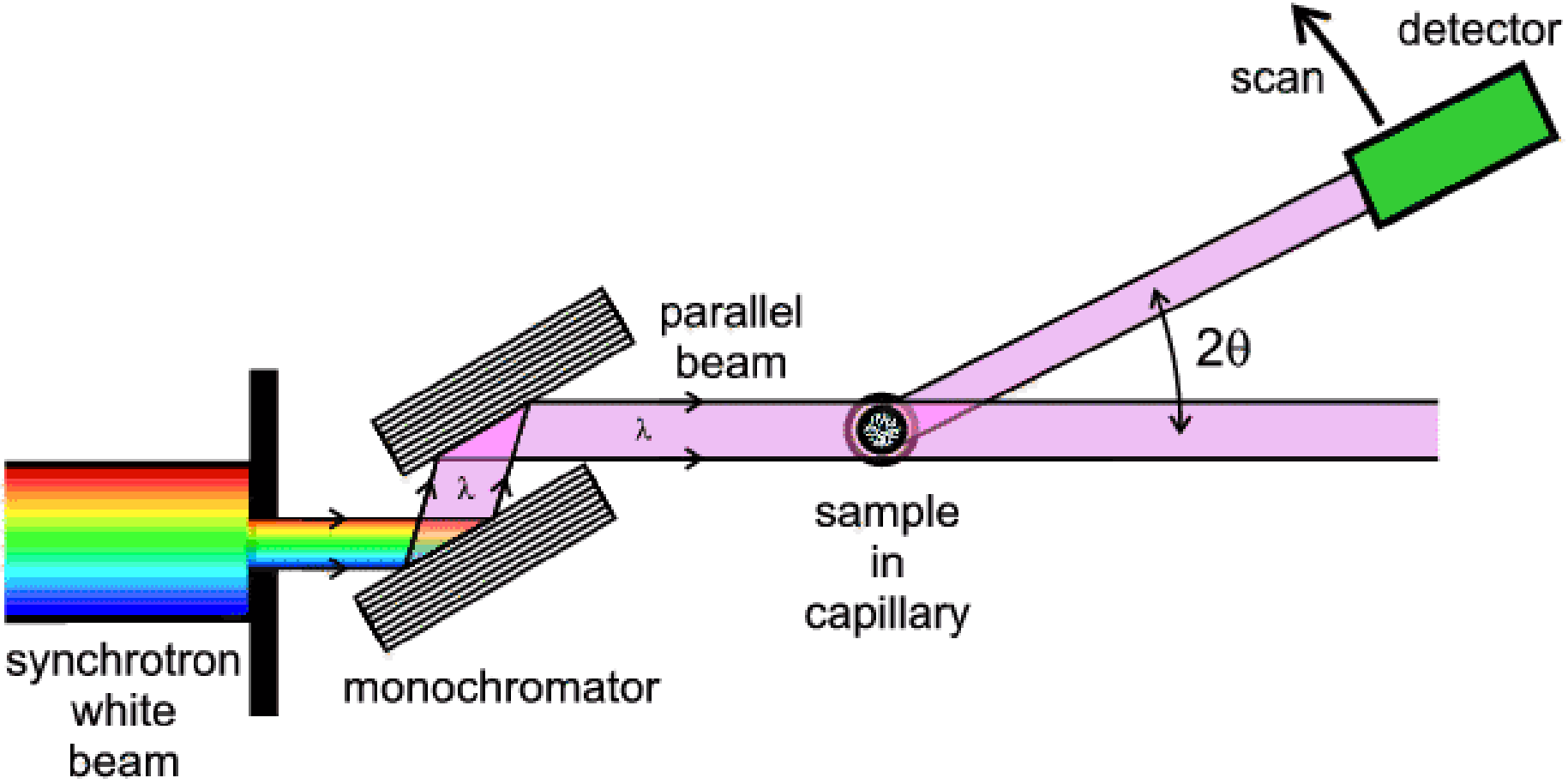

Diffraction geometries in synchrotrons

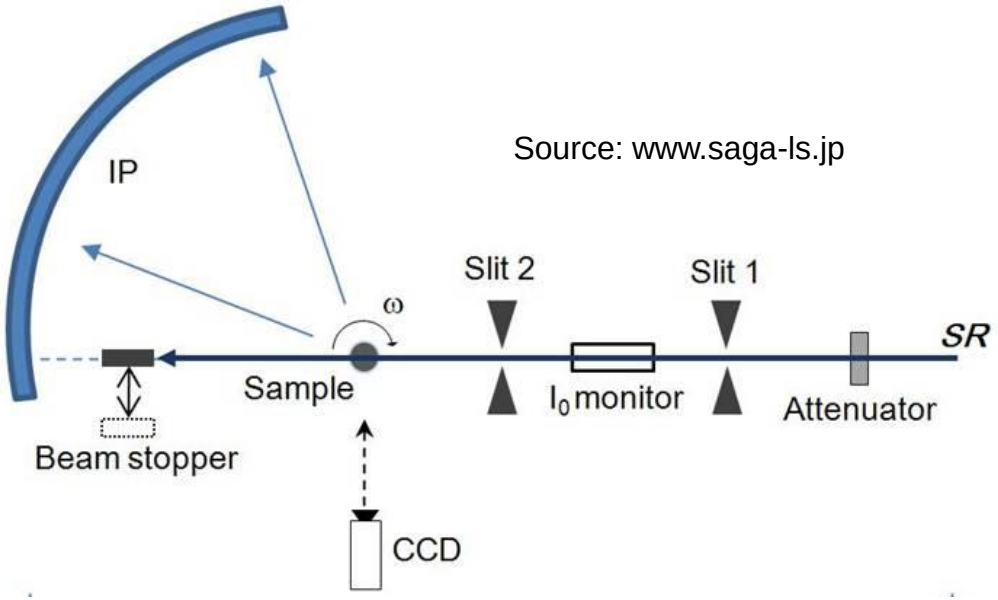

Source: www.saga-ls.jp

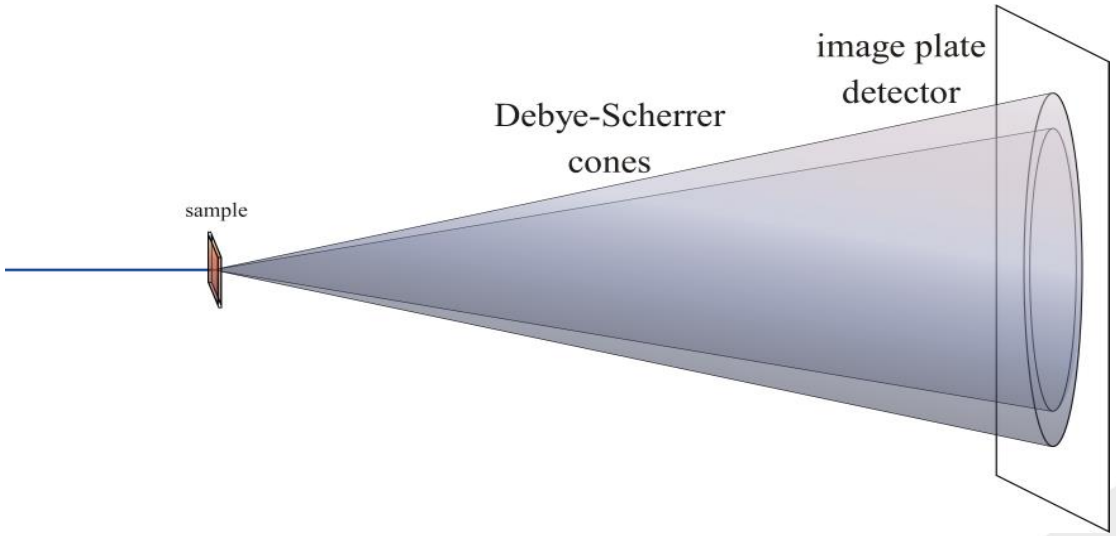

Elettra
Sincrotrone
Trieste

Diffraction geometries in synchrotrons

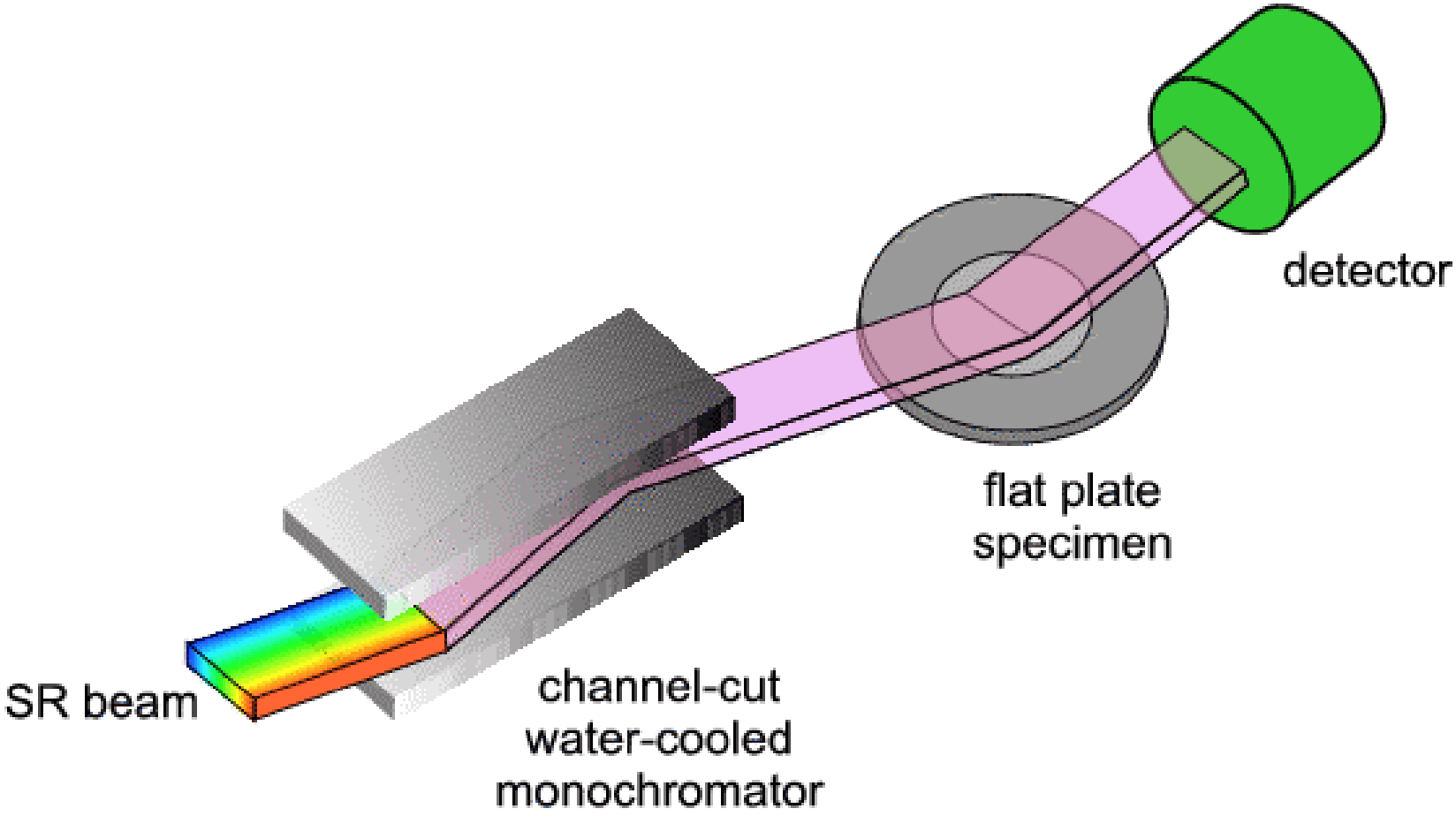

Diffraction geometries in synchrotrons

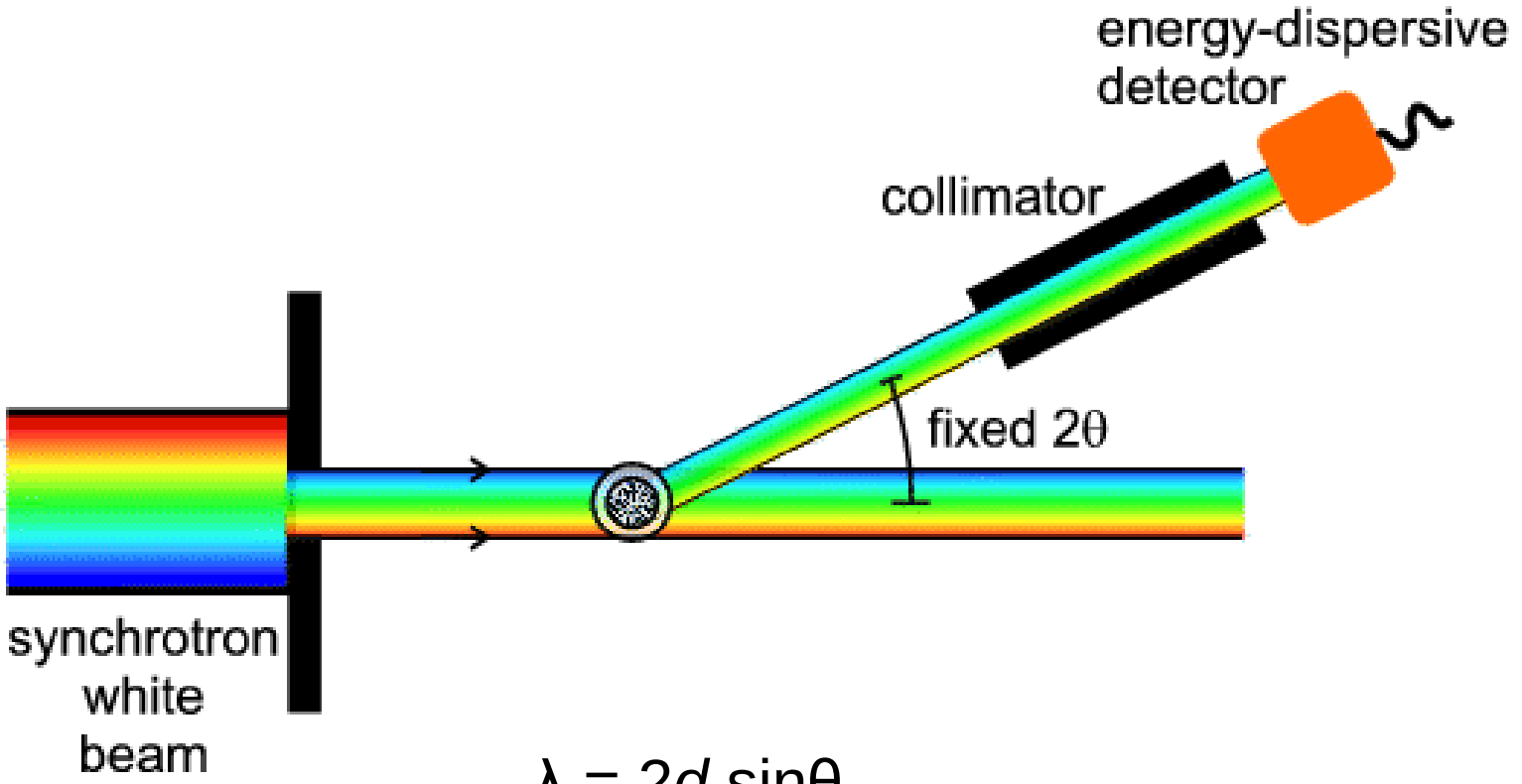

$$\lambda = 2d \sin\theta$$

scanned variable (by ED detector)

determined variable

fixed (by collimator)

Elettra Sincrotrone Trieste

Advantages of XPRD at synchrotrons

- **High X-ray flux** : Millions count counting statistics in reflection (Bragg-Brentano) as well as in transmission (Debye-Scherrer) modes even with low quantities of powder available

- **Highly collimated photon beam**: angular resolution better due to narrow instrumental profile. FWHM better than 0.01° 2θ obtained with new generation solid state microstrip detectors and down to 0.002° 2θ using multicrystal analyser detectors

- **Tunable photon energy up to high energies:**
  - anomalous scattering experiments
  - collect fluorescence-free XRPD data
  - Extension of d-space that can be probed.
  - depth analysis by varying energy

Elettra
Sincrotrone
Trieste

Instrumentation for X-ray Powder Diffraction at Synchrotrons

ESRF – ID22

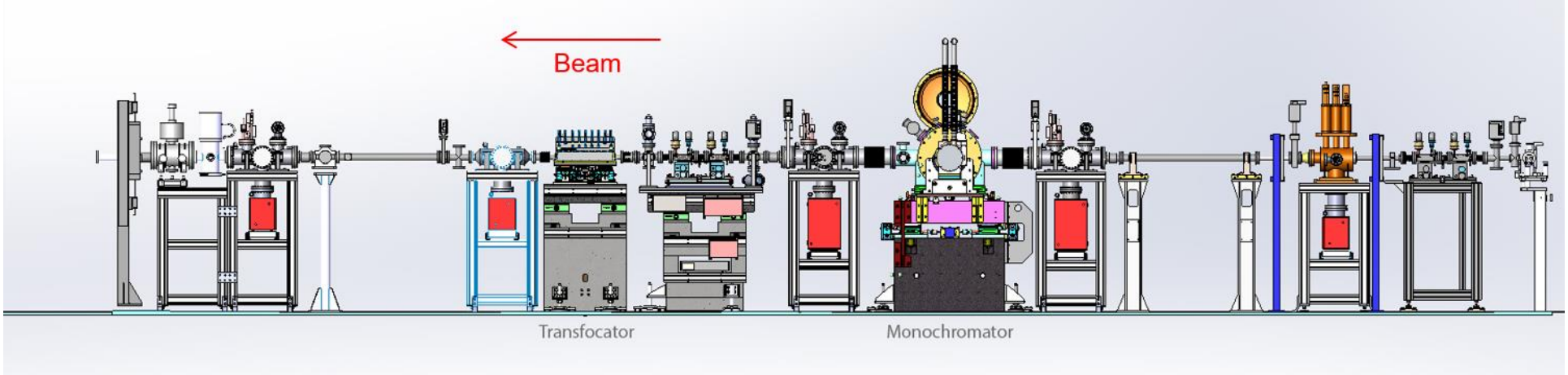

Light source:

In vacuum undulator

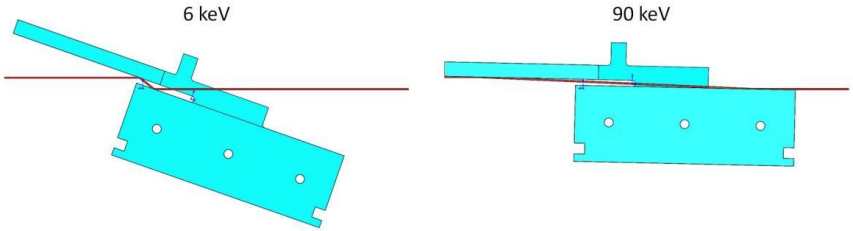

X-rays at **sample:**

Energy range : 6-80 keV

Beam size can be focused to 50 um

Elettra
Sincrotrone
Trieste

Elettra - MCX

Light source:
Bending magnet
Critical energy : 3.2keV (2.0) , 5.5keV (2.4)

X-rays at sample:
Energy range : 6-21 keV
Photon flux : 10^{11} photons/sec
Beam size at sample : 10x1 mm^2 - 0.3x0.3 mm^2
Energy resolution : $\Delta E/E$ $2x10^{-4}$

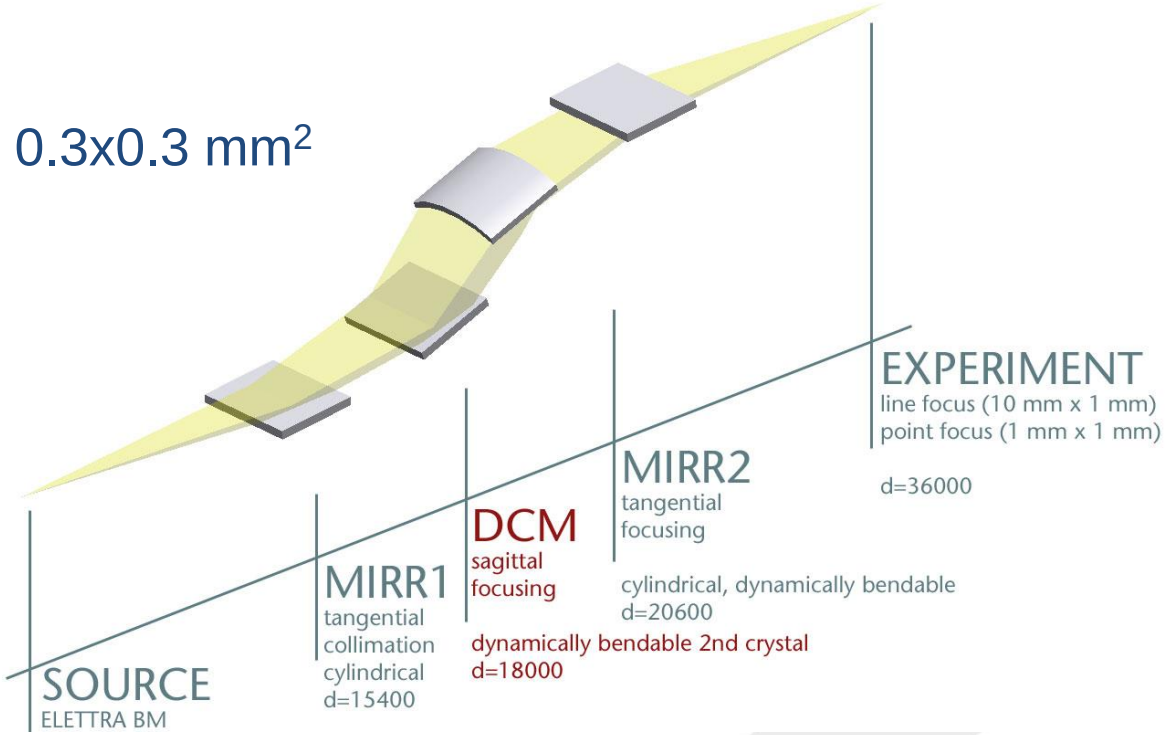

Elettra
Sincrotrone
Trieste

Diffractometer MCX

Elettra
Sincrotrone
Trieste

Diffractometer ID22-ESRF

X-ray detectors

0D – (spot) detectors: Scintillators

N

1D – Line detectors: Gas detectors, Strip

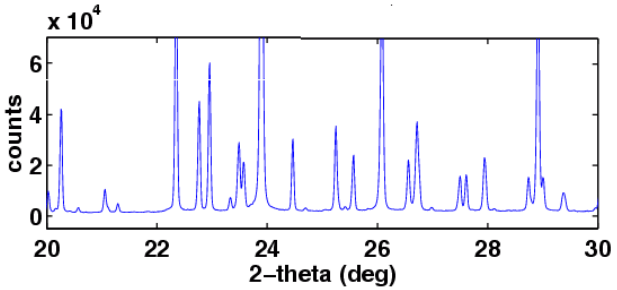

2D -- Area detectors: Image plate, CCD, Pixel

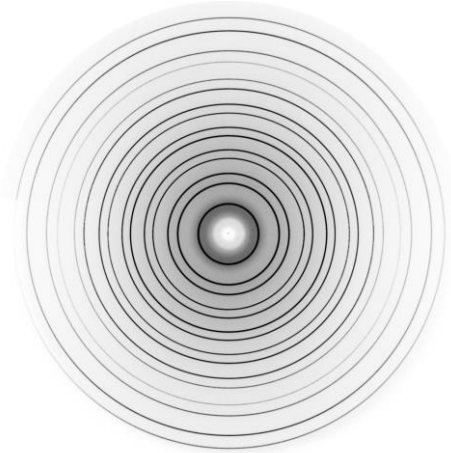

Scintillator detector (0D)

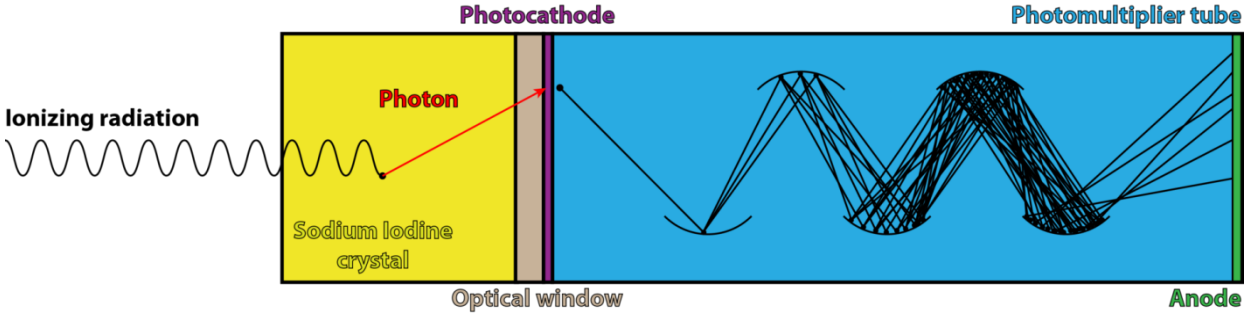

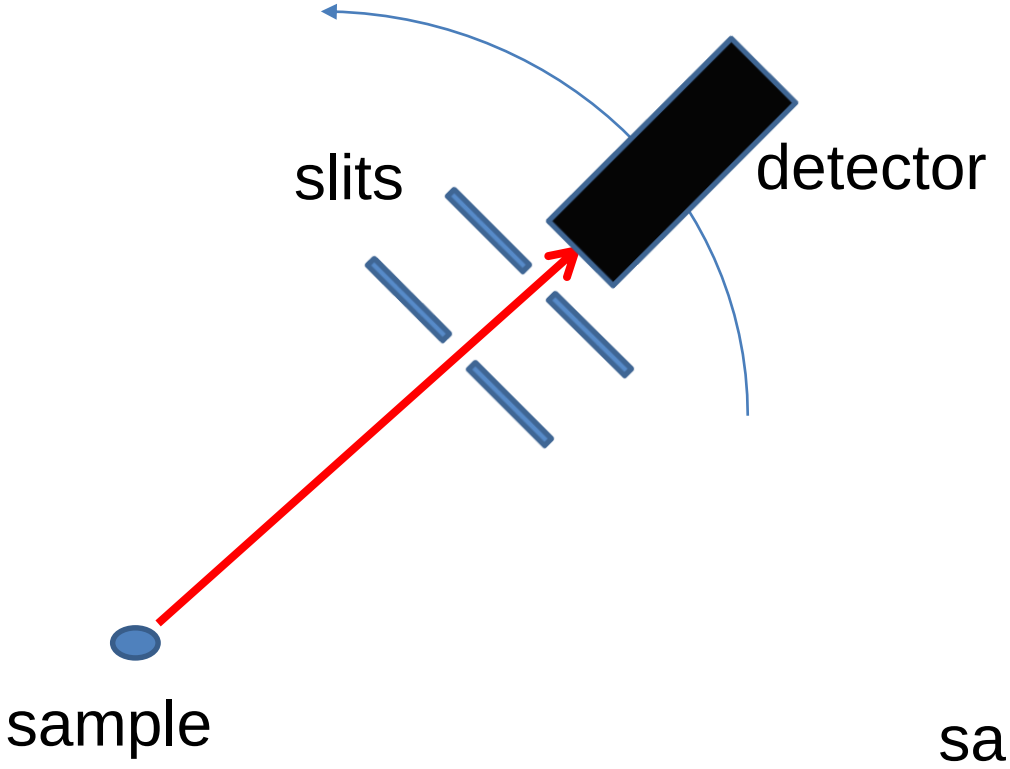

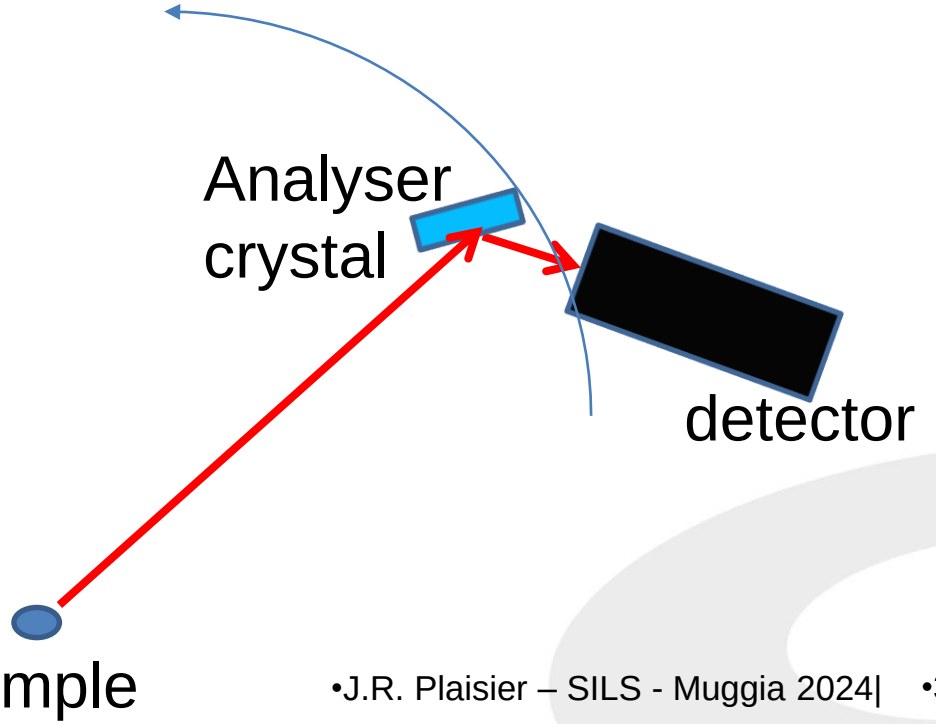

Elettra
Sincrotrone
Trieste

Image plate (2D)

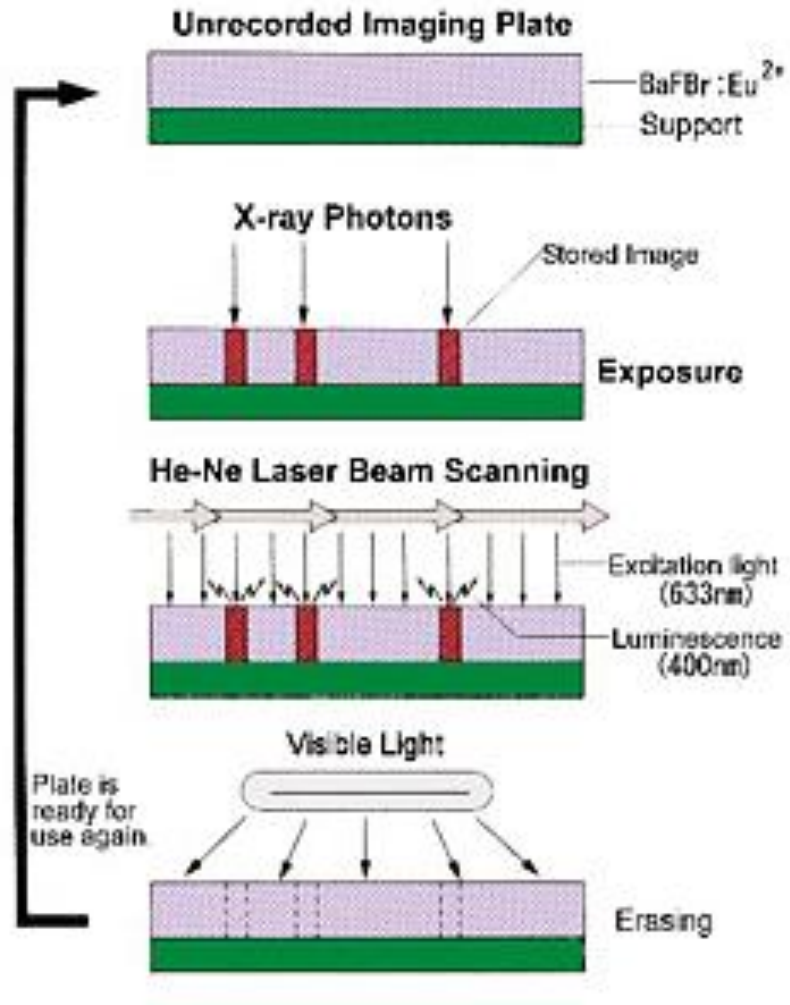

Elettra
Sincrotrone
Trieste

Mythen detector (1D)

Pilatus detector (2D)

Source: XRD1 - elettra

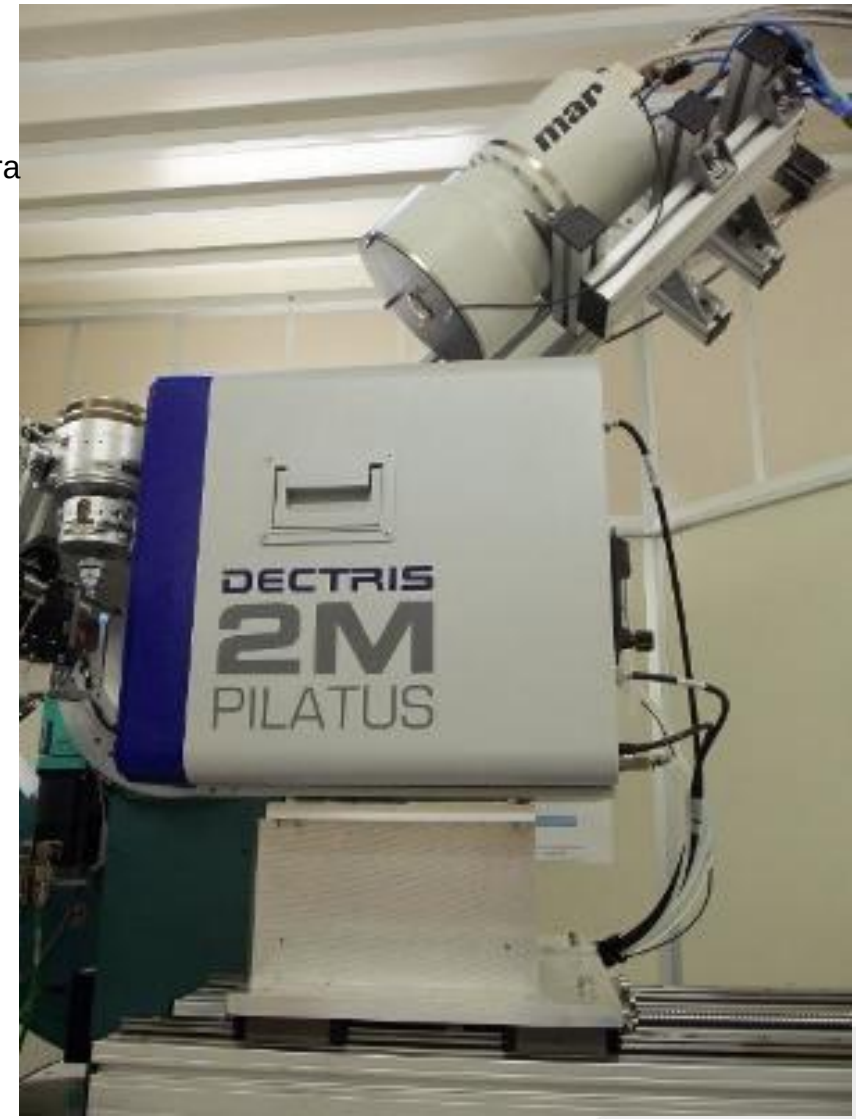

Source: www.psi.ch

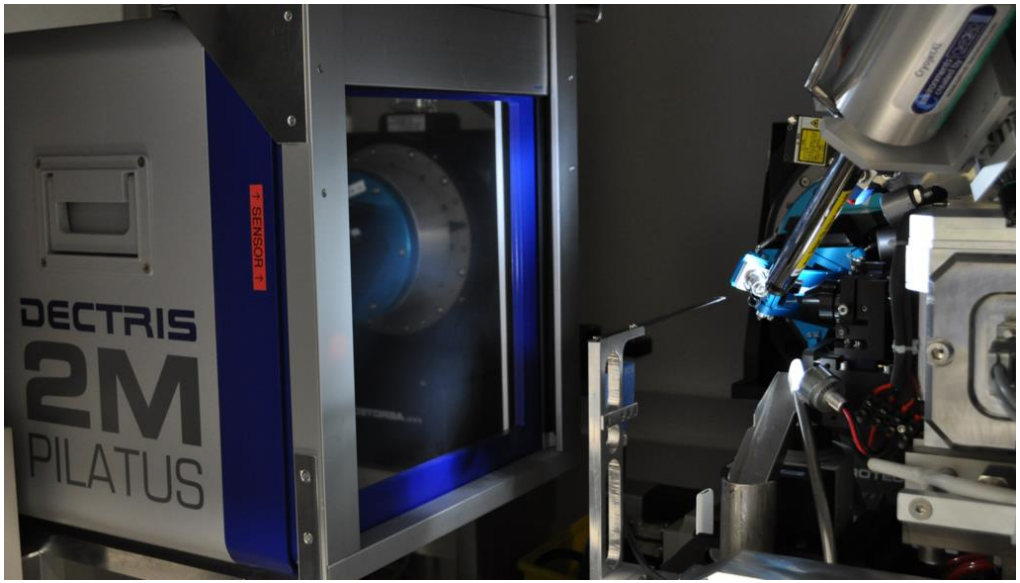

Elettra
Sincrotrone
Trieste

Pilatus detector (2D)

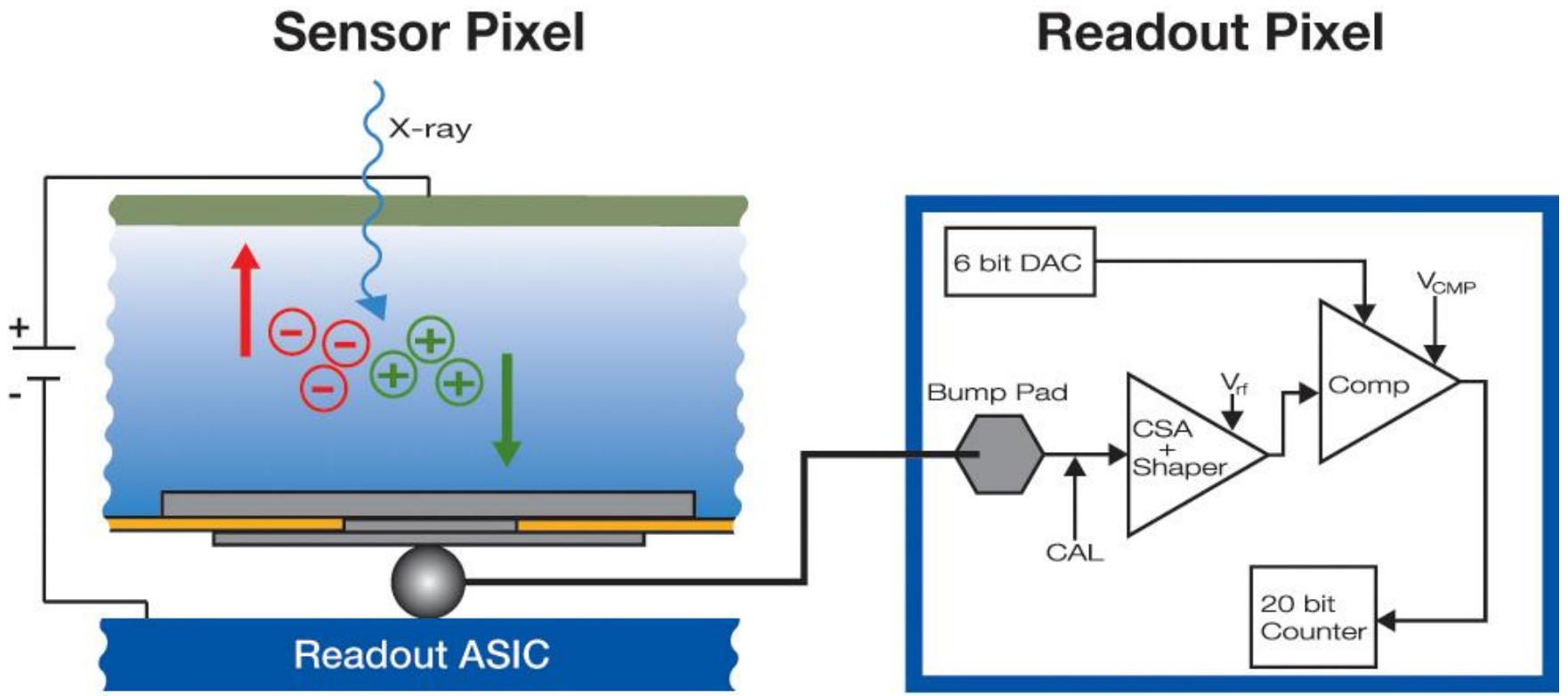

Direct detection of X-rays in semiconductor sensor

→ Point Spread Function 1 pixel

Single Photon Counting ASIC

→ No readout noise or dark current
→ High dynamic range (20 bit)
→ Fast readout

Elettra Sincrotrone Trieste

Mythen (1D) and Pilatus (2D)

Sensor material	Silicon
Sensor	Reverse biased pn-junction array
Detection principle	Single photon counting
Sensor thickness [µm]	320, 450, 1000
Number of channels/module	1280
Sensitive area (width x length) [mm²]	64 x 8
Dimensions of one channel (width x length) [µm²]	50 x 8000
Read out time [ms]	0.3
Maximum count rate per channel [X-rays/s]	>1x10^6
Energy range [keV]	5 – 40
Point-spread function	1 channel
Dynamic range [bit]	4, 8, 16, 24 (1 : 16777216)

Sensor material	Silicon
Sensor	Reverse biased pn-junction array
Detection principle	CMOS hybrid-pixel technology - single photon counting
Sensor thickness [µm]	320
Number of pixels/module	1475 x 1679 = 2476525 pixels
Sensitive area (width x length) [mm²]	254 x 289
Dimensions of one pixel (width x length) [µm²]	172 x 172
Read out time [ms]	3.6 (frame rate 30Hz)
Maximum count rate per channel [X-rays/s]	>1x10^6
Energy range [keV]	3 - 30 keV (quantum efficiency: 3 keV 80%; 8 keV 99%; 15 keV 55%)
Point-spread function	1 pixel

Elettra
Sincrotrone
Trieste

Diffractometer ID22-ESRF

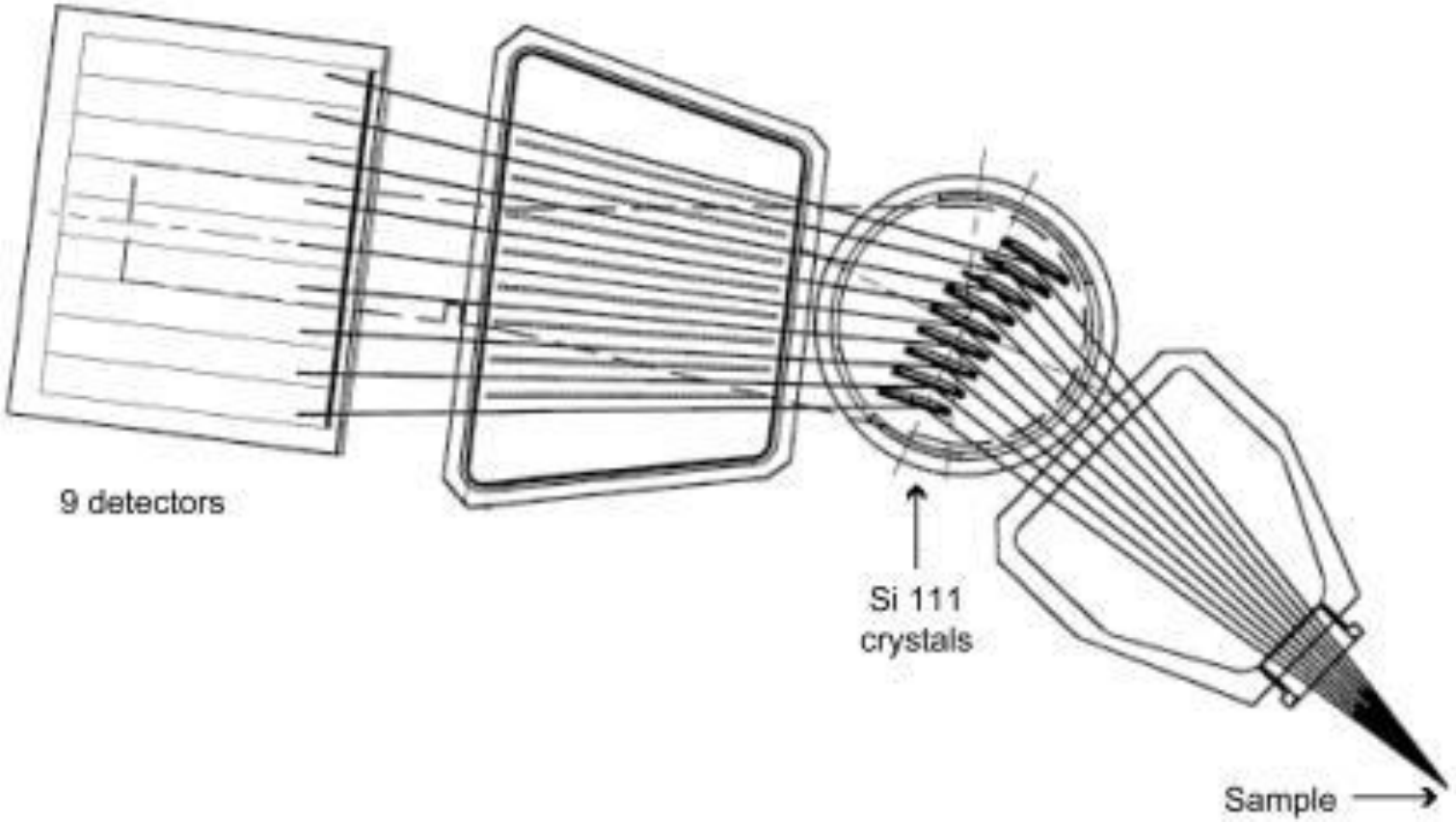

Elettra
Sincrotrone
Trieste

Diffractometer I11 - Diamond

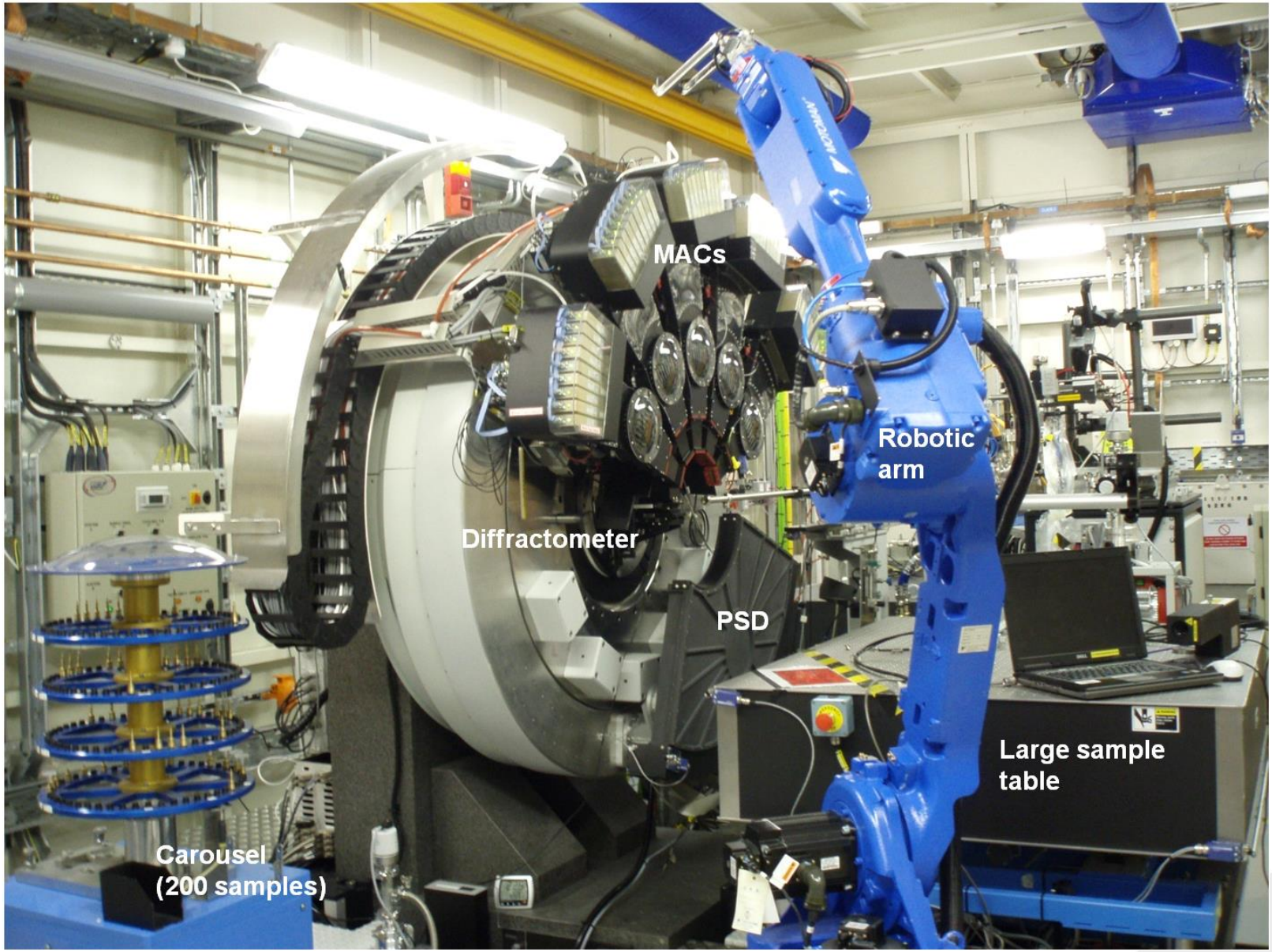

Elettra
Sincrotrone
Trieste

Diffractometer MS

Elettra
Sincrotrone
Trieste

Information from Powder Diffraction

Information from powder diffraction

- The diffraction peak positions give information on the size and shape of the unit cell.
- Shifts in peak positions give information about deformation (eg. Residual stress)

$$\lambda = 2d \sin\theta$$

$$\frac{1}{d_{hkl}^2} = h^2 \frac{b^2c^2 \sin^2\alpha}{V^2} + k^2 \frac{a^2c^2 \sin^2\beta}{V^2} + l^2 \frac{a^2b^2 \sin^2\gamma}{V^2}$$
$$+ 2hk \frac{abc^2(\cos\alpha\cos\beta - \cos\gamma)}{V^2} + 2kl \frac{a^2bc(\cos\beta\cos\gamma - \cos\alpha)}{V^2}$$
$$+ 2lh \frac{ab^2c(\cos\gamma\cos\alpha - \cos\beta)}{V^2}$$

Information from powder diffraction

$$d_{hkl} = \frac{a_0}{\sqrt{h^2 + k^2 + l^2}}$$

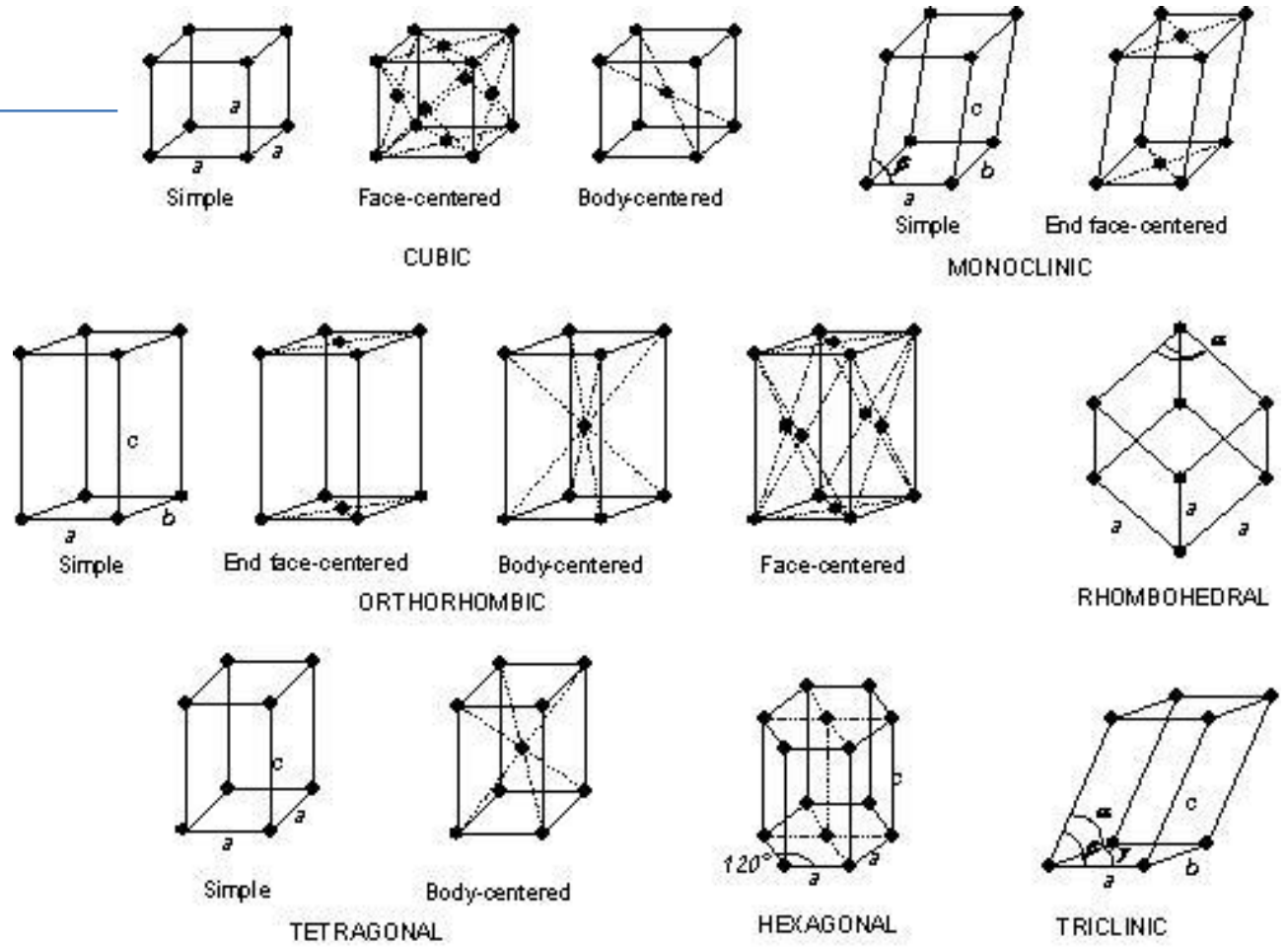

Information from powder diffraction

- The Intensity of a diffracted beam, I_{hkl} is related to an imaginary number called the structure factor, F_{hkl} : $I_{hkl} \propto |F_{hkl}|^2$

$$F(hkl) = \sum_n f_n N_n e^{2\pi i(hx_n + ky_n + lz_n)} e^{-B\sin^2\theta/\lambda}$$

- The Intensity of a diffracted beam gives information on the positions of the atoms in the unit cell and hence the 'atomic structure' of the material

- In case of mixtures the intensities give information on the quantity of various materials in the mixture

Structure determination

- **Steps in structure determination from SR-XRPD:**
  - Indexing (DICVOL ecc.)
  - Space group determination
  - Finding a model structure
    - Direct methods
    - Simulated annealing etc. (eg. DASH)
    - Model from similar compounds
  - Refining the structure (Rietveld)

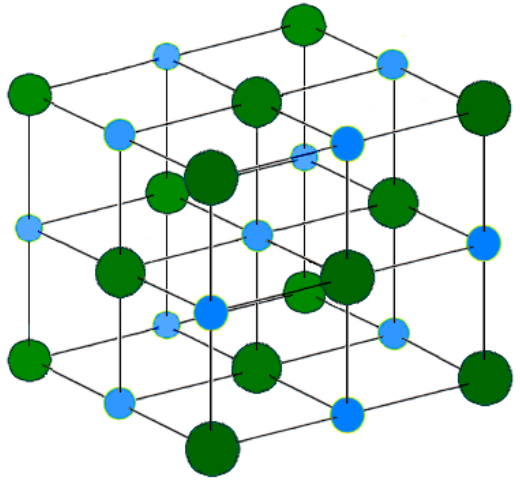

Elettra Sincrotrone Trieste

Structure determination Indexing

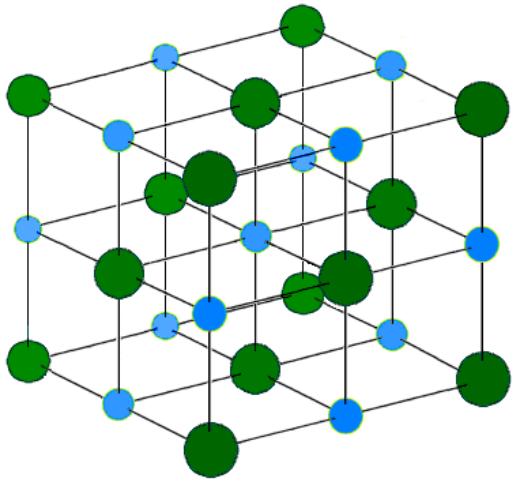

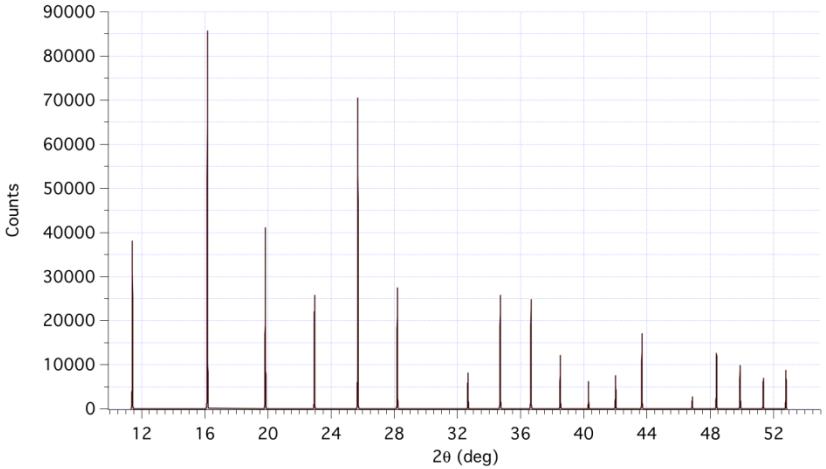

- Known parameters: peak positions
- Unknowns:
  - Unit cell a,b,c, α, β, γ
  - Miller indices: h, k ,lfor each reflection
  - Zero shift ($2\Theta_0$)

$$\frac{1}{d_{hkl}^2} = h^2\frac{b^2c^2\sin^2\alpha}{V^2} + k^2\frac{a^2c^2\sin^2\beta}{V^2} + l^2\frac{a^2b^2\sin^2\gamma}{V^2}$$

$$+2hk\frac{abc^2(\cos\alpha\cos\beta-\cos\gamma)}{V^2} + 2kl\frac{a^2bc(\cos\beta\cos\gamma-\cos\alpha)}{V^2}$$

$$+2lh\frac{ab^2c(\cos\gamma\cos\alpha-\cos\beta)}{V^2}$$

$$d = \lambda/\,2\sin(\Theta - 2\Theta_0/2)$$

Elettra
Sincrotrone
Trieste

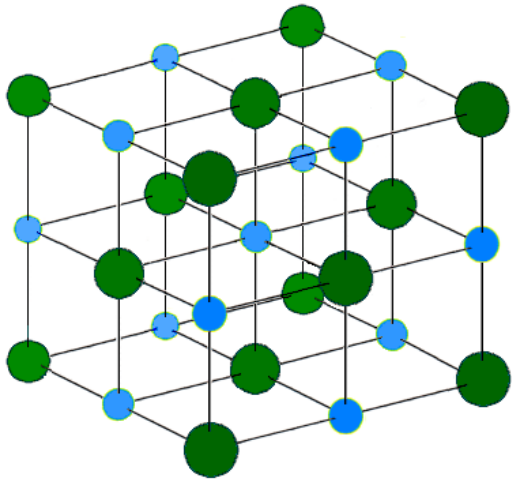

Structure determination
Fining the space group

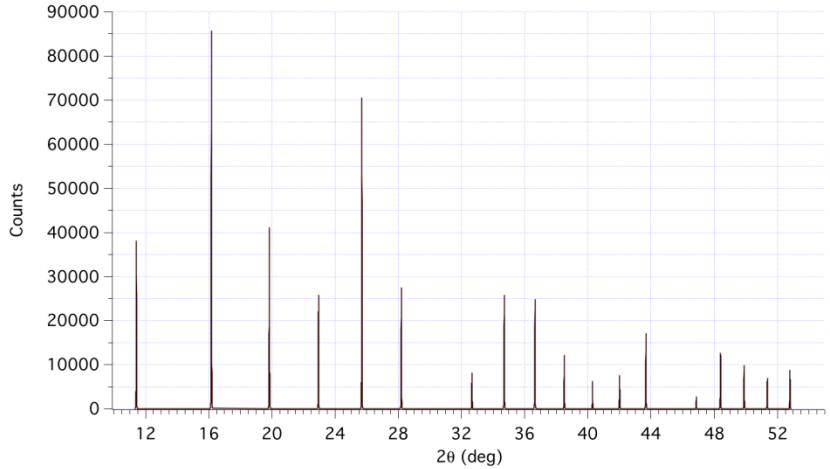

- The space group describe the symmetry in the unit cell (e.g. Centering, mirror planes, rotation axes)
- Some symmetry elements may cause certain reflections to have zero intensity.
- Indentifying these reflection conditions allows to identify the proper space group candidates.

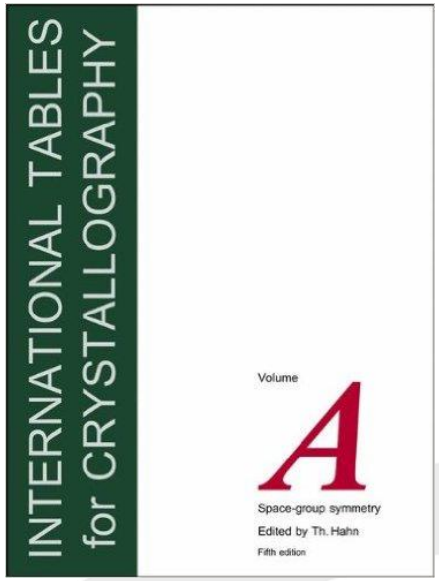

Elettra
Sincrotro
Trieste

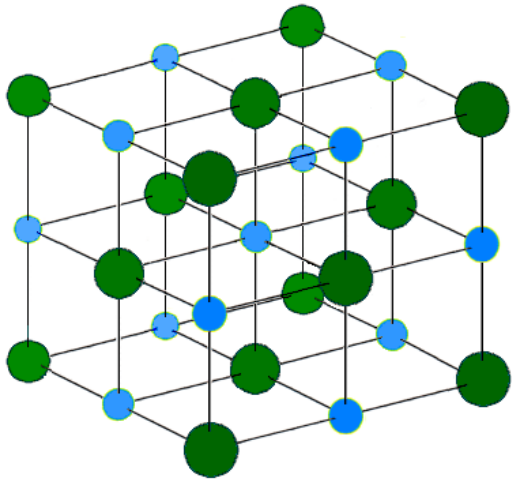

Structure determination
Finding the space group

Unit-Cell Geometry	Inferred Crystal System(s)	No. of Space Groups
$a \neq b \neq c$ and $\alpha \neq \beta \neq$ & gamma; & ne; 90°	Triclinic	2
$a \neq b \neq c$ and $\alpha = \gamma = 90°$ and $\beta \neq 90°$	Monoclinic	13
$a \neq b \neq c$ and $\alpha = \beta = \gamma = 90°$	Orthorhombic	59
$a = b \neq c$ and $\alpha = \beta = \gamma = 90°$	Tetragonal	68
$a = b = c$ and $\alpha = \beta = \gamma \neq 90°$	Trigonal (Rhombohedral)	7
$a = b \neq c$ and $\alpha = \beta = 90°$ and $\gamma = 120°$	Trigonal or Hexagonal	45
$a = b = c$ and $\alpha = \beta = \gamma = 90°$	Cubic	36

Elettra Sincrotrone Trieste

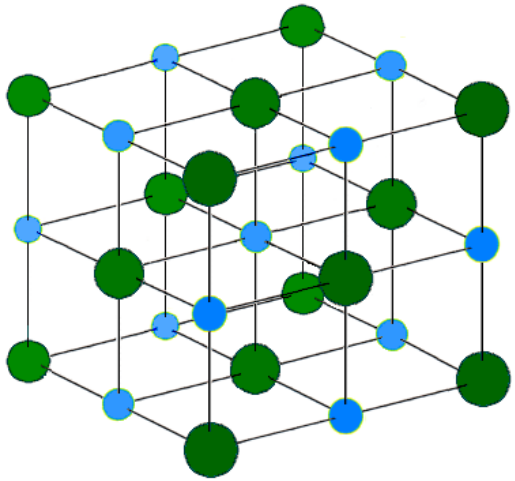

Structure determination
Finding the space group

Reflection Condition(s)		Possible Space Group(s)	
None	→	$P2$ Pm $P2/m$	(3) (6) (10)
$0k0$: $k = 2n$	→	$P2_1$ $P2_1/m$	(4) (11)
$h0l$: $l = 2n$	→	Pc $P2/c$	(7) (13)
$h0l$: $l = 2n$ and $0k0$: $k = 2n$	→	$P2_1/c$	(14)
hkl: $h + k = 2n$	→	$C2$ Cm $C2/m$	(5) (8) (12)
hkl: $h + k = 2n$ and $h0l$: $l = 2n$	→	Cc $C2/c$	(9) (15)

Elettra
Sincrotrone
Trieste

Structure determination
Finding a starting model

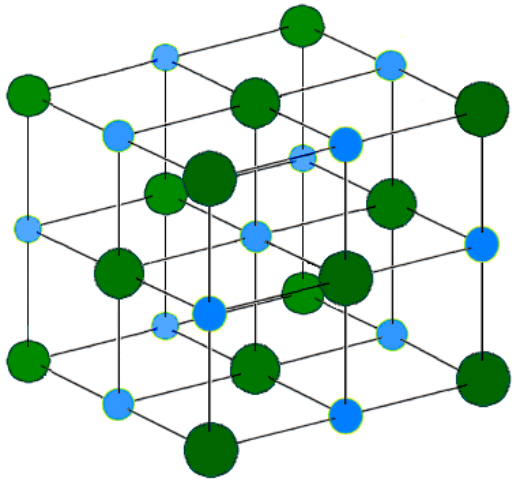

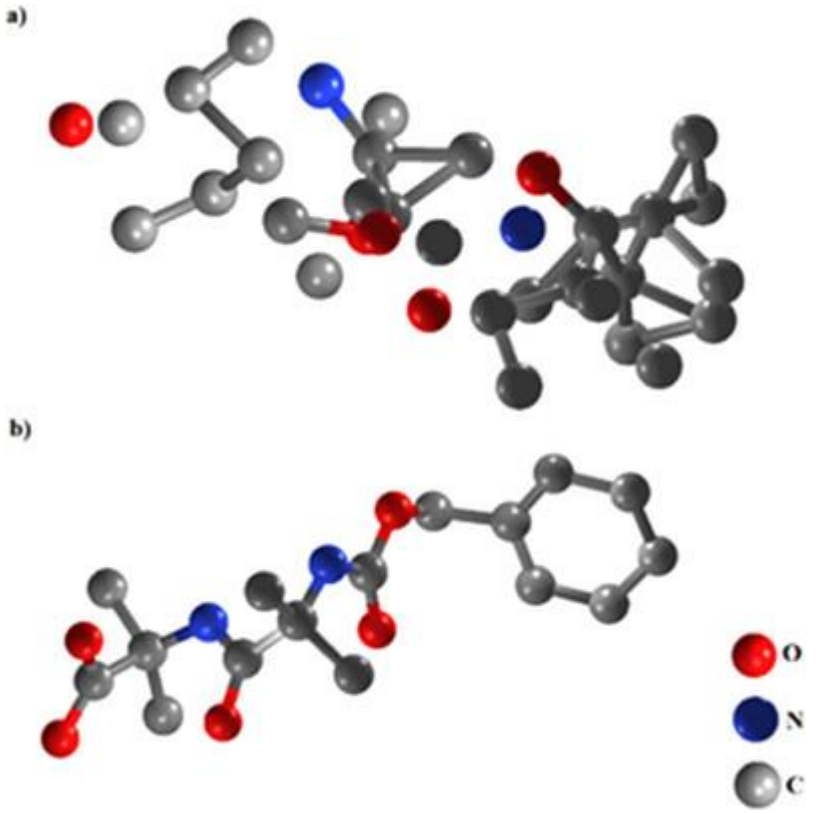

Elettra
Sincrotrone
Trieste

Structure Determination

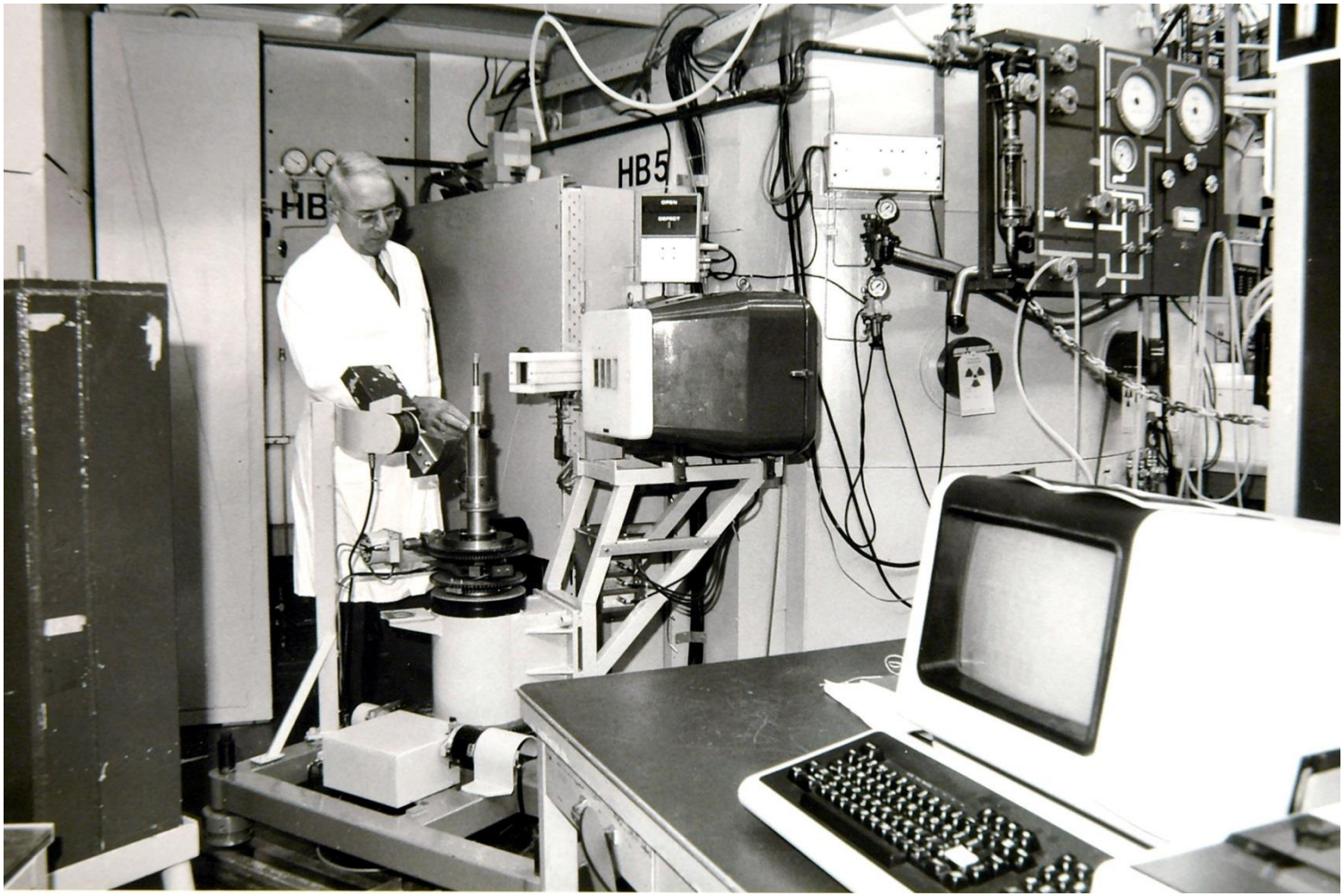

Elettra Sincrotrone Trieste

Structure determination

Parameters refined in Rietveld refinement:

- Background (fixed, functions)
- Peak shape (microstructural parameters, functions)
- Lattice constants – Zero pont correction – Sample displacement
- Scaling – phase fractions
- Structural parameters (Atoms positions, occupancies, B)
- Preferred orientation
- Absorption

Parameters are adjusted, and a diffraction pattern is calculated until the best fit wih the measured pattern is obtained

Elettra Sincrotrone Trieste

Structure determination

$$F(hkl) = \sum_n f_n N_n e^{2\pi i(hx_n + ky_n + lz_n)} e^{-B\sin^2\theta/\lambda}$$

$$I(hkl) \sim |F(hkl)|^2$$

$$y_i = I_k \exp\left[\frac{-4\ln(2)}{H_k^2}(2\theta_i - 2\theta_k)^2\right]$$

$$H_k^2 = U\tan^2\theta_k + V\tan\theta_k + W$$

$$M = \sum_i W_i \left\{ y_i^{obs} - \frac{1}{c} y_i^{calc} \right\}^2$$

Elettra
Sincrotrone
Trieste

Structure determination

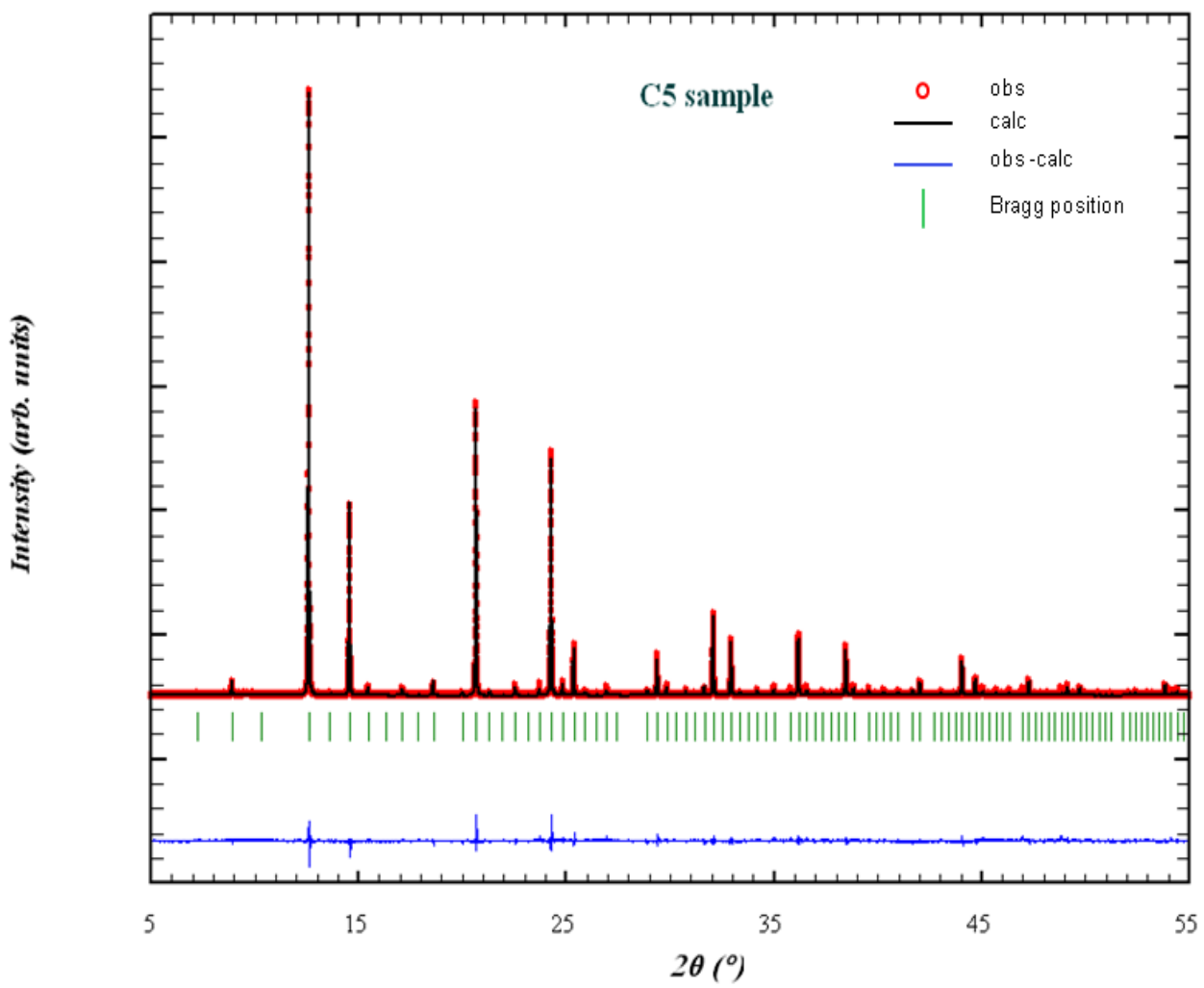

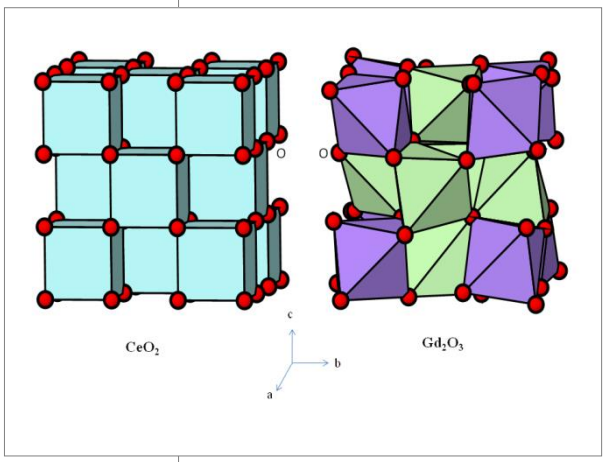

Elettra Sincrotrone Trieste

Information from powder diffraction

- **1895** Rontgen discovered X-rays
- **1912** Laue measured the first diffraction pattern of crystal
- **1913** Braggs published first crystal structures
- **1918** Paul Scherrer published the Scherrer formula to determine the size of nanocrystals

Information from powder diffraction

$$B(2\theta) = \frac{K\lambda}{L\cos\theta}$$

- Peak width (*B*) is inversely proportional to the nanocrystal size *(L).*

P. Scherrer, “Bestimmung der Grösse und der inneren Struktur von Kolloidteilchen mittels Röntgenstrahlen,” *Nachr. Ges. Wiss. Göttingen* **26** (1918) pp 98-100.

Information from powder diffraction

- The shape of the peak give information about the microstructure of the materials

A diffraction peak is a **convolution** ( ) of *profile components* produced by different sources.
These are instrumental factors (IP) and effects due to domain size (S), microstrain (D), faulting (F), anti-phase domain boundaries (APB), stoichiometry fluctuations (C), grain surfacerelaxation (GSR), etc.

$$I(s) = I_{IP}(s) \otimes I_S(s) \otimes I_D(s) \otimes I_F(s) \otimes I_{APB}(s) \otimes I_C(s) \otimes I_{GRS}(s)...$$

Elettra
Sincrotrone
Trieste

Information from powder diffraction

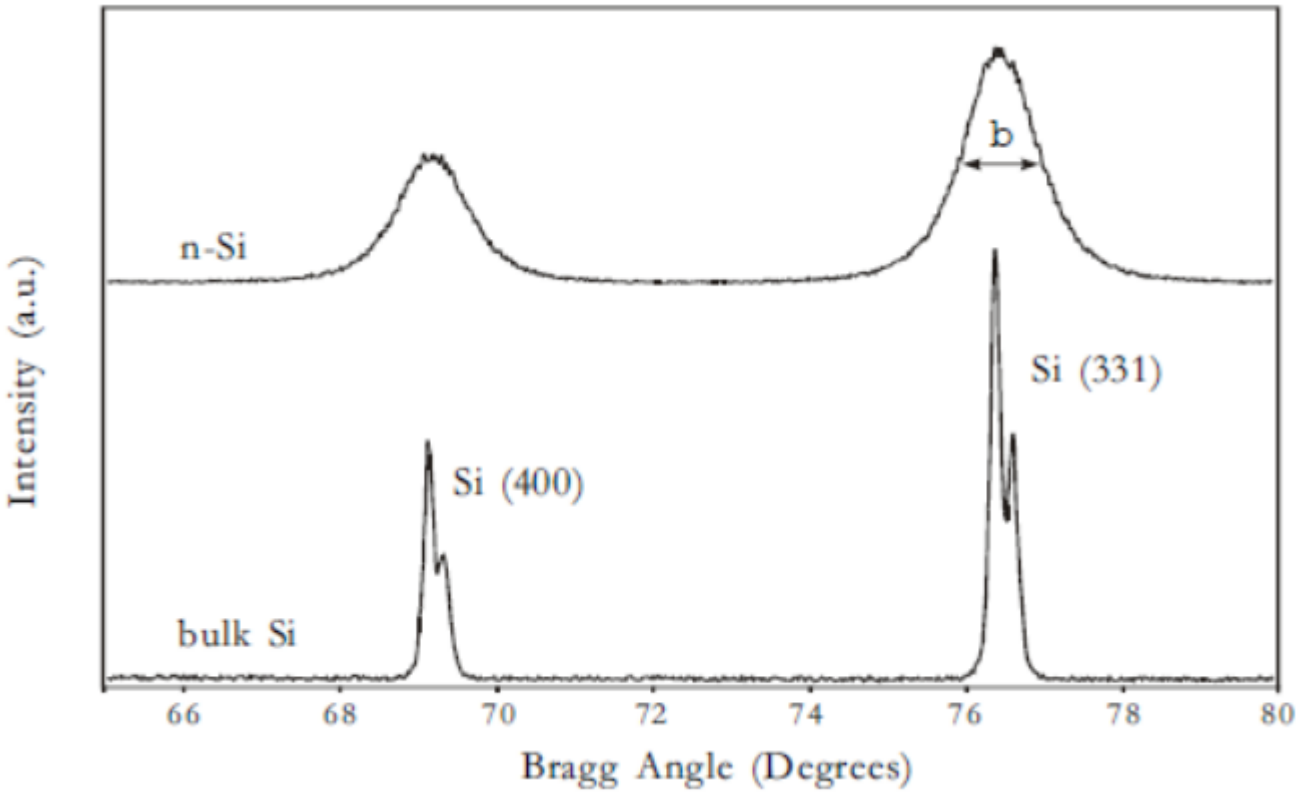

Elettra
Sincrotrone
Trieste

Instrumental profile

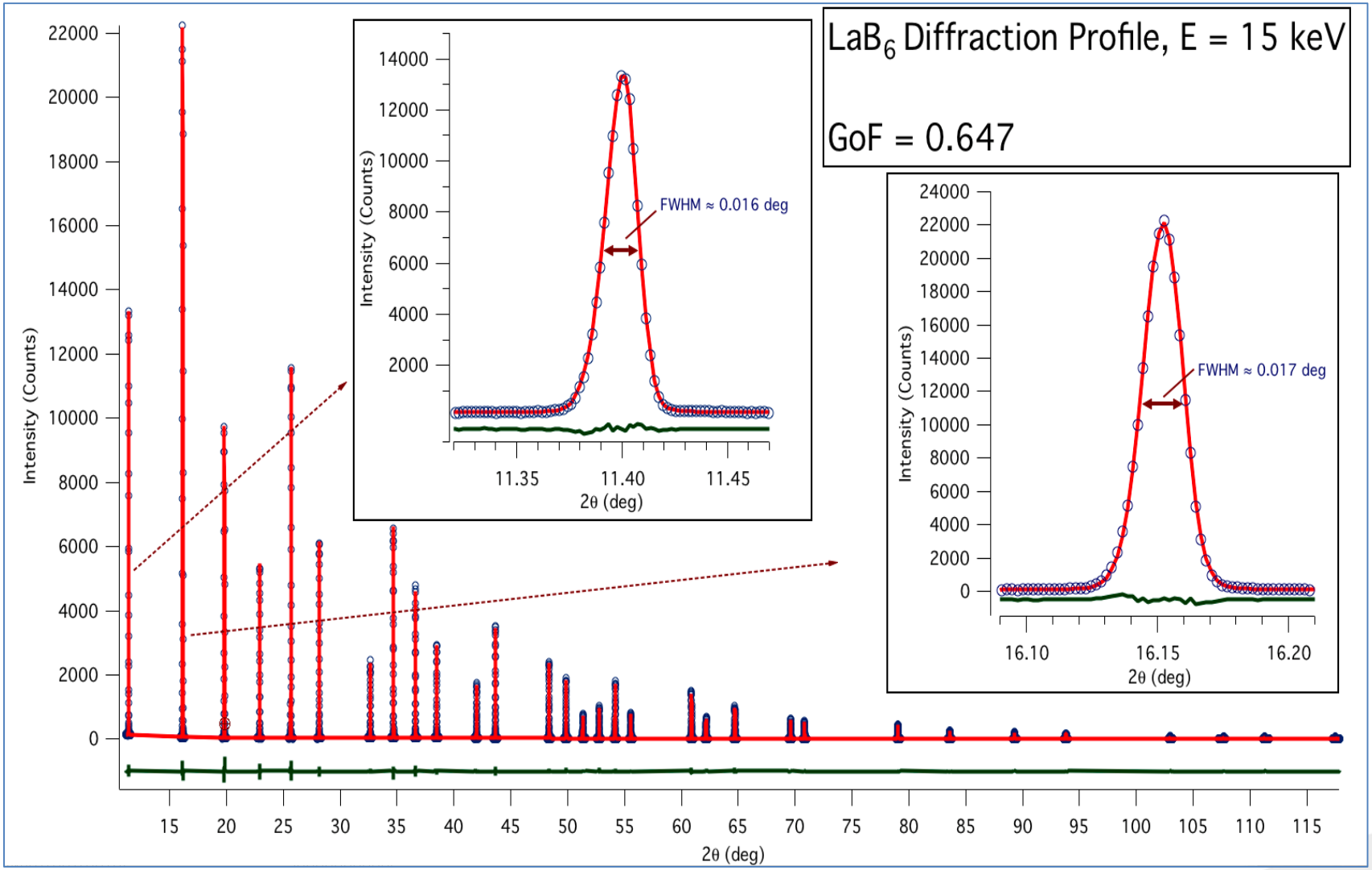

Obtaining information from XRPD

- We want to measure the intensity profile in reciprocal space
  - position of diffraction peaks (d_{hkl})
  - intensity (I_{hkl})
  - peak profile

- **IMPORTANT**: a correct measurement assumes:
  - the homogeneous spatial distribution of the crystallites in the sample
  - the homogeneous probing of the material by the beam
  - the statistically correct measurement of intensity

Elettra
Sincrotrone
Trieste

Texture

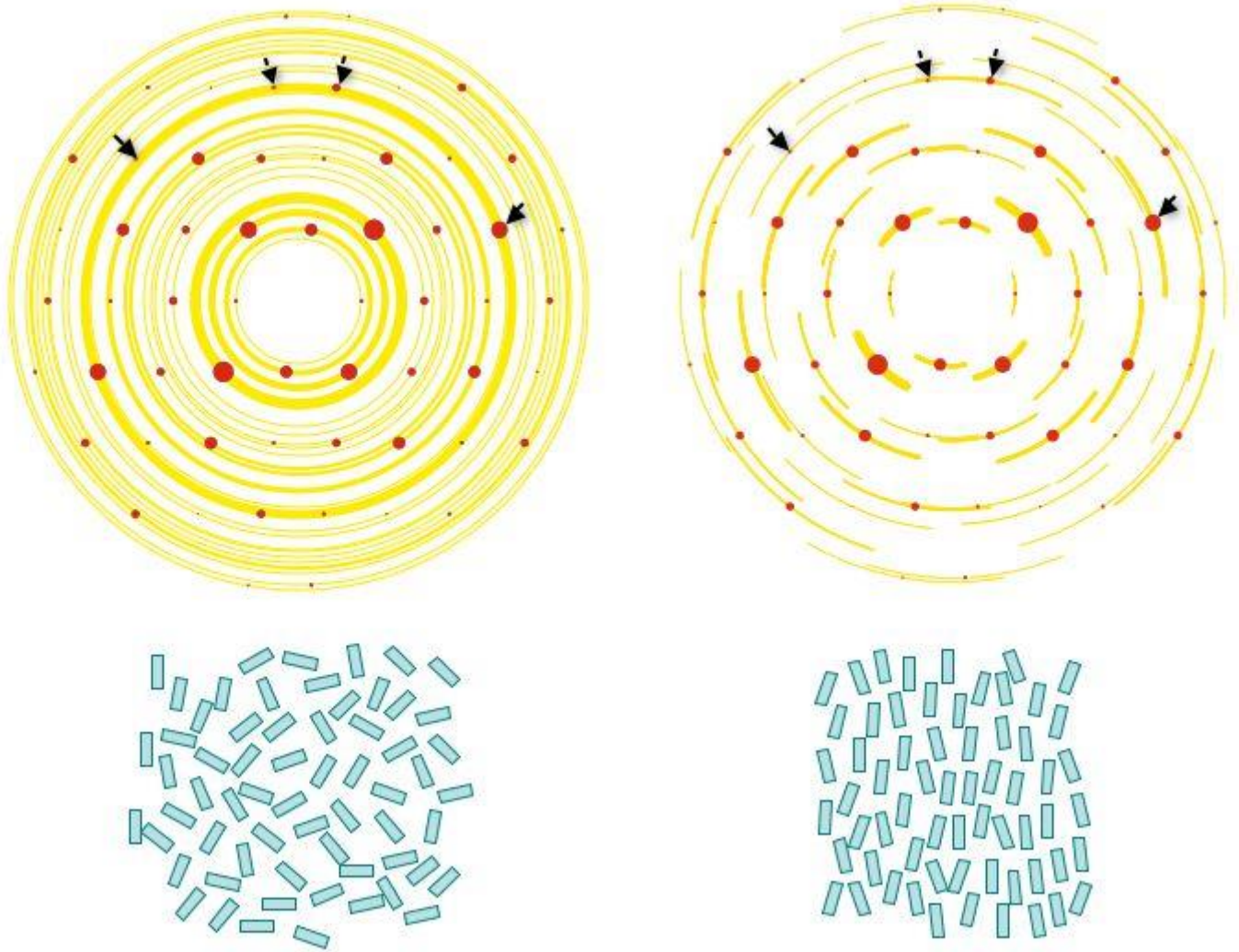

Elettra
Sincrotrone
Trieste

Texture

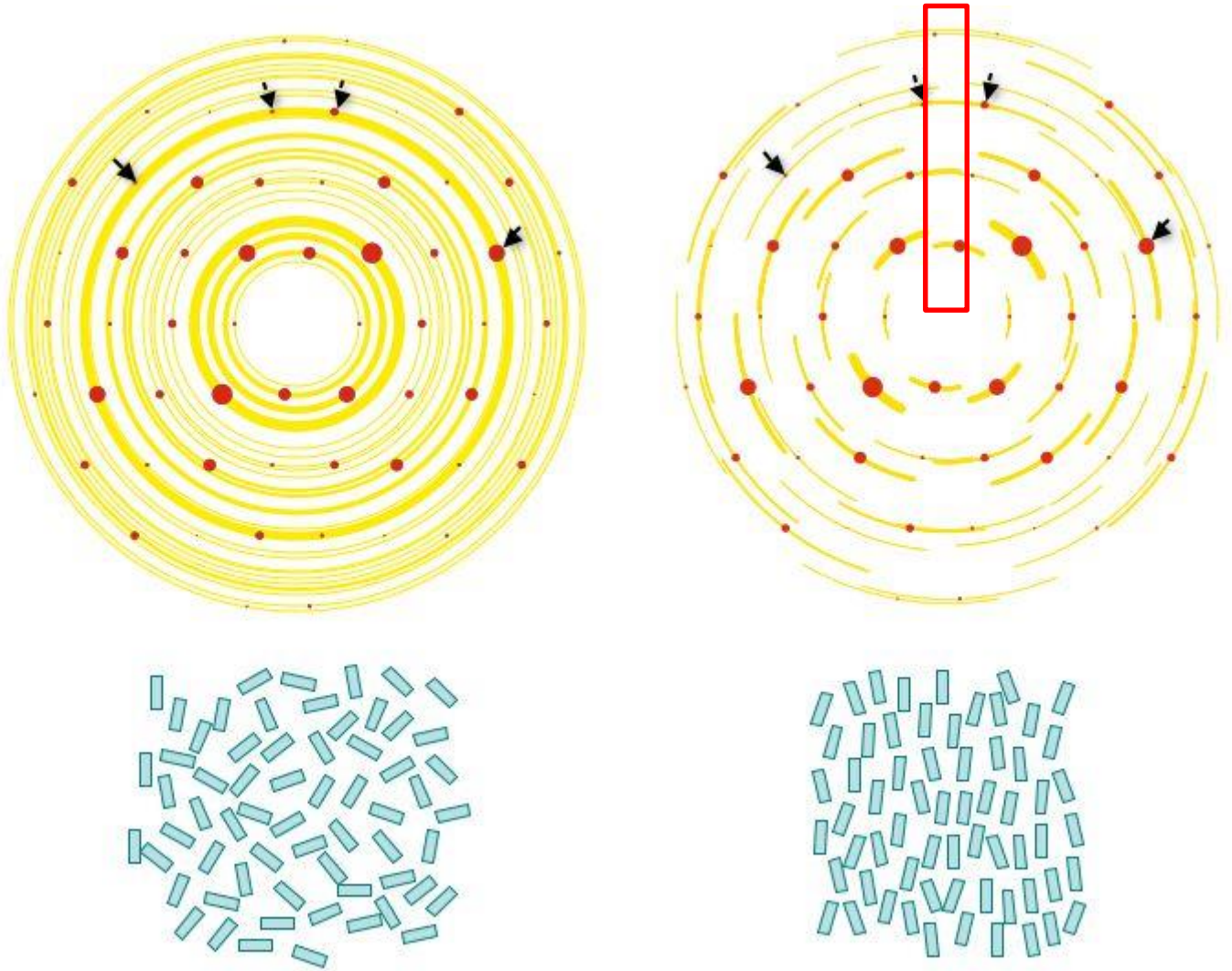

Elettra
Sincrotrone
Trieste

Few cristallites

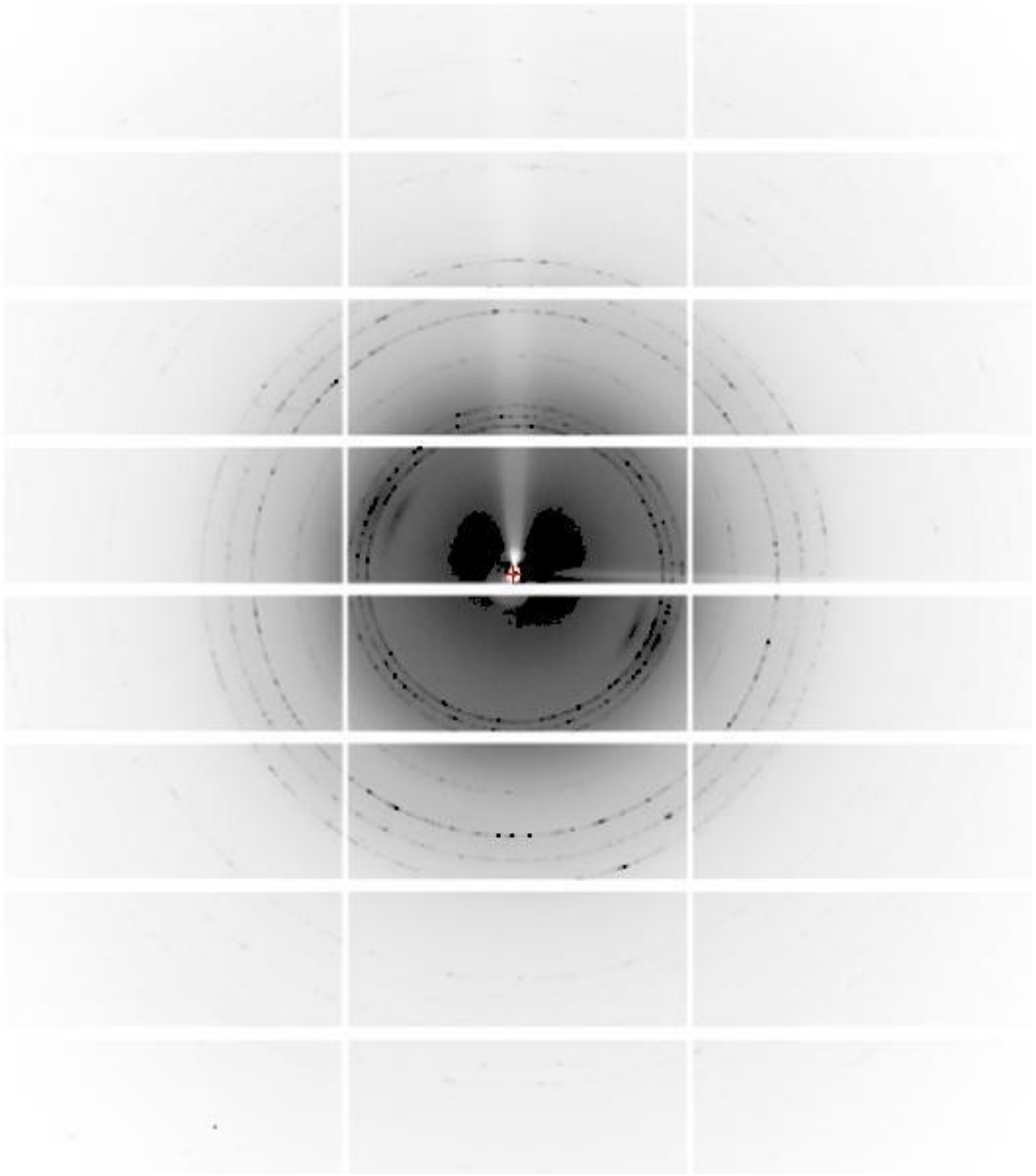

Polarisation

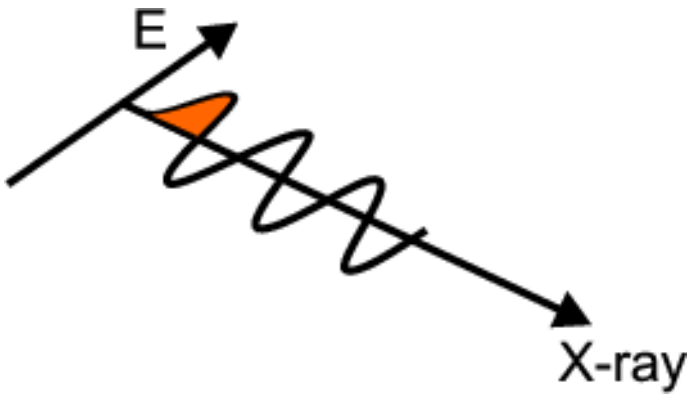

Synchrotron
Radiation is horizontally polarised in the plane of the electron orbit

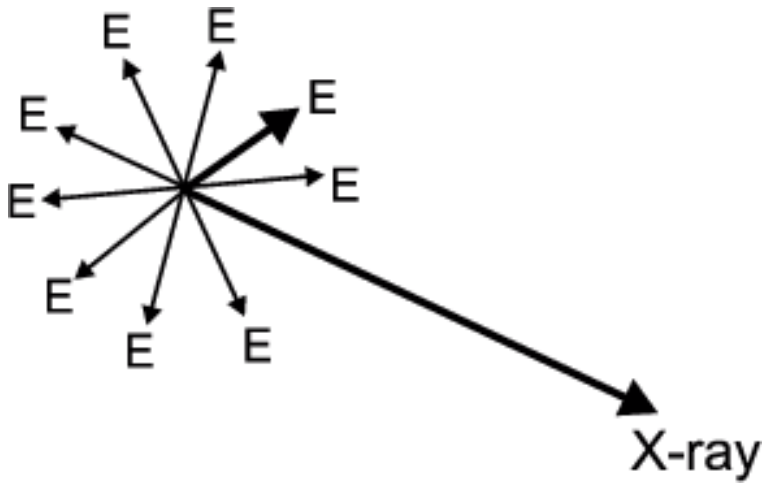

Laboratory source
Unpolarised radiation

Polarisation

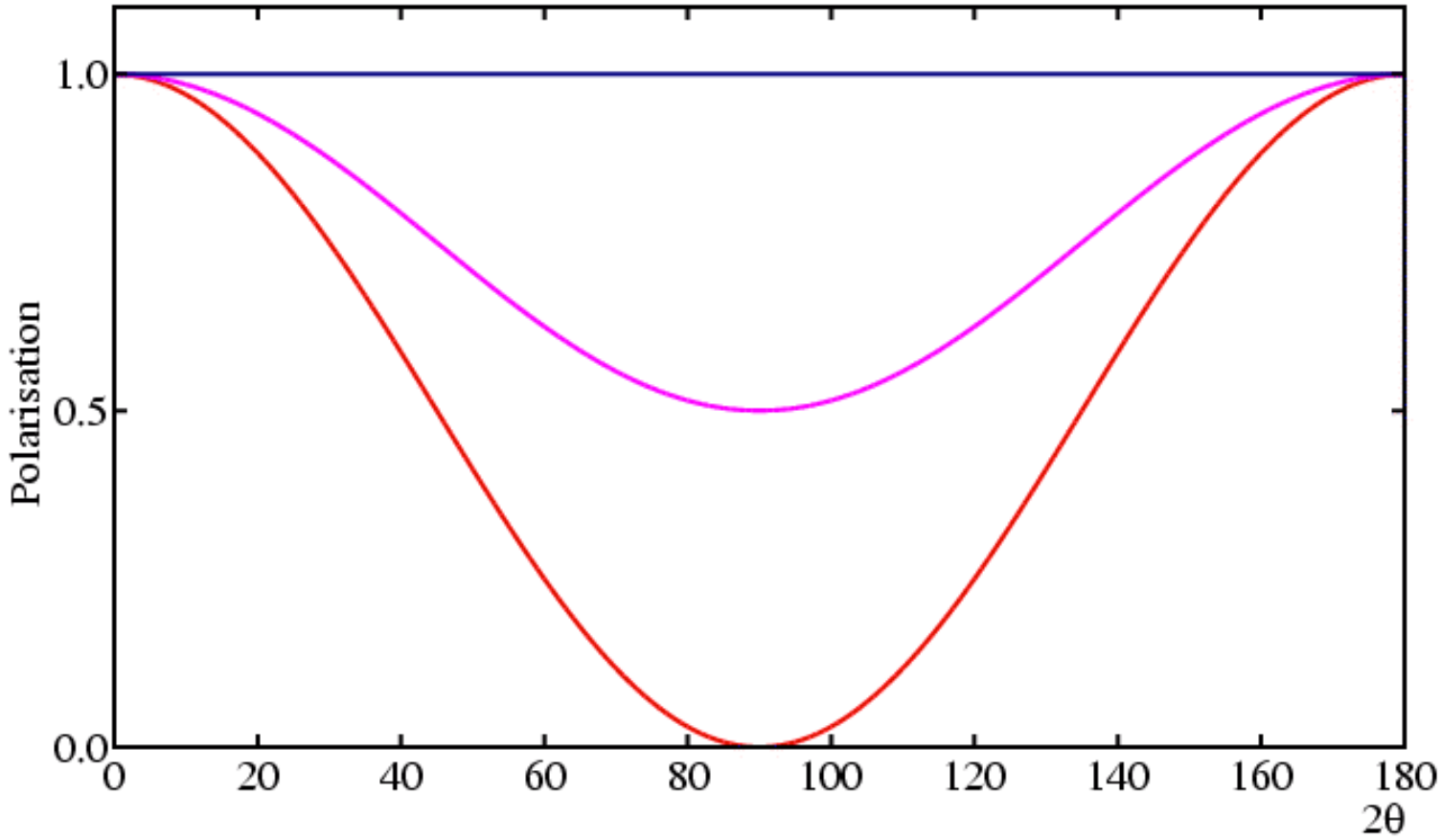

Red: Polarisation in plane of scattering $P = \cos^2 2\theta$

Blue: Polarisation perpendicular to plane of scattering $P = 1$

Pink: Unpolarised X-rays $P = (1 + \cos^2 2\theta)/2$

Elettra
Sincrotrone
Trieste

Polarisation

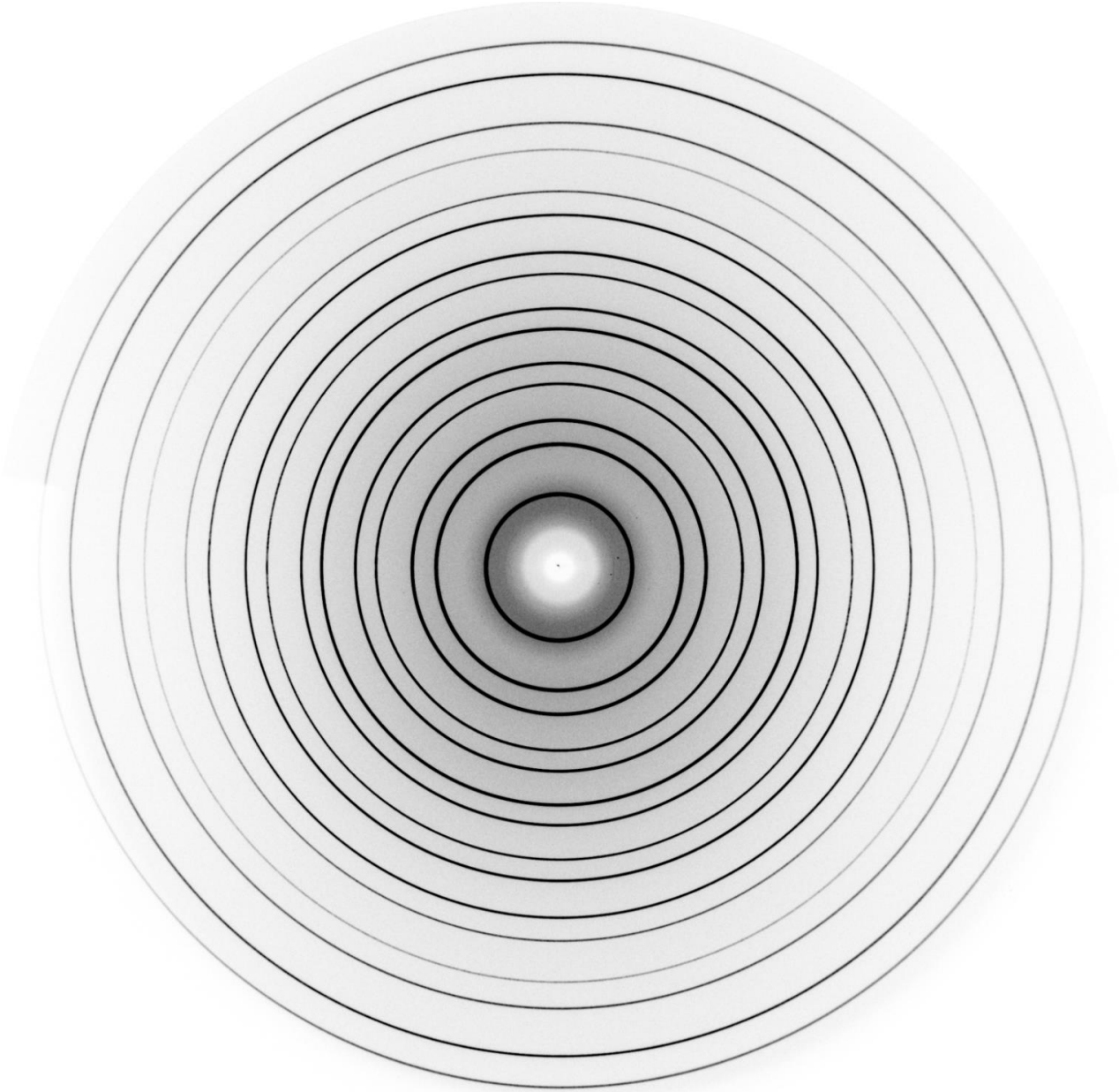

Absorption

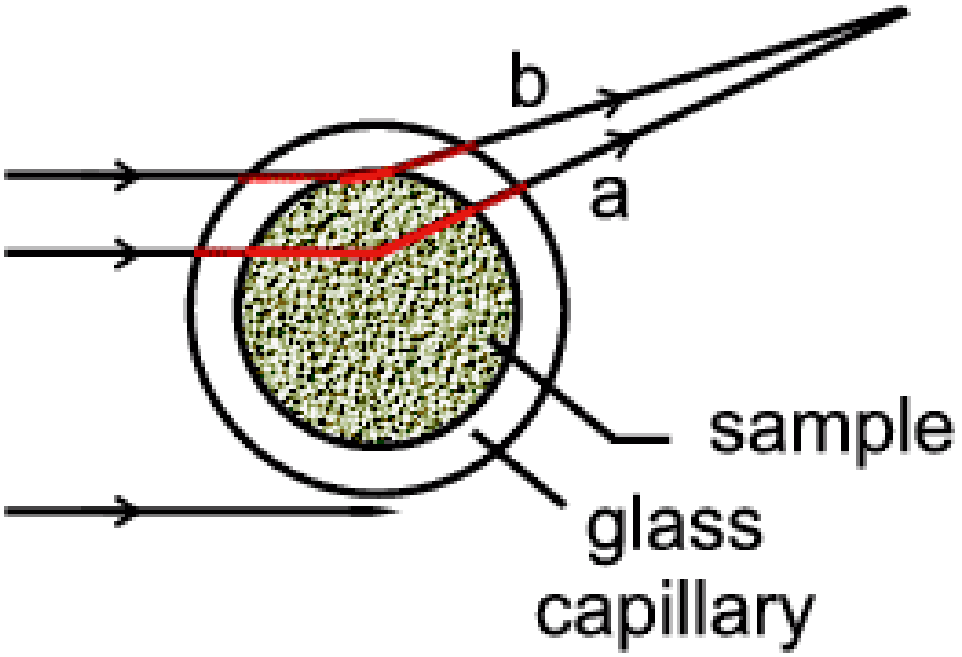

Capillary: The effect is not easy to calculate but the result is satisfying. As the example above illustrates, some paths appear to be like transmission (a) and others like reflection (b). Correction for this effect can be made if the absorption of the sample is not too large.

Elettra
Sincrotrone
Trieste

Absorption

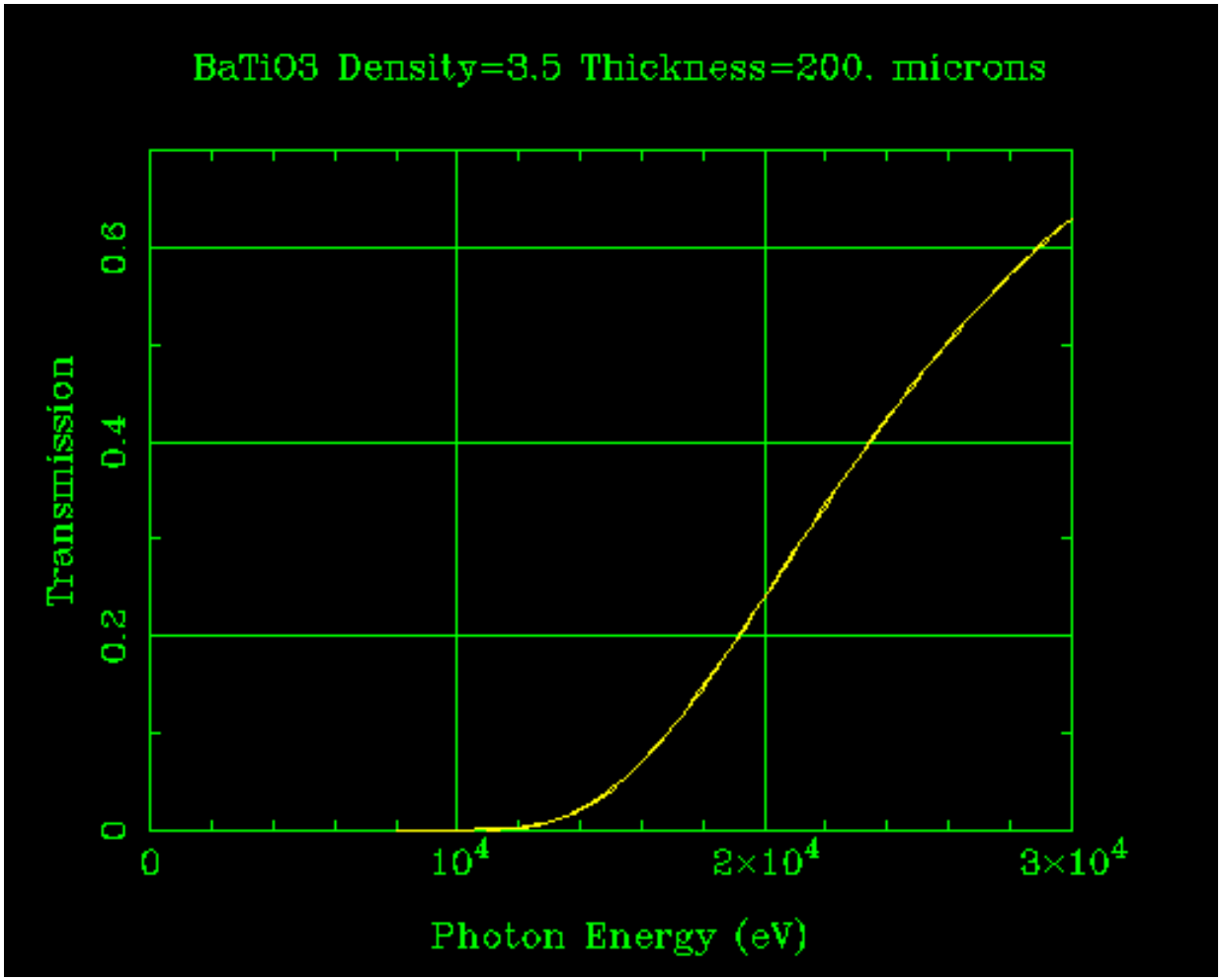

Absorption

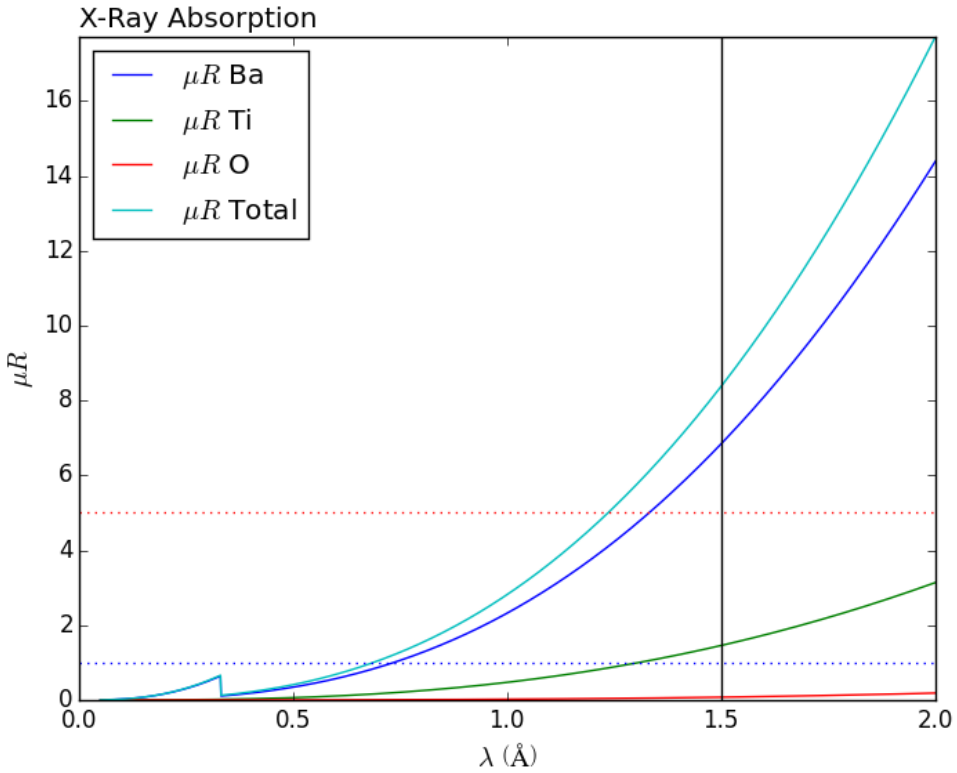

The plot above shows the absorption for each input element and for the specified composition as a function of X-ray wavelength/energy. The blue dotted line indicates a muR value of 1. In a capillary (Debye-Scherrer) geometry, it is ideal when muR is 1 or below, as sample absorption is minimal and no correction is usually needed. The red dotted line indicates a muR value of 5. For muR >= 5, measurements are generally not possible in a capillary geometry, as there will be very severe levels of absorption and corrections are inaccurate. (source: http://11bm.xray.aps.anl.gov/absorb/absorb.php)

Absorption

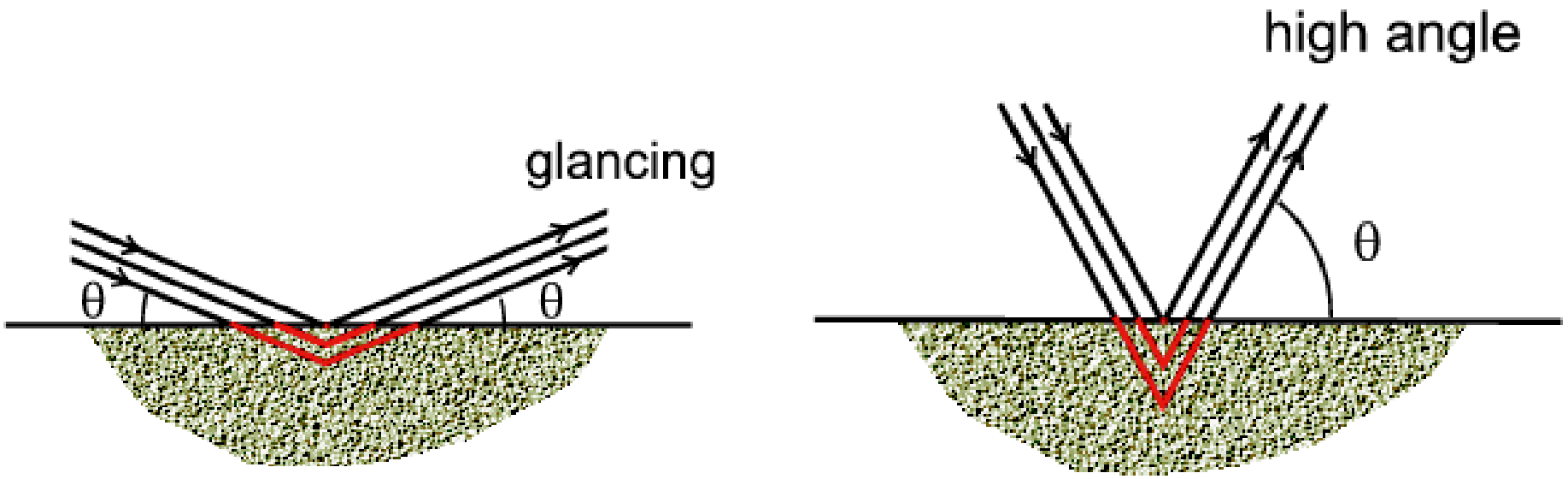

Bragg-Brentano: The effect might not be so obvious how to calculate but result is that when all the possible path lengths are taken in to account, the net absorption remains constant with θ. This means that the effect of absorption can effectively be ignored in this case since it affects all reflections equally. Therefore this geometry may be an alternative when dealing with strongly absorbing samples

Elettra Sincrotrone Trieste

Applications of XRPD

- Phase identification (search match procedures)
- Crystal structure determination (ab initio solution and refinement)
- Quantitative Phase Analysis (QPA)
- Amorphous phase analysis and total Scattering – PDF analysis
- Crystalline domain size/shape and lattice defect analysis (LPA)
- Determination of preferred orientations (Texture Analysis)
- Residual Stress Analysis
- … and more

Phase identification - example

Basilica dei santi Giovanni e Paolo

XIII-XVI century
End XV large stained glass windows

Phase identification - example

Glass samples: Grisaille

- Low melting glass (SiO_2, PbO,)
- Pigment (metal oxides)
- Paint medium (water, vinegar, oil)
- Firing to fuse the grisaille on the glass

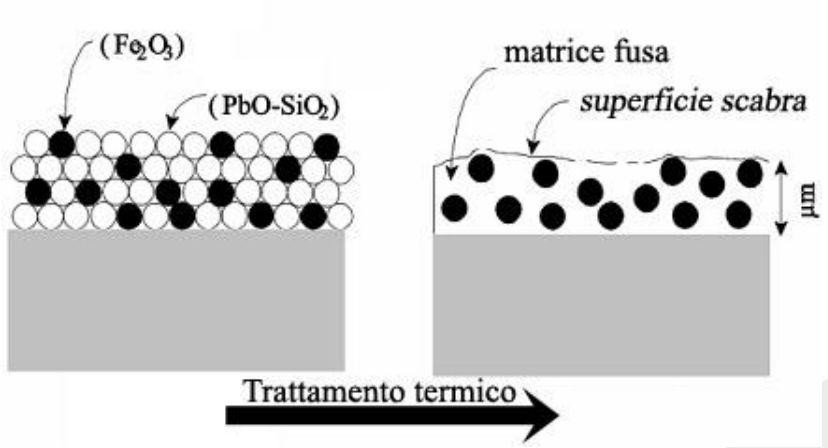

Phase identification - example

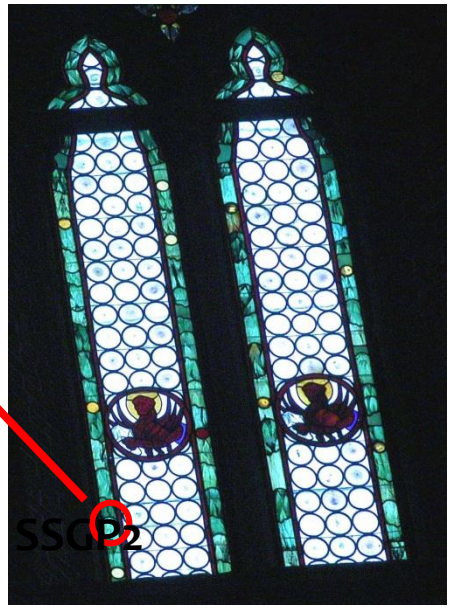

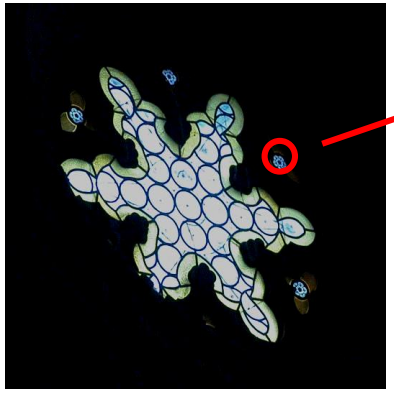

Phase identification - example

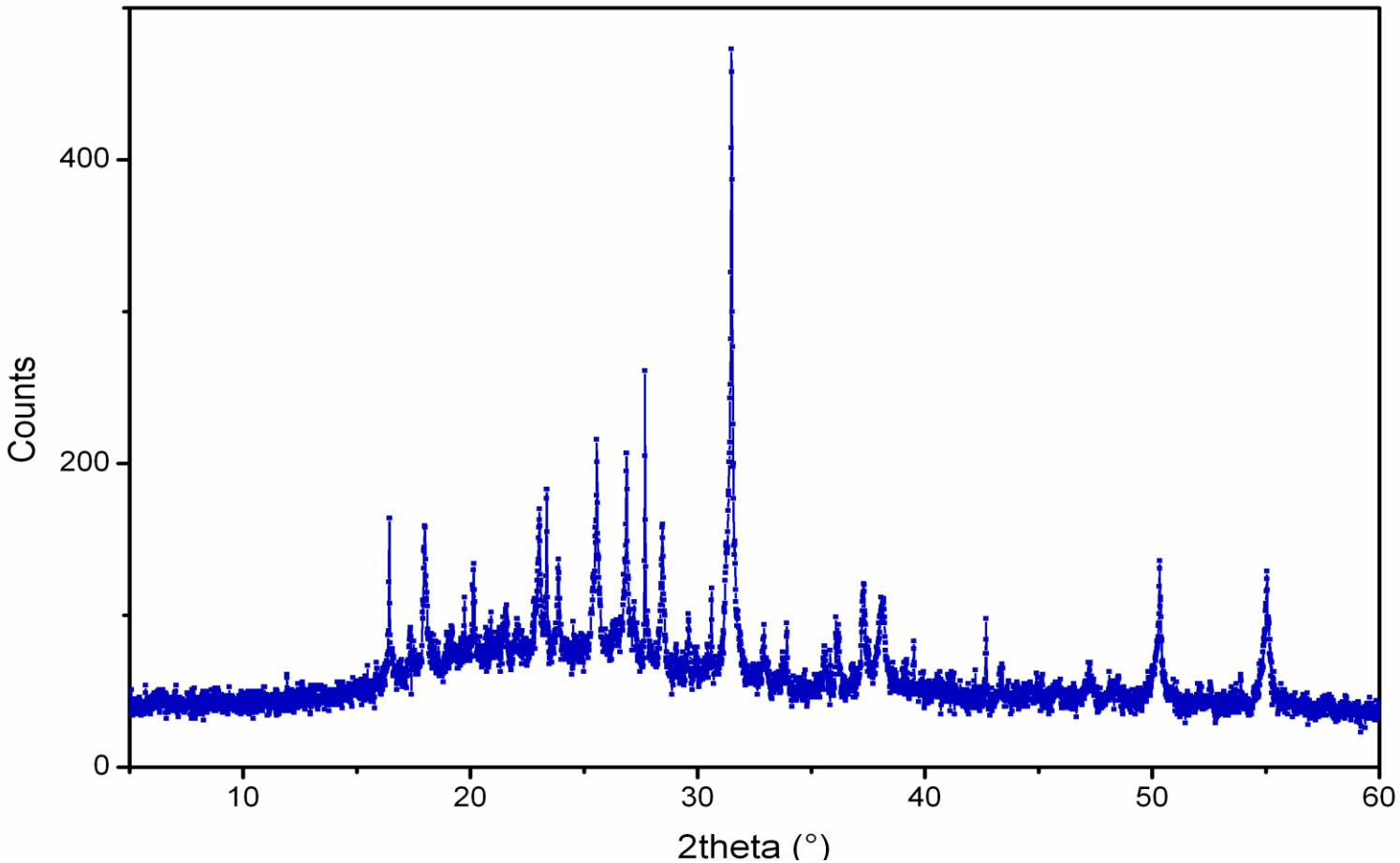

E = 9.4 keV
λ = 1.319Å

Phase identification - example

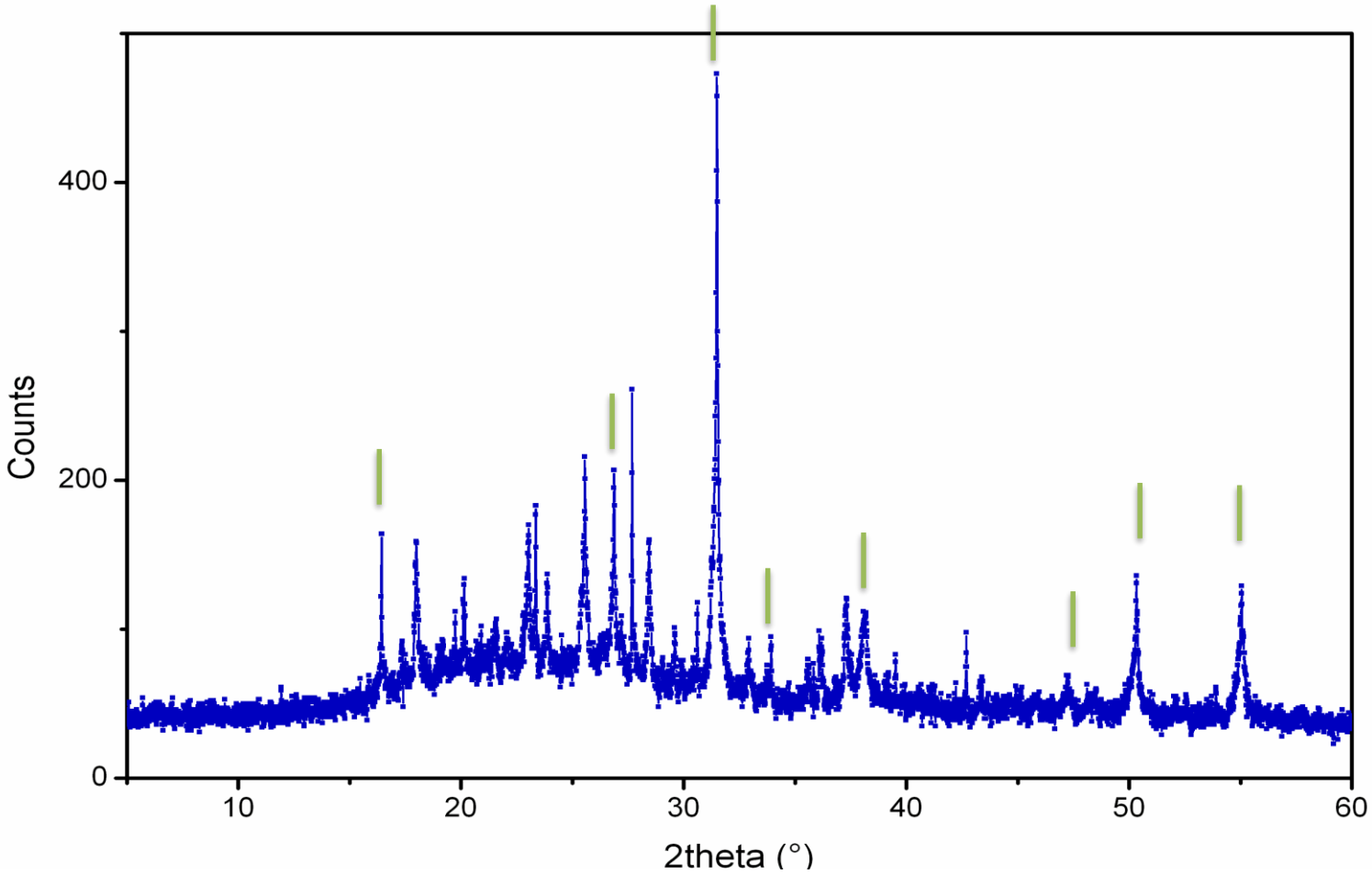

Spinel
$CoAl_2O_4$
01-082-2422

Phase identification - example

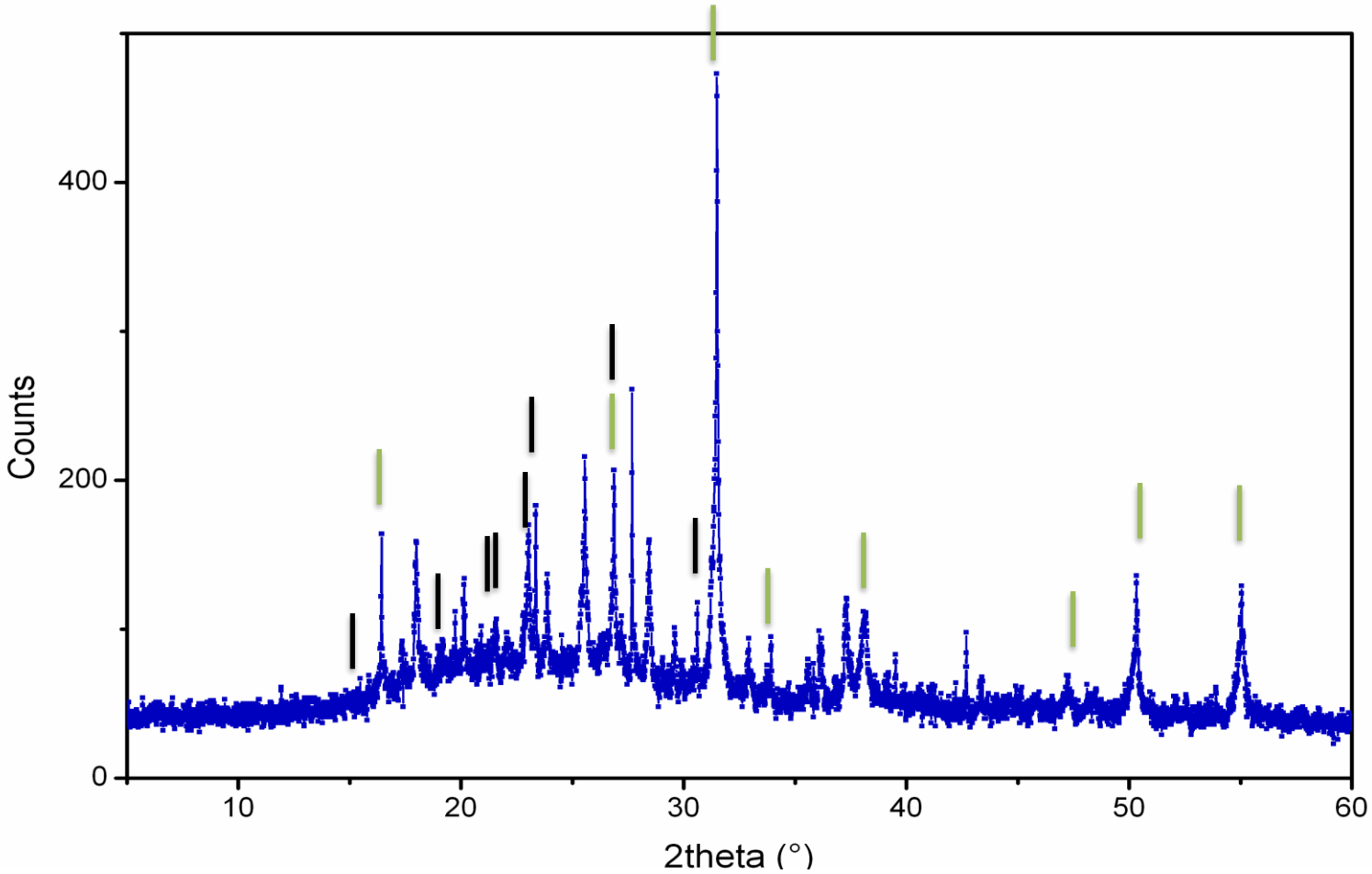

Spinel
$CoAl_2O_4$
01-082-2422

Laurionite
PbCl(OH)
04-012-3672

Phase identification - example

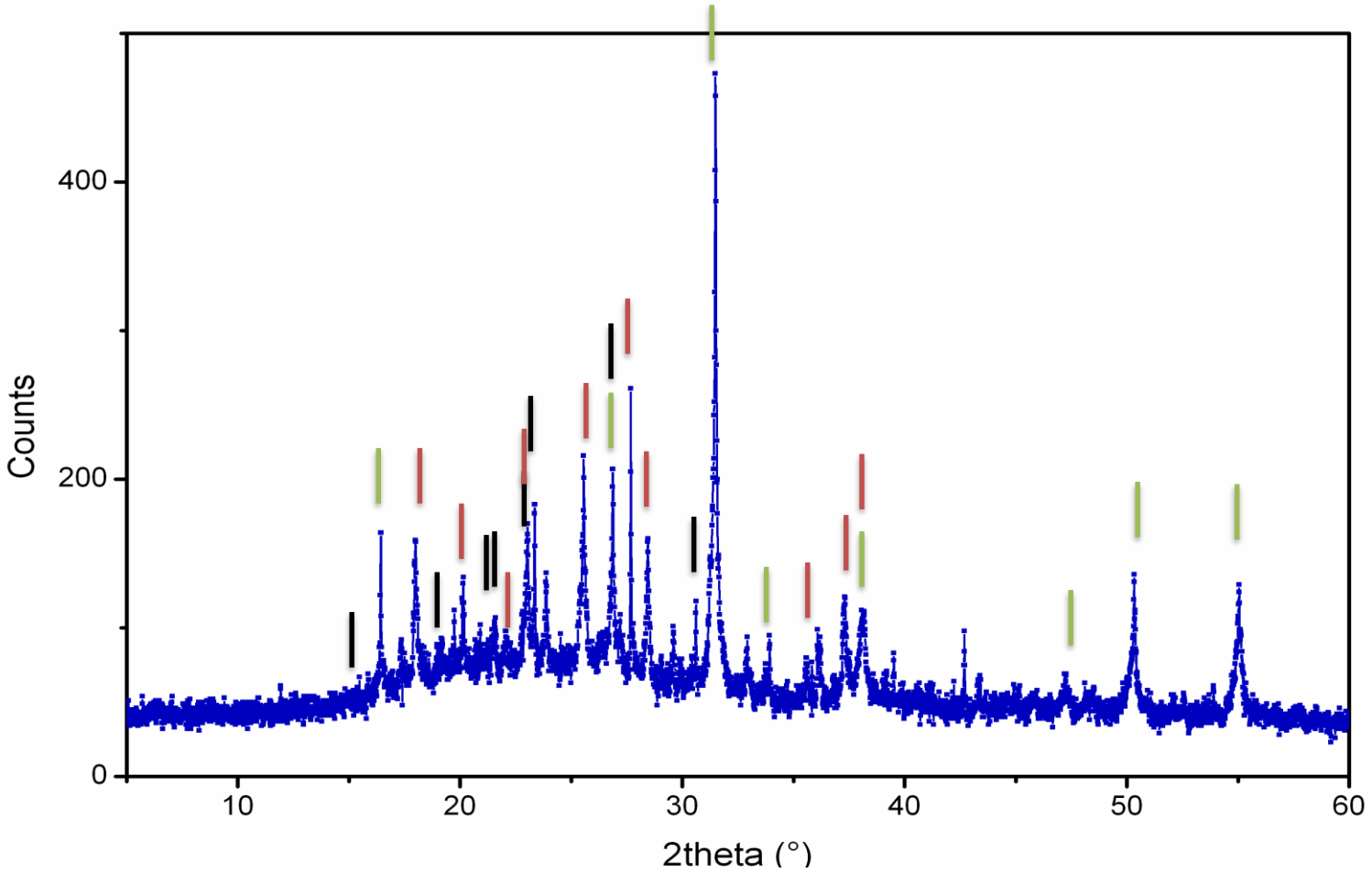

Spinel
$CoAl_2O_4$
01-082-2422

Laurionite
PbCl(OH)
04-012-3672

Anglesite
$PbSO_4$
04-008-8386

Phase identification - example

	GRISAGLIA	PATINA
	$CoAl_2O_4$; $PbSO_4$; $Pb(OH)Cl$	Amorphous
	$Pb_2Sb_2O_7$; $PbSO_4$; $CaSO_4(H_2O)_2$; $CaAl_2Si_2O_8$	$FeO(OH)$; $FeSO_4(OH)(H_2O)_2$ $PbSO_4$; $CaSO_4(H_2O)_2$; $Al_2Si_2O_5(OH)_4$
	$CoAl_2O_4$; $PbSO_4$; $CaPO_3(OH)_2H_2O$	SiO_2; PbS; $PbSO_4$; $CaCO_3$ (vat), $CaPO_3(OH)_2H_2O$

Phase identification - example

- **$Pb_2Sb_2O_7$** : original pigment
- **SO_4^{2-}, S^{2-}, CO_3^{2-}** : alteration product seawater-aerosol , acid rain
- **FeO(OH); $FeSO_4(OH)(H_2O)_2$** : alteration product of original pigments
- **CO_3^{2-},PO_3^{3-}**: biological origin
- **$CoAl_2O_4$** : intervention at later date?

Elettra
Sincrotrone
Trieste

XRPD in non ambient conditions

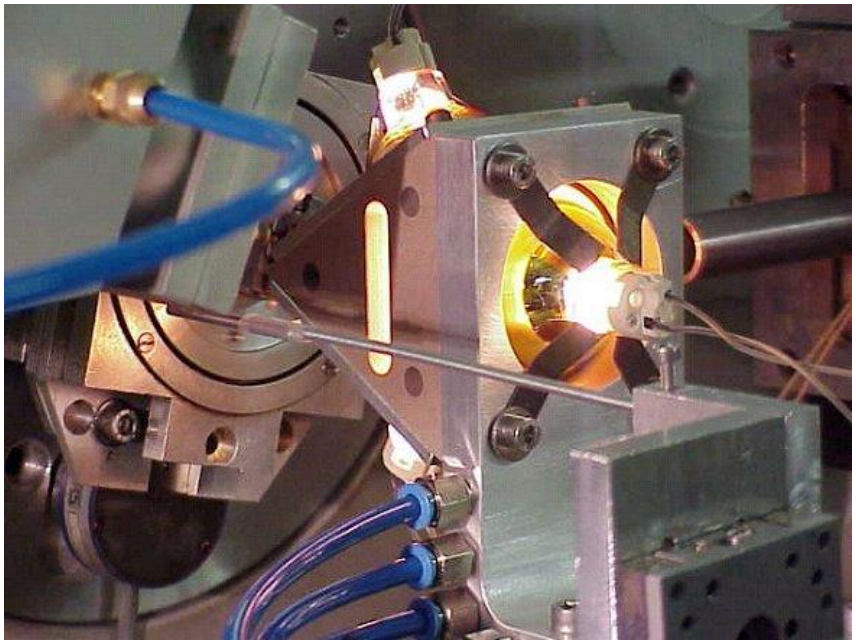

Elettra
Sincrotrone
Trieste

XRPD in non ambient conditions

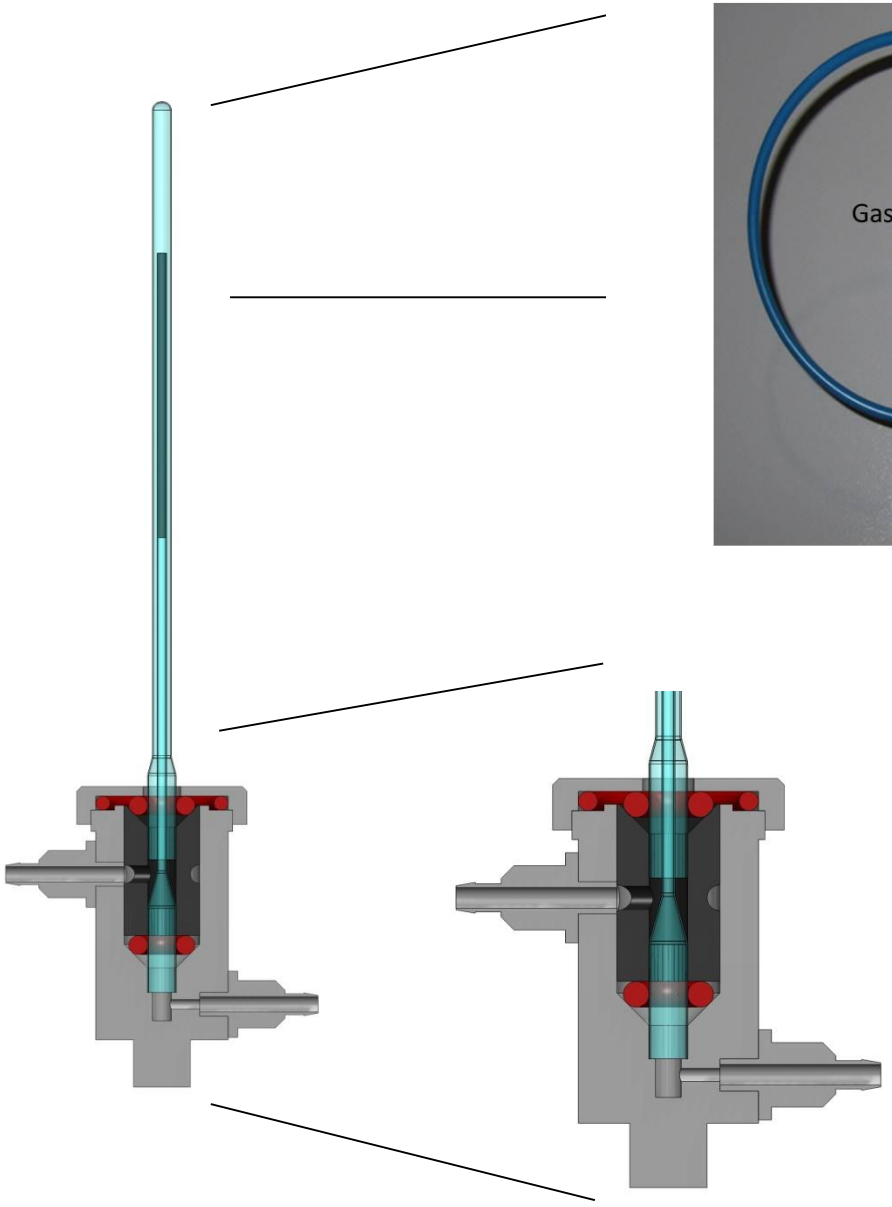

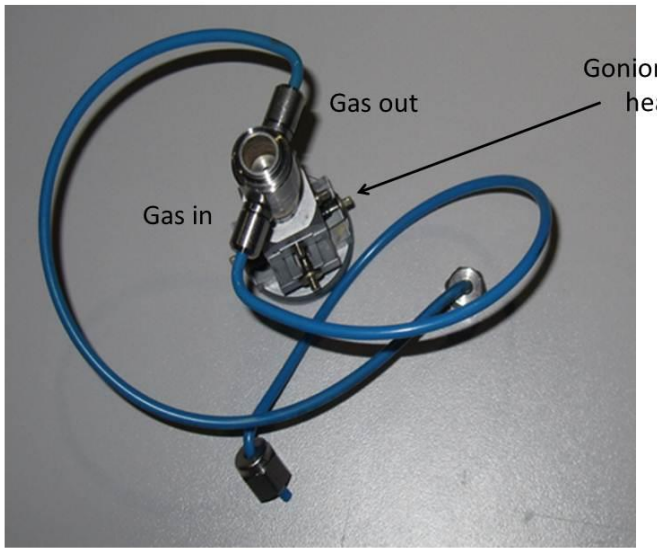

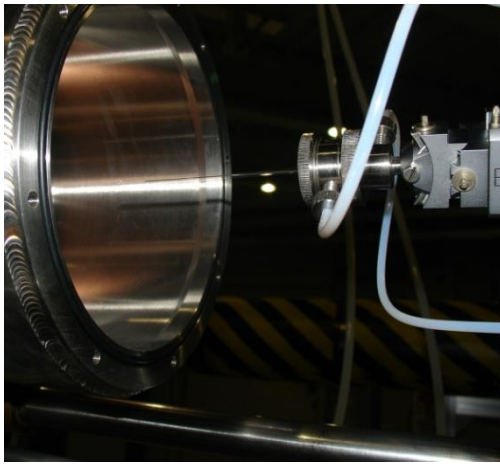

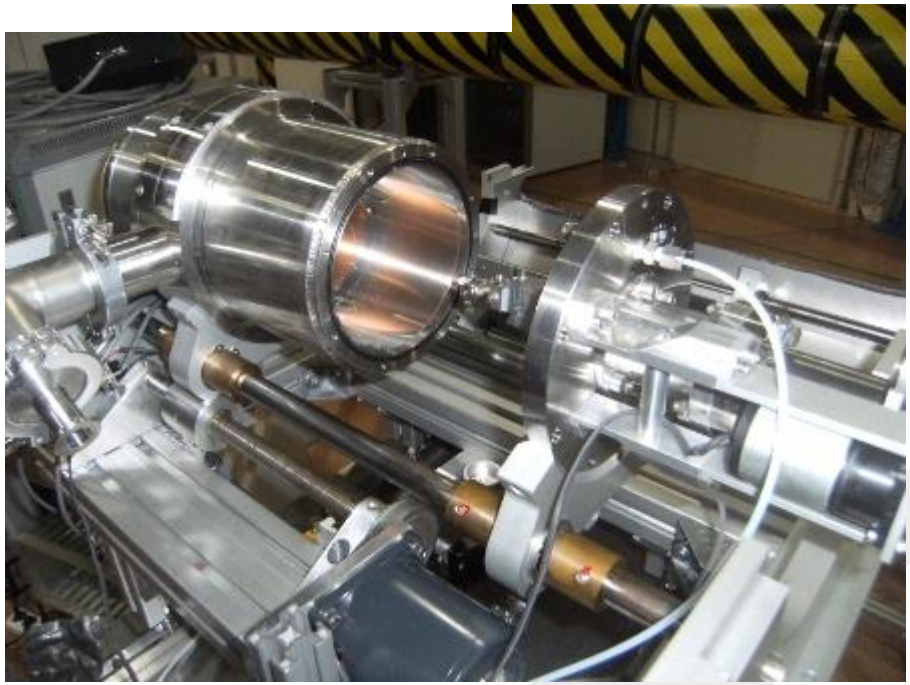

Elettra
Sincrotrone
Trieste

Furnace Design

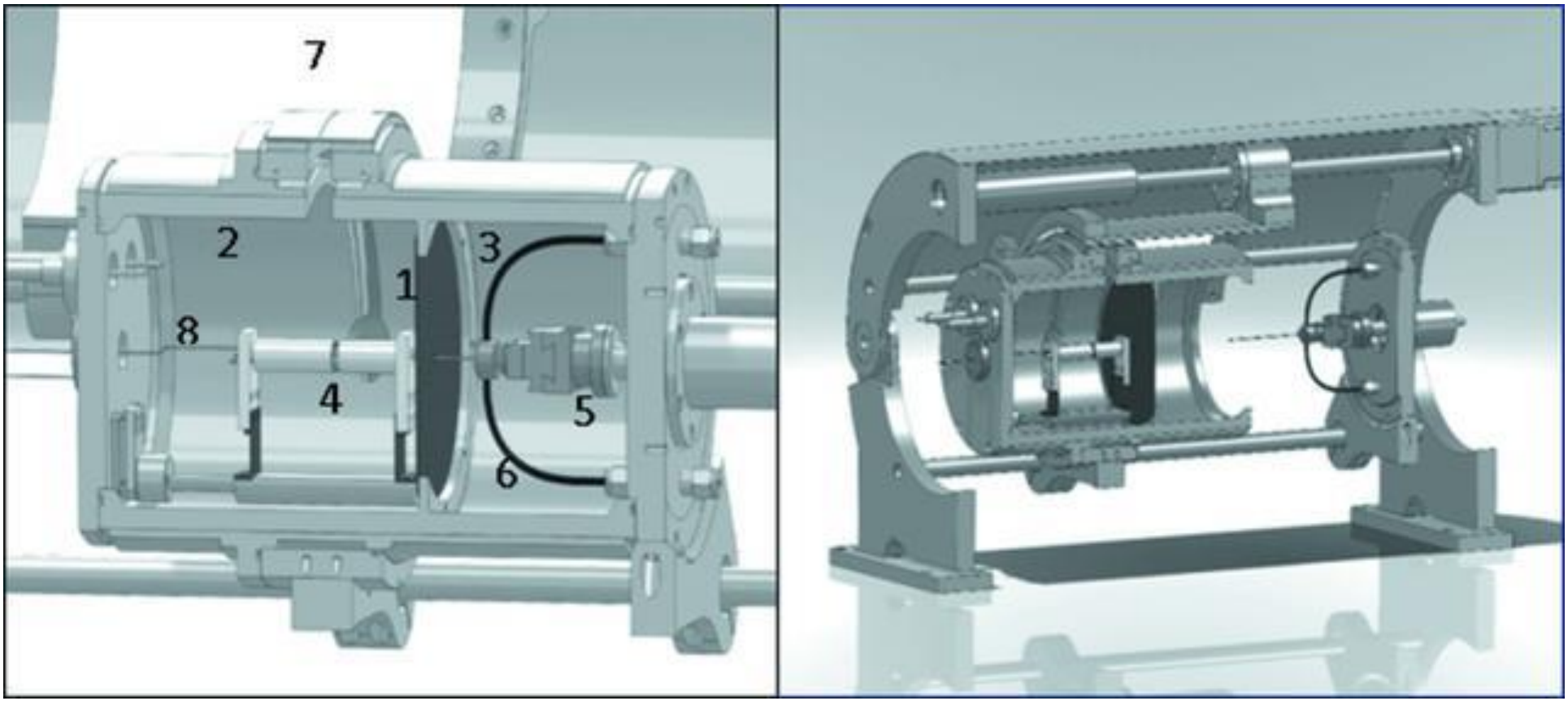

In situ reaction furnace for real-time XRD studies
Riello P., Lausi A., MacLeod J., Plaisier J.R., Zerauschek G., Fornasiero P.
Journal of Synchrotron Radiation, Vol. 20 - 1, pp. 194-196 (2013)

XRPD in non ambient conditions

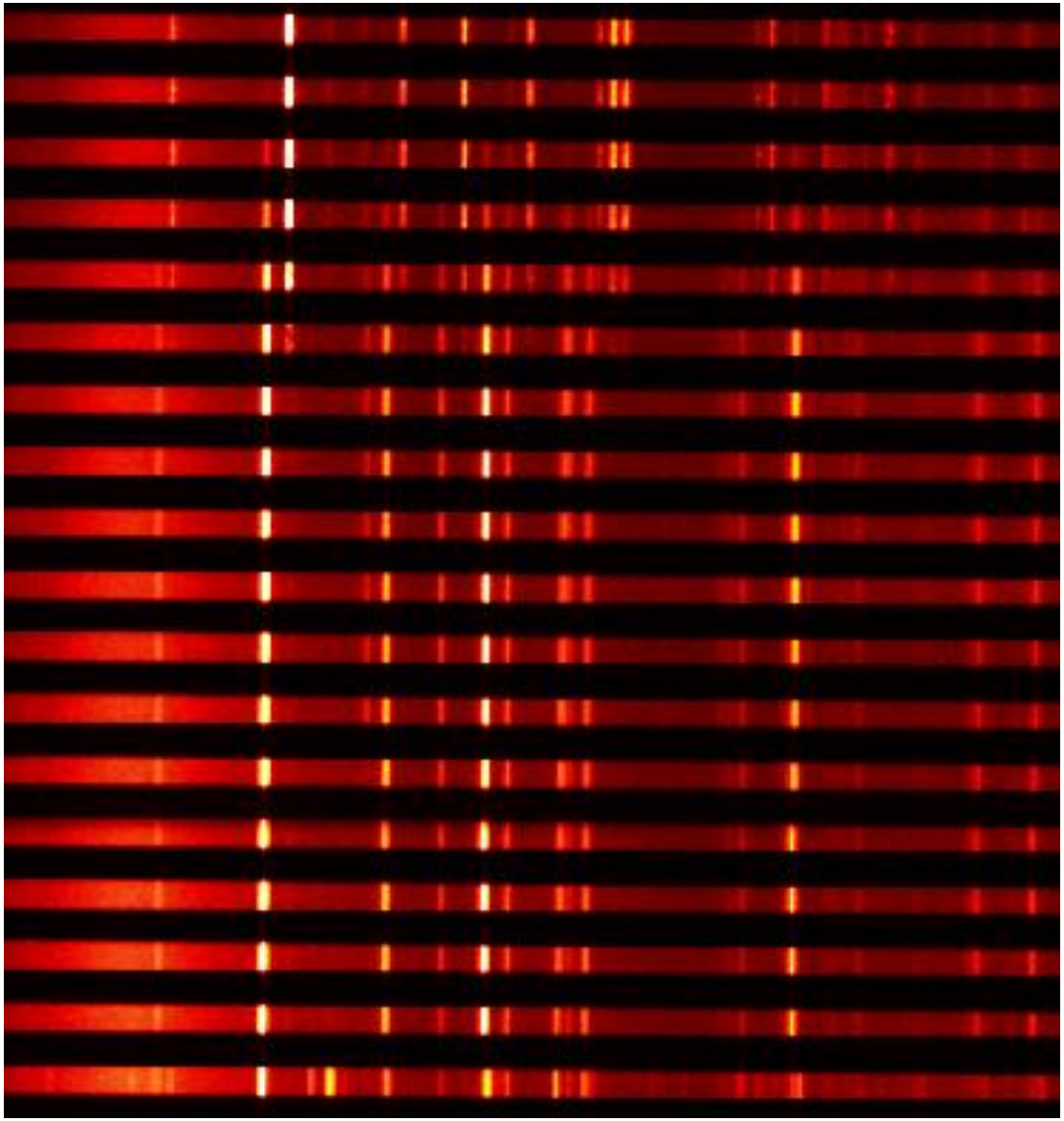

600 °C

800°C

1000 °C

XRPD in non ambient conditions

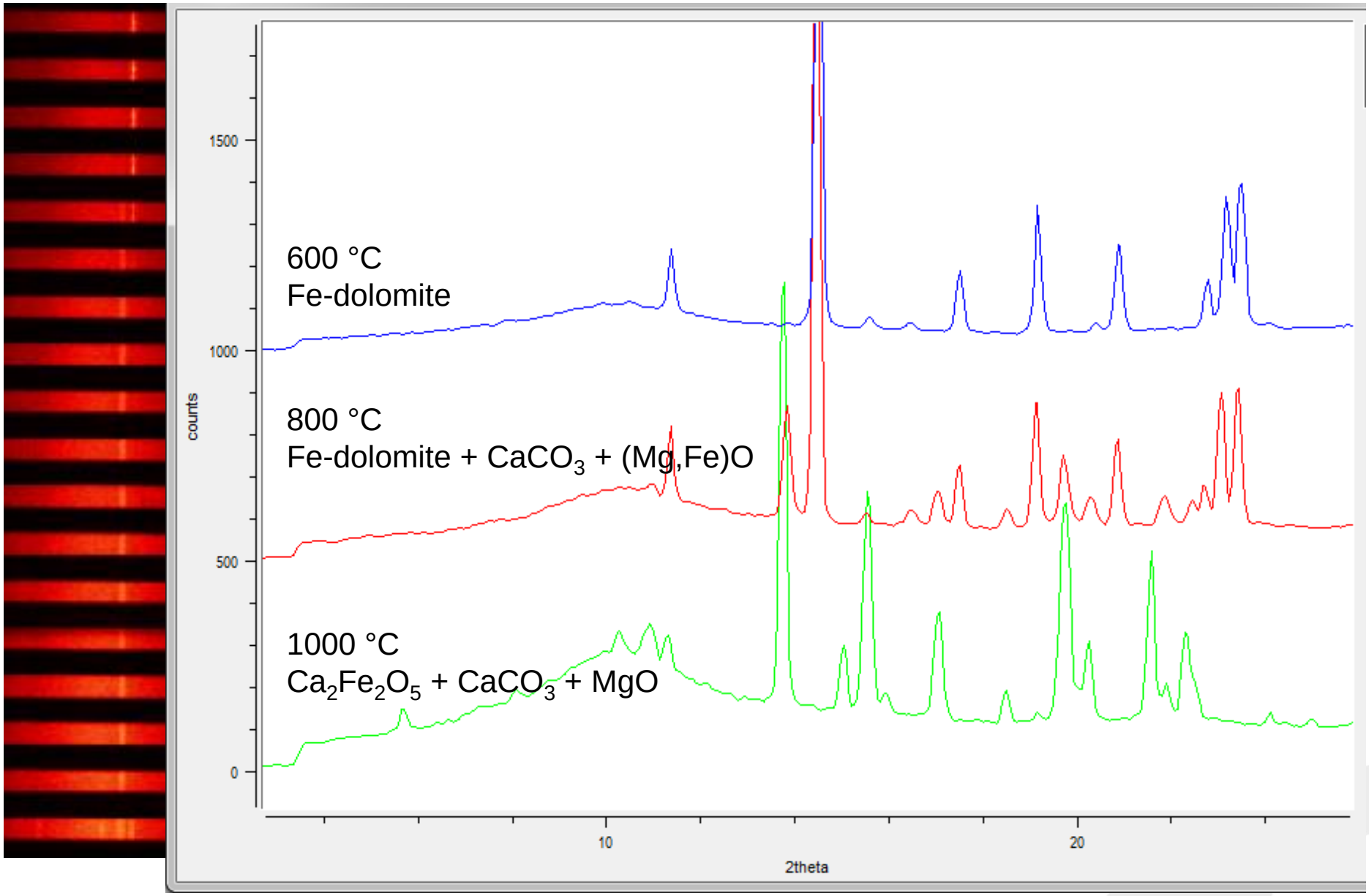

Elettra Sincrotrone Trieste

2D-3D transition In $Cu–TiS_2$ system

- Phase transitions between 2D (layered) and 3D (cubic) phases in Cu_xTiS_2 (x = 0-0.5) intercalation compounds have been studied ***in situ*** by the X-ray diffraction technique in the temperature range 20–1000 °C.

- The discovery of CDW (charge density wave) quantum states and superconductivity in the $Cu–TiSe_2$ system arouses interest to isostructural materials, but known phase transformations to the spinel structure make comparison difficult.

- Samples were prepared by intercalation of Cu at room temperature. All samples had the layered hexagonal structure.

2D-3D transition in $Cu–TiS_2$ system
Shkvarina EG, Titov AA, Doroschek AA, Shkvarin AS, Starichenko DV, Plaisier JR, Gigli L, Titov AN.
The Journal of Chemical Physics 147, 044712 (2017)

Elettra
Sincrotrone
Trieste

2D-3D transition
In Cu–TiS_2 system

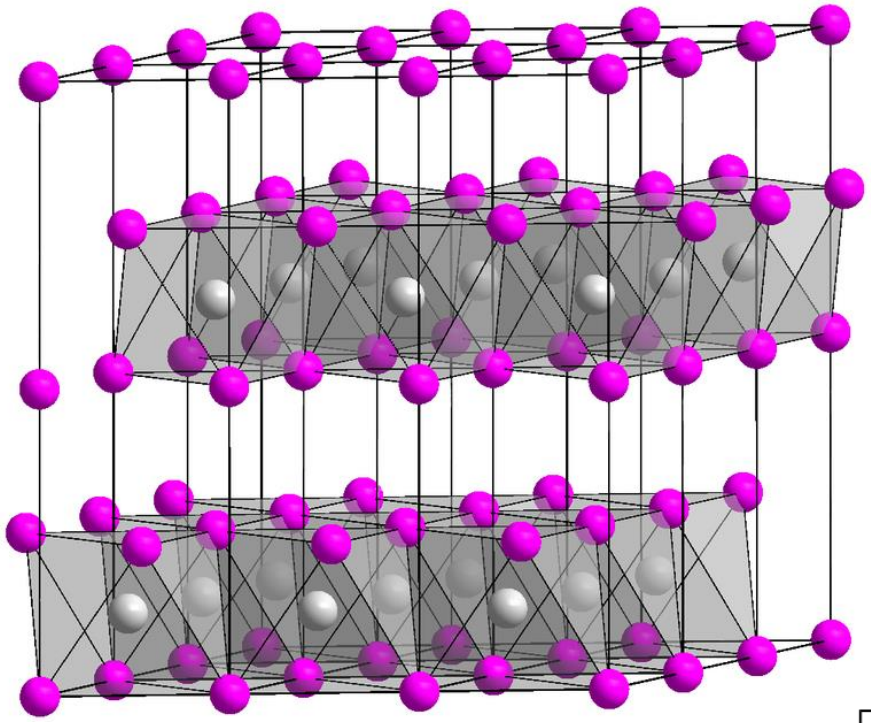

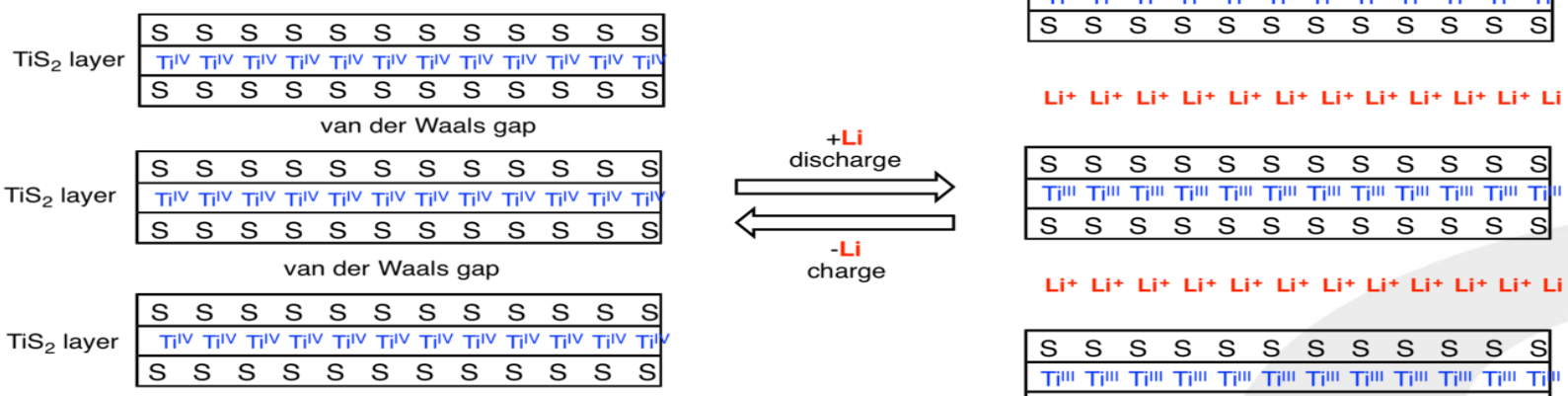

Elettra
Sincrotrone
Trieste

2D-3D transition
In Cu–TiS_2 system

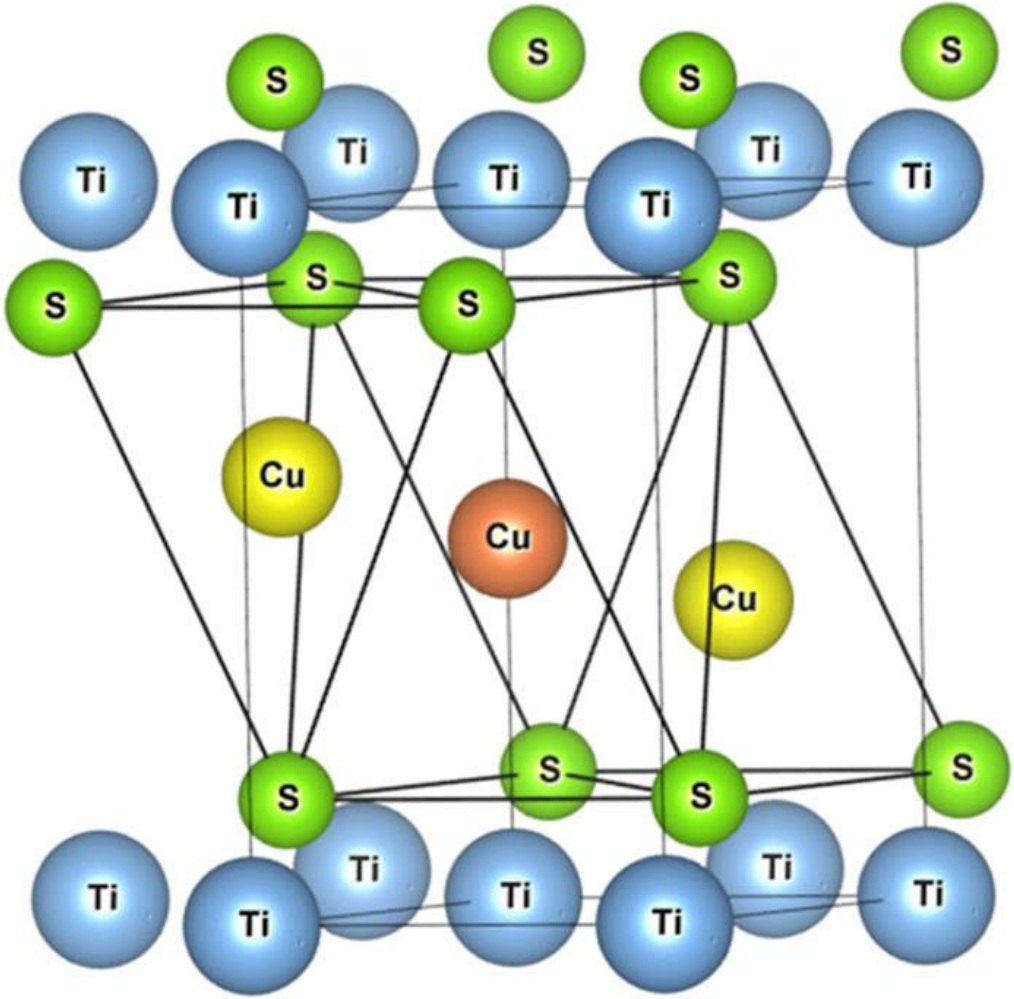

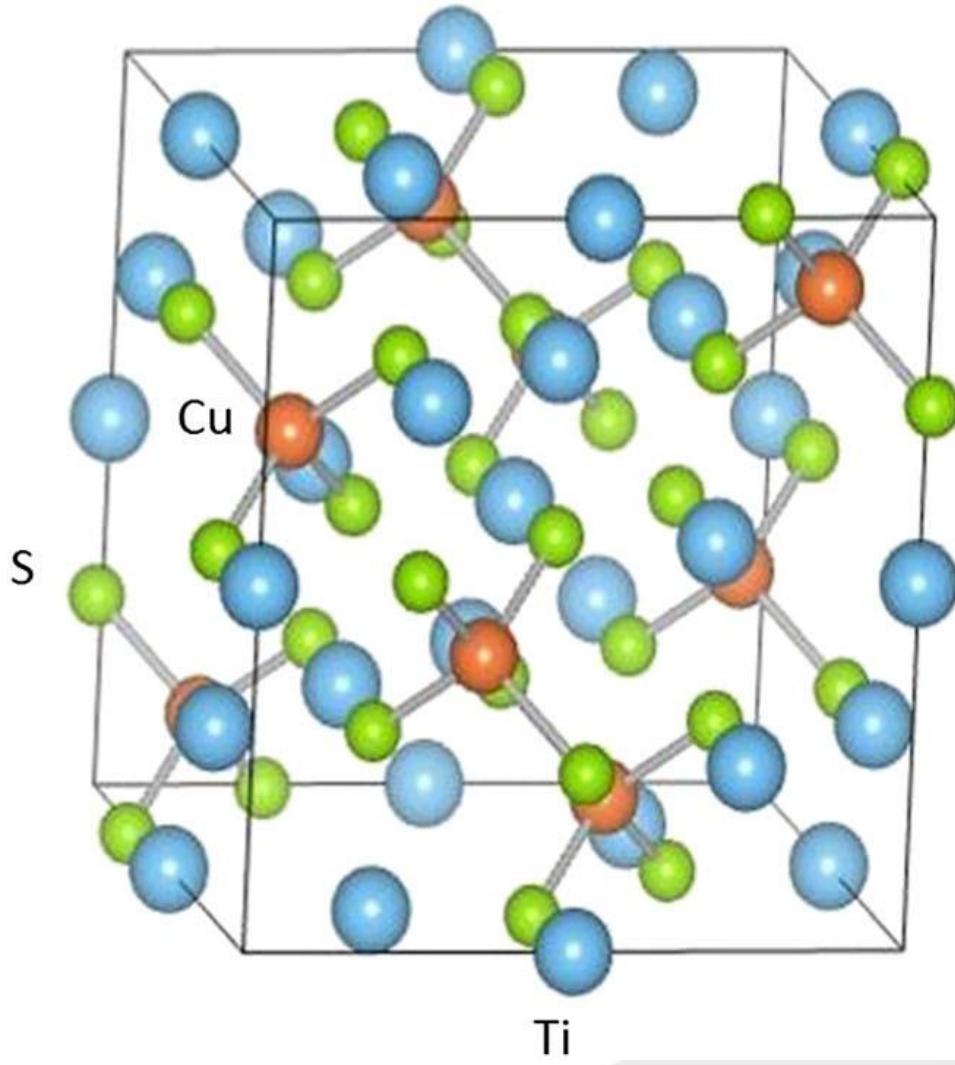

Elettra
Sincrotrone
Trieste

2D-3D transition In $Cu–TiS_2$ system

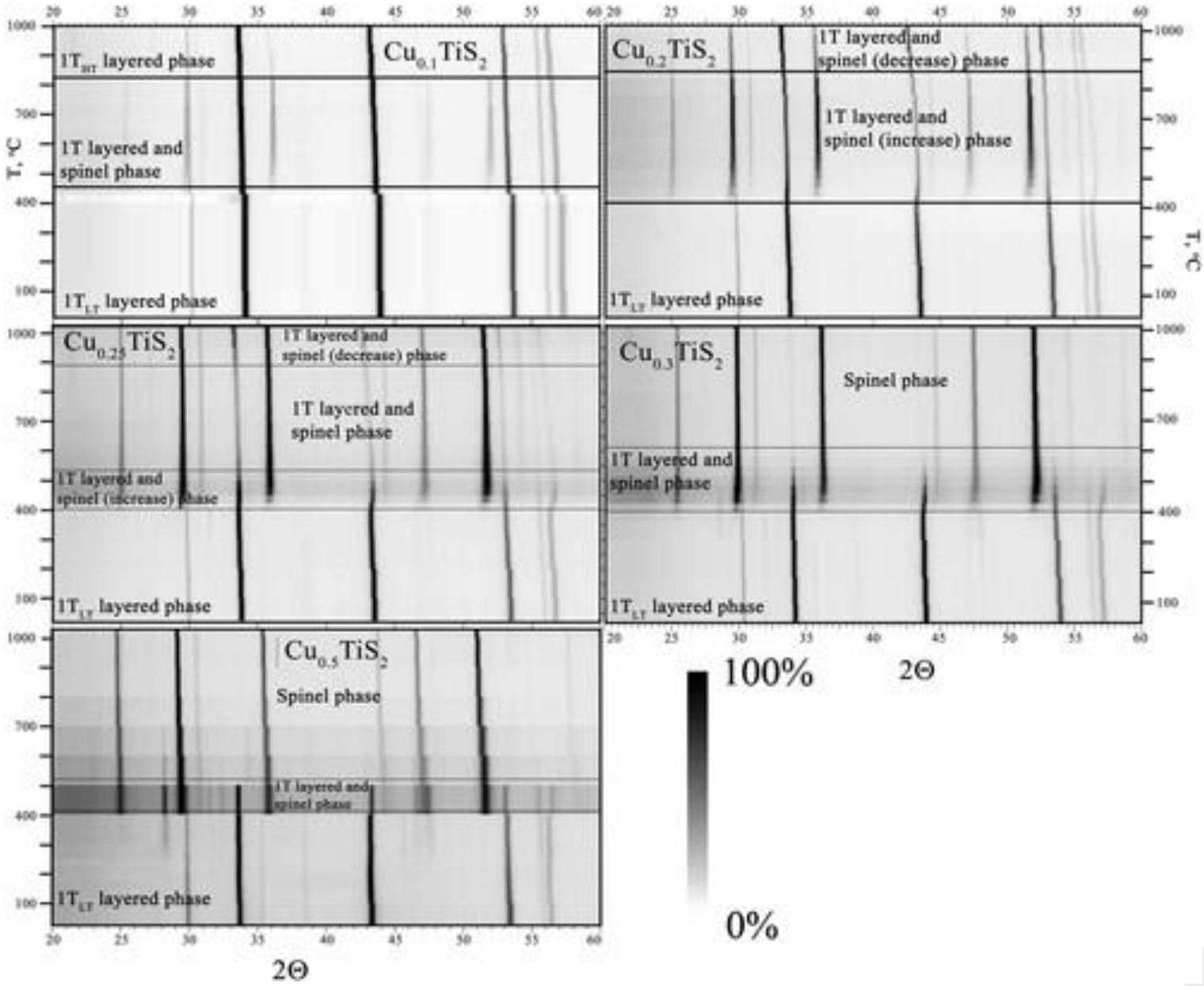

Elettra
Sincrotrone
Trieste

2D-3D transition In Cu–TiS_2 system

T (°C)	1T layered phase							Cubic spinel phase			R_F^2 (%)	χ^2
	a	c	S (⅓ ⅔ z)	Cu (0 0 ½)	Cu (⅓ ⅔ z)		Ti (0 0 ½)	a	Cu (⅛⅛⅛)	S (x x x)		
			z	Occupation	z	Occupation	Occupation		Occupation	x		
						$Cu_{0.2}TiS_2$						
206	3.4269(1)	5.8106(2)	0.2438(5)	0.198(2)	...	...	...	...	...	...	5.96	1.880
320	3.4331(1)	5.8252(2)	0.2452(5)	0.195(2)	...	...	...	...	...	...	6.44	1.688
451	3.4401(1)	5.8037(2)	0.2593(8)	0.064(2)	...	...	0.005(3)	9.9816(4)	0.763(8)	0.2502(5)	3.90	1.123
483	3.4405(1)	5.7942(3)	0.249(1)	0.059(3)	...	...	...	9.9631(3)	0.611(5)	0.2526(3)	2.89	1.136
514	3.4421(1)	5.7937(3)	0.253(1)	0.045(3)	...	...	0.017(4)	9.9592(2)	0.564(4)	0.2530(2)	3.18	1.064
546	3.4441(1)	5.7982(4)	0.260(1)	0.030(4)	...	...	0.018(5)	9.9604(2)	0.521(3)	0.2529(3)	2.78	1.138
606	3.4482(1)	5.8083(4)	0.243(1)	0.005(3)	...	...	0.074(6)	9.9642(1)	0.512(3)	0.2536(2)	4.55	1.107
637	3.4498(1)	5.8133(4)	0.249(1)	0.038(3)	...	...	0.018(5)	9.9660(1)	0.503(3)	0.2532(1)	1.86	1.105
735	3.4543(1)	5.8365(4)	0.246(1)	0.057(3)	0.45(3)	0.013(2)	0.020(5)	9.9726(1)	0.467(3)	0.2538(2)	2.89	1.565
828	3.4603(1)	5.8677(3)	0.243(1)	0.032(3)	0.454(7)	0.037(2)	0.029(4)	9.9846(1)	0.474(3)	0.2536(2)	2.72	1.296
874	3.4626(1)	5.8881(2)	0.240(1)	0.040(2)	0.431(6)	0.041(2)	0.031(4)	9.9908(1)	0.498(4)	0.2535(2)	2.92	1.770
918	3.4654(1)	5.9051(3)	0.239(1)	0.060(2)	0.445(8)	0.032(2)	0.001(4)	9.9662(4)	0.533(6)	0.2540(3)	4.12	2.410
						$Cu_{0.1}TiS_2$						
525	3.4422(1)	5.7990(2)	0.2460(6)	0.044(2)	0.35(2)	0.013(2)	0.024(3)	9.9701(8)	0.66(2)	0.2547(8)	8.16	5.921
647	3.4494(1)	5.8129(2)	0.2448(6)	0.038(2)	0.37(2)	0.015(2)	0.023(4)	9.9690(4)	0.50(2)	0.2544(6)	7.05	5.813
918	3.4650(1)	5.8691(2)	0.2428(7)	0.055(2)	0.42(2)	0.020(3)	0.002(4)	...	...	...	9.65	10.47
						$Cu_{0.25}TiS_2$						
918	3.4664(2)	5.9140(8)	0.236(2)	0.009(6)	0.46(1)	0.052(4)	...	10.0075(1)	0.512(4)	0.2531(2)	6.42	10.81

Elettra
Sincrotrone
Trieste

2D-3D transition In $Cu–TiS_2$ system

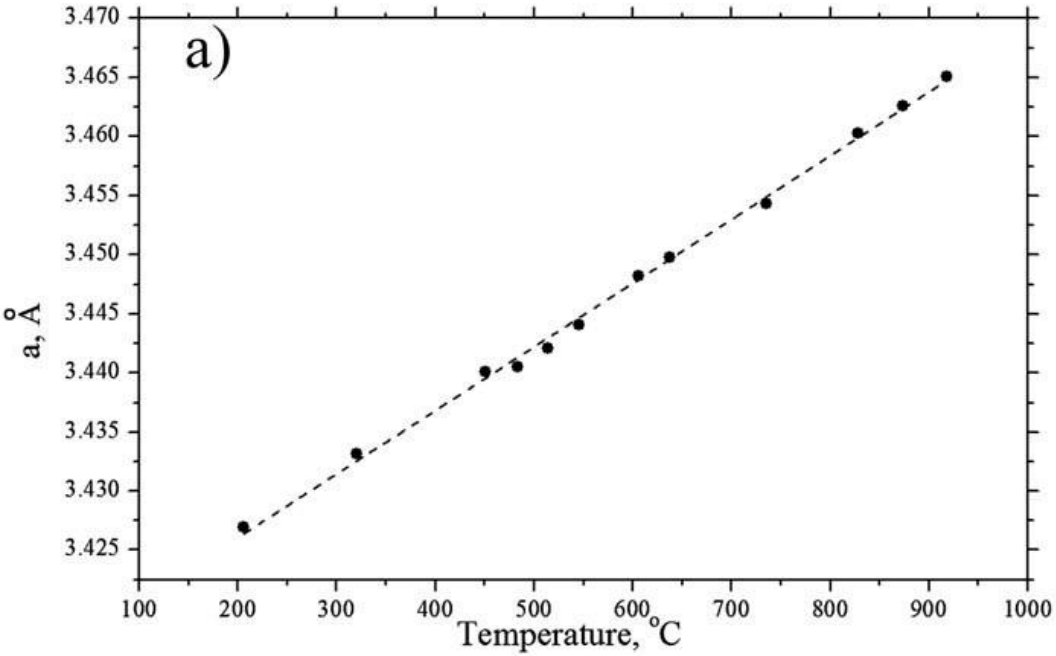

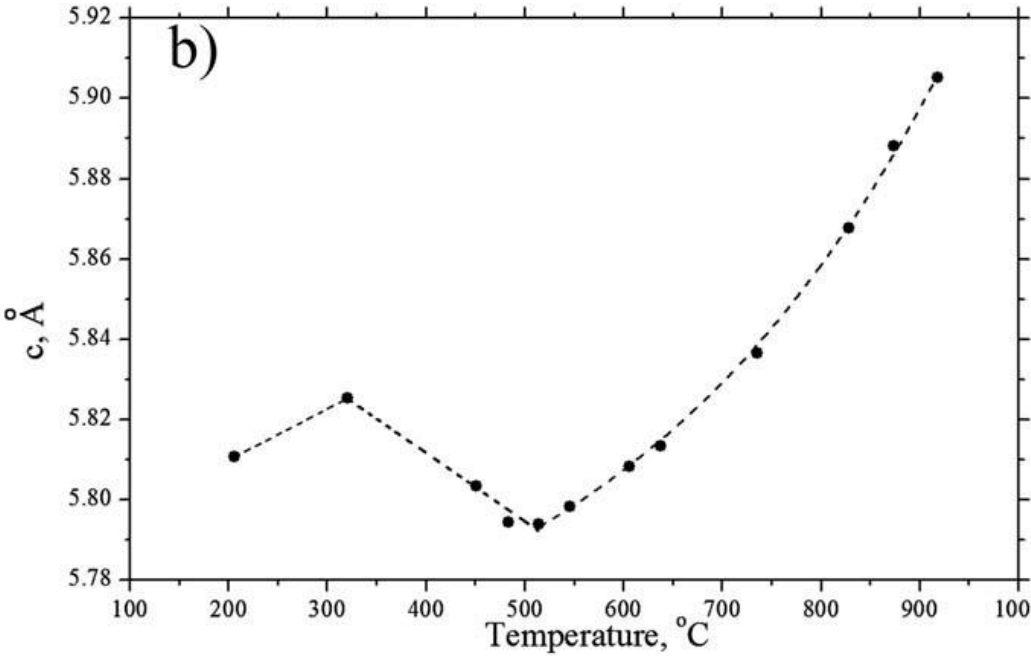

Elettra
Sincrotrone
Trieste

2D-3D transition In $Cu–TiS_2$ system

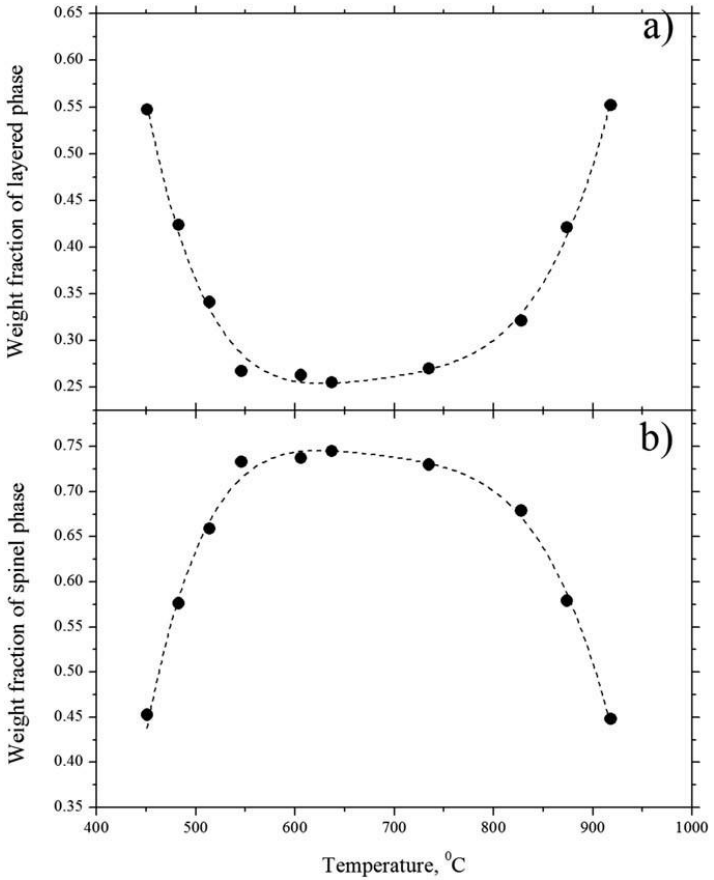

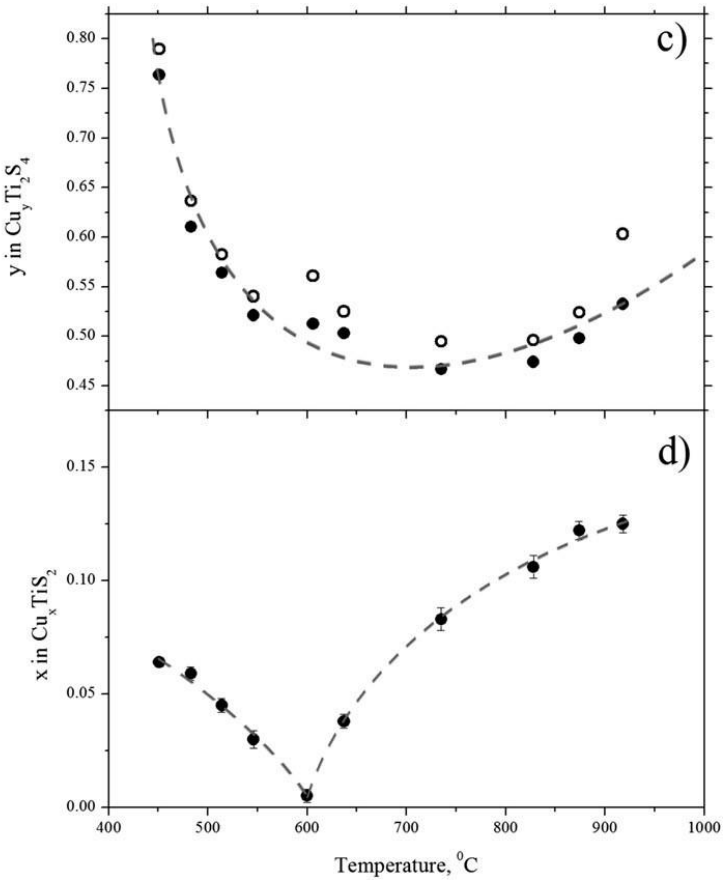

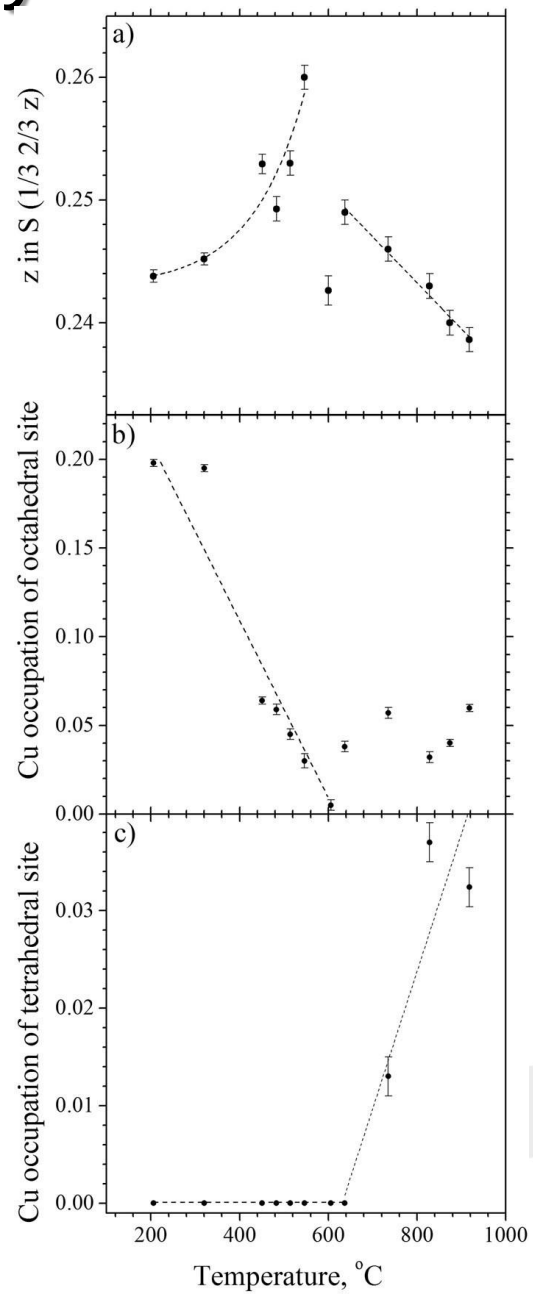

Elettra
Sincrotrone
Trieste

2D-3D transition In $Cu–TiS_2$ system

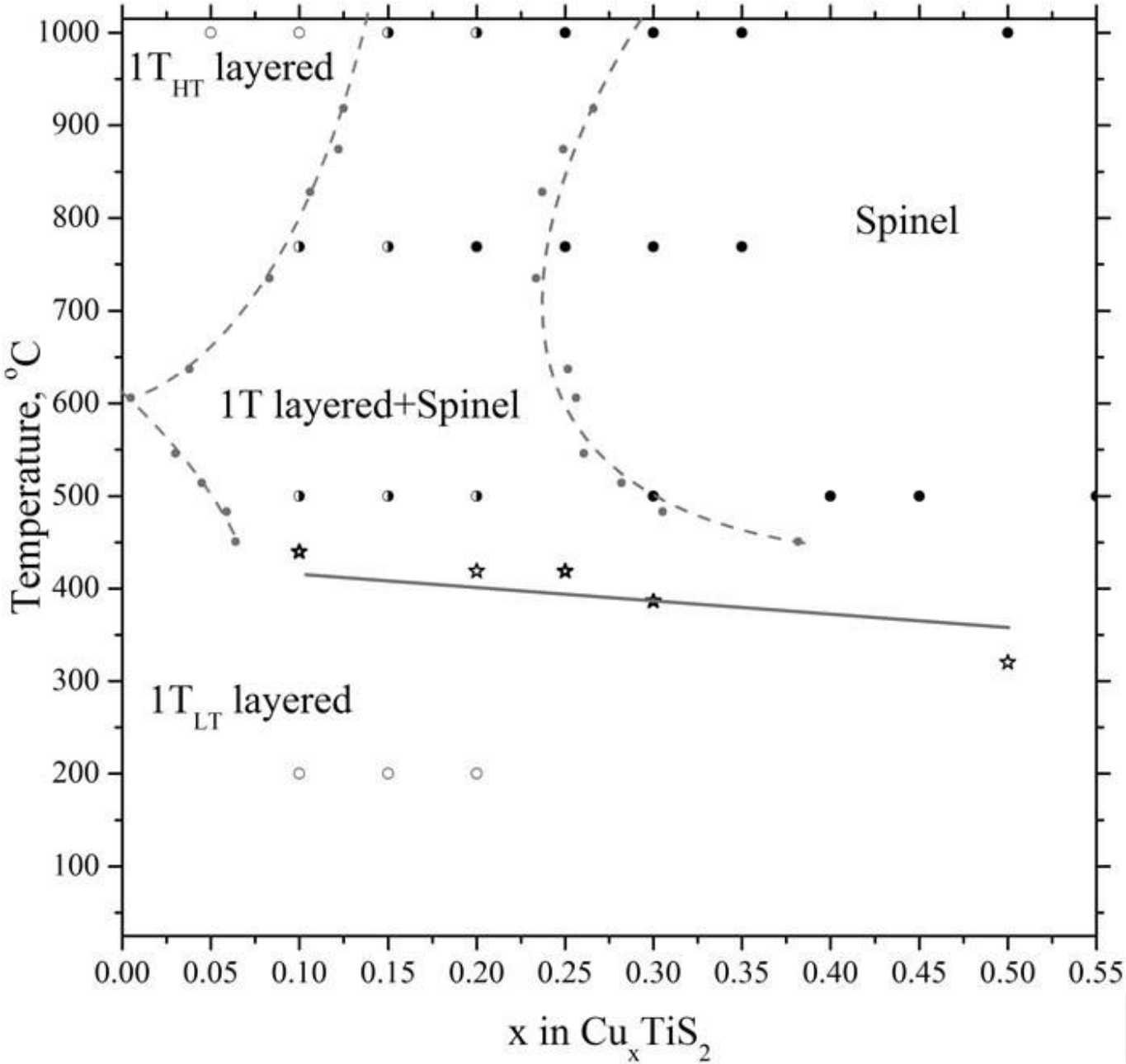

Elettra
Sincrotrone
Trieste

2D-3D transition In $Cu–TiS_2$ system

- It has been found that the stability of the layered phase is determined by the distribution of copper atoms between the octahedral and tetrahedral crystallographic sites.
- The occupation of octahedral sites dominates at low temperatures.
- Upon heating, tetrahedral site occupation is limited and the layered phase becomes unstable and transforms to the spinel.
- Further heating allows the distribution of copper between octahedral and tetrahedral sites; the layered phase becomes stable again.

Elettra
Sincrotrone
Trieste

XRPD in non ambient conditions

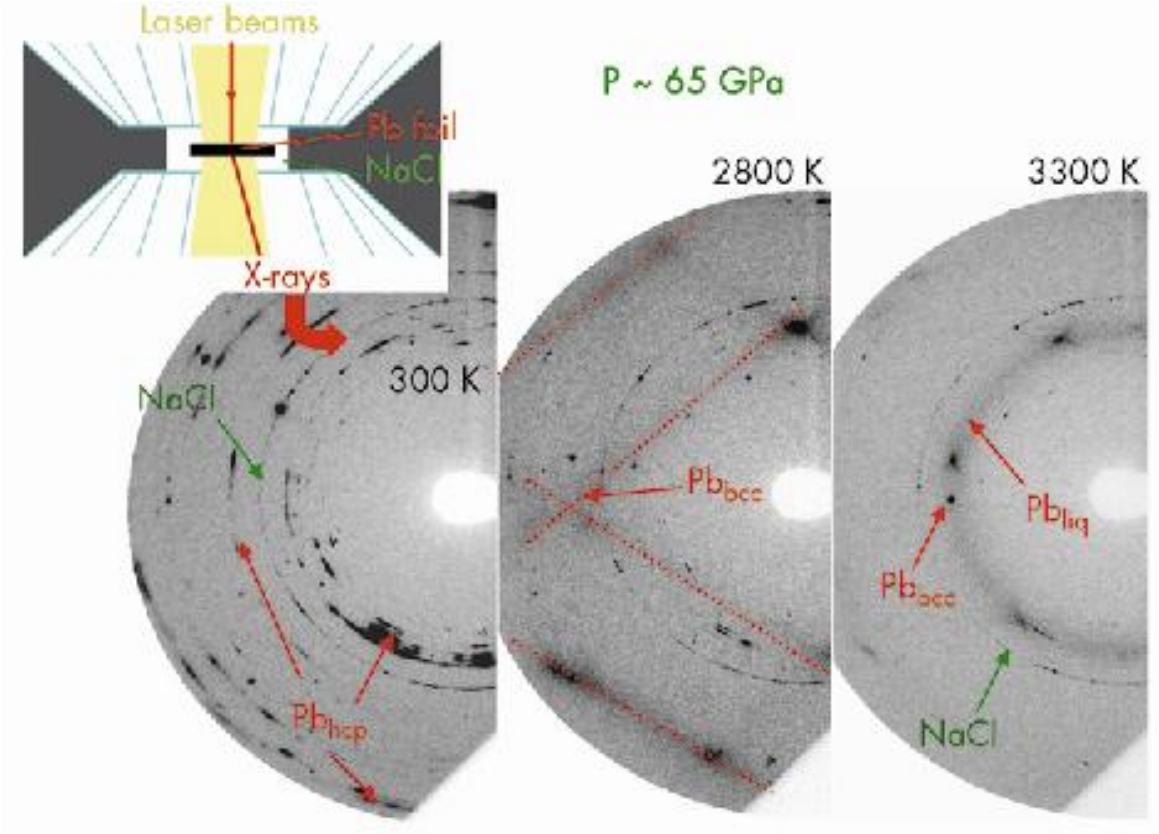

Source: www.esrf.eu

Elettra
Sincrotrone
Trieste

Diffraction for stress analysis

- The stresses in a material are the sum of the contributions from any externally applied load (applied stress) and those arising from the interactions between individual grains or components that are not completely relaxed when no external load is present (residual stresses).

- Stresses lead to deformation, the distances between lattice planes changes in the direction where stress is present.

- Measuring how the peak position (related to the lattice plane distance by braggs law) changes, at different orientations of the sample gives us information on the amount of stress

Diffraction for stress analysis

- Not being aware of residual tensile stresses, that make materials weaker can have disastrous consequences in construction for example:

Residual stress is often a cause of premature failure of critical components, and was one factor in the collapse of the suspension bridge at Silver Bridge in West Virginia in December 1967. The eyebar links were castings which showed high levels of residual stress, which in one eyebar, encouraged crack growth. When the crack reached a critical size, it grew catastrophically, and from that moment, the whole structure started to fail in a chain reaction. Because the structure failed in less than a minute, 46 drivers and passengers in cars on the bridge at the time were killed.

Diffraction for stress analysis

- On the other hand residual stresses may be induced in materials on purpose. Compressive residual stress maybe induced in order to strengthen it and increase its fatigue life

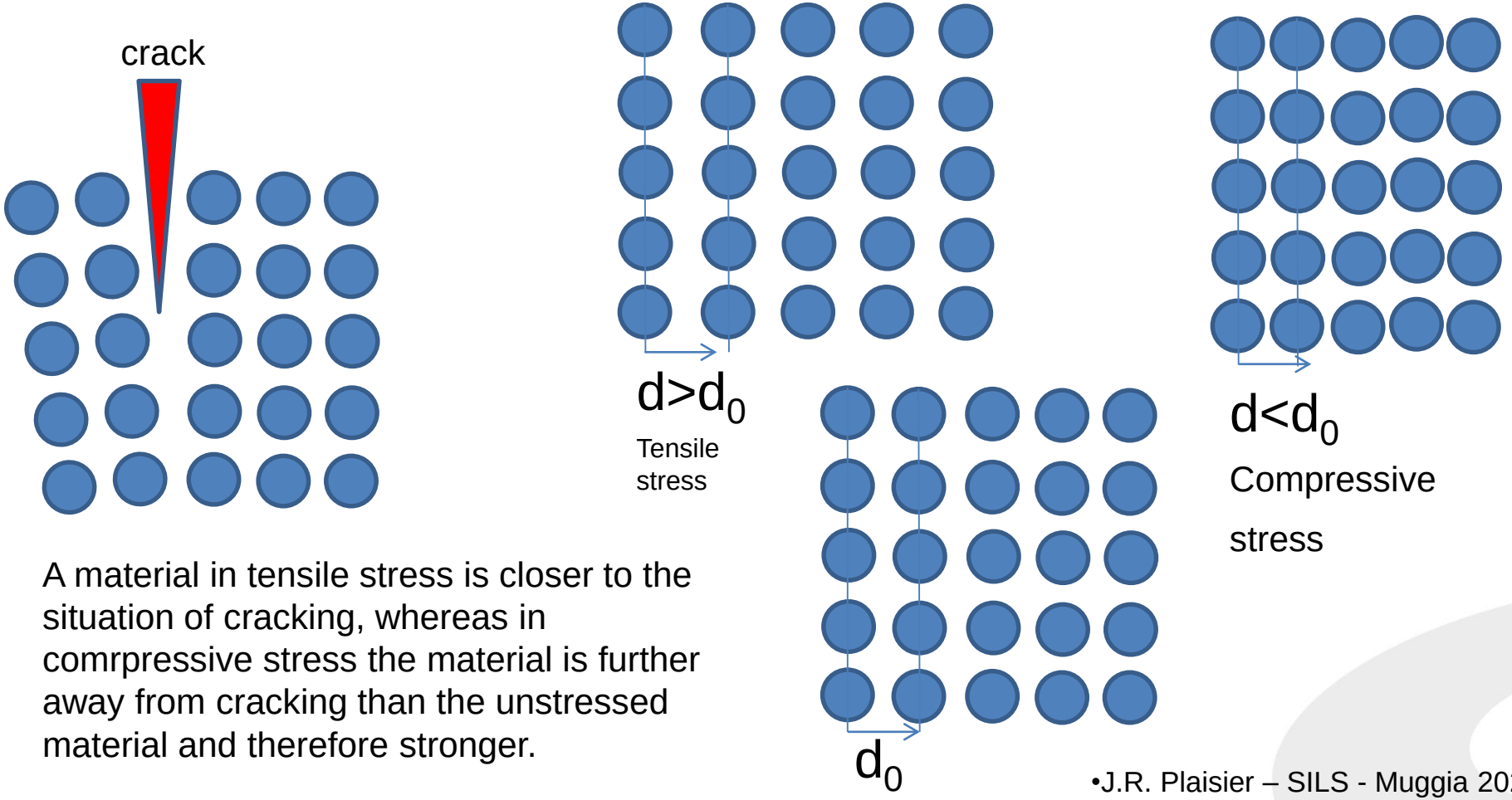

- A material in tensile stress is closer to the situation of cracking, whereas in comrpressive stress the material is further away from cracking than the unstressed material and therefore stronger.

Elettra
Sincrotrone
Trieste

Diffraction for stress analysis

- It is strain that is actually measured: $\Delta d/d_0$
- Residual strain changes interplanar spacings, which shifts the positions of diffraction peaks.
- Strain is resolved differently in different physical directions in the sample.
- Engineering materials are polycrystalline, so some grains are always oriented to diffract enabling stress tensors to be determined.

Diffraction for stress analysis

- When the d-spacing of a reflection is measured, only grains with the planes oriented in a given direction contribute to diffraction. If we change the orientation of the specimen and remeasure the d-spacing we are looking at a different population of grains and we get a different d-spacing due to different stress levels

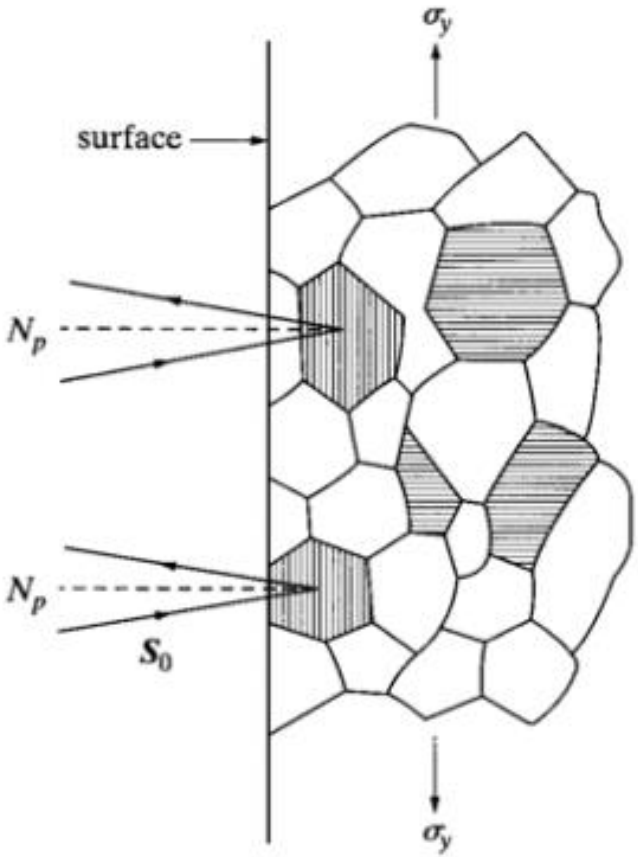

Diffraction for stress analysis

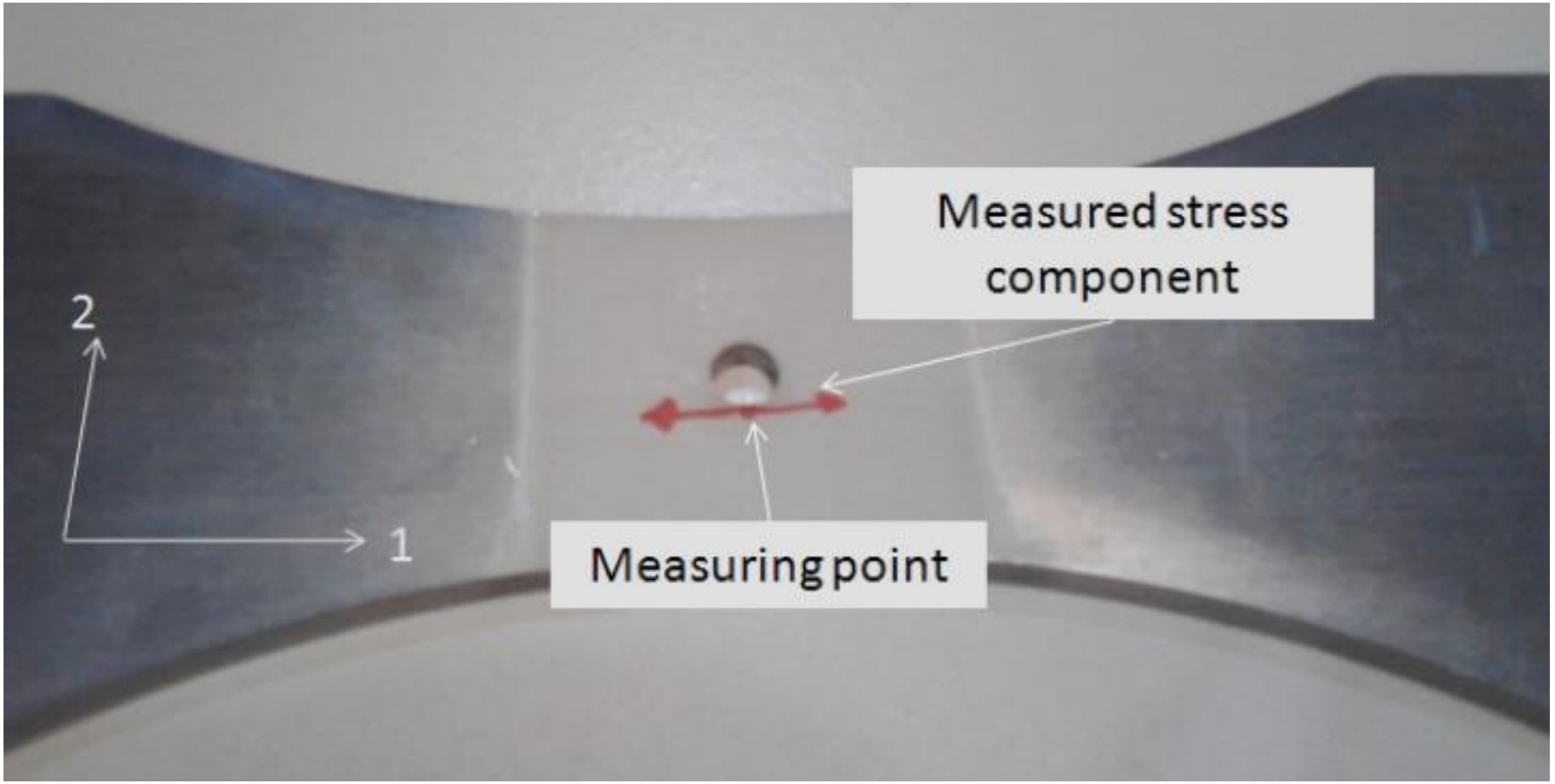

- Alloys of aluminium used in the airplane industry were measured to see the effectiveness of laser peening around a hole.

Elettra
Sincrotrone
Trieste

Diffraction for stress analysis

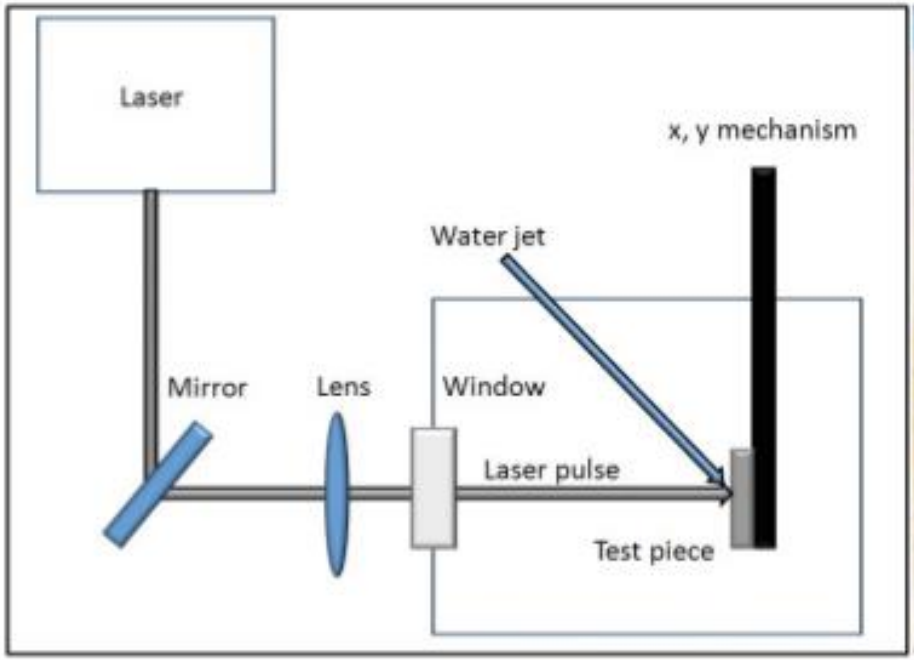

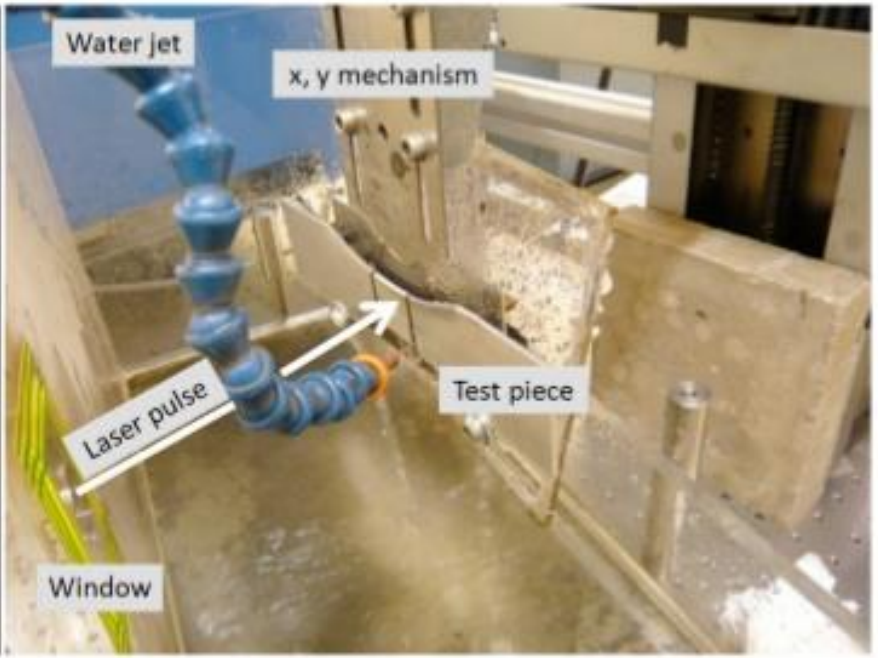

Elettra
Sincrotrone
Trieste

Diffraction for stress analysis

- The same diffraction peak is measured for different orientatons of the sample

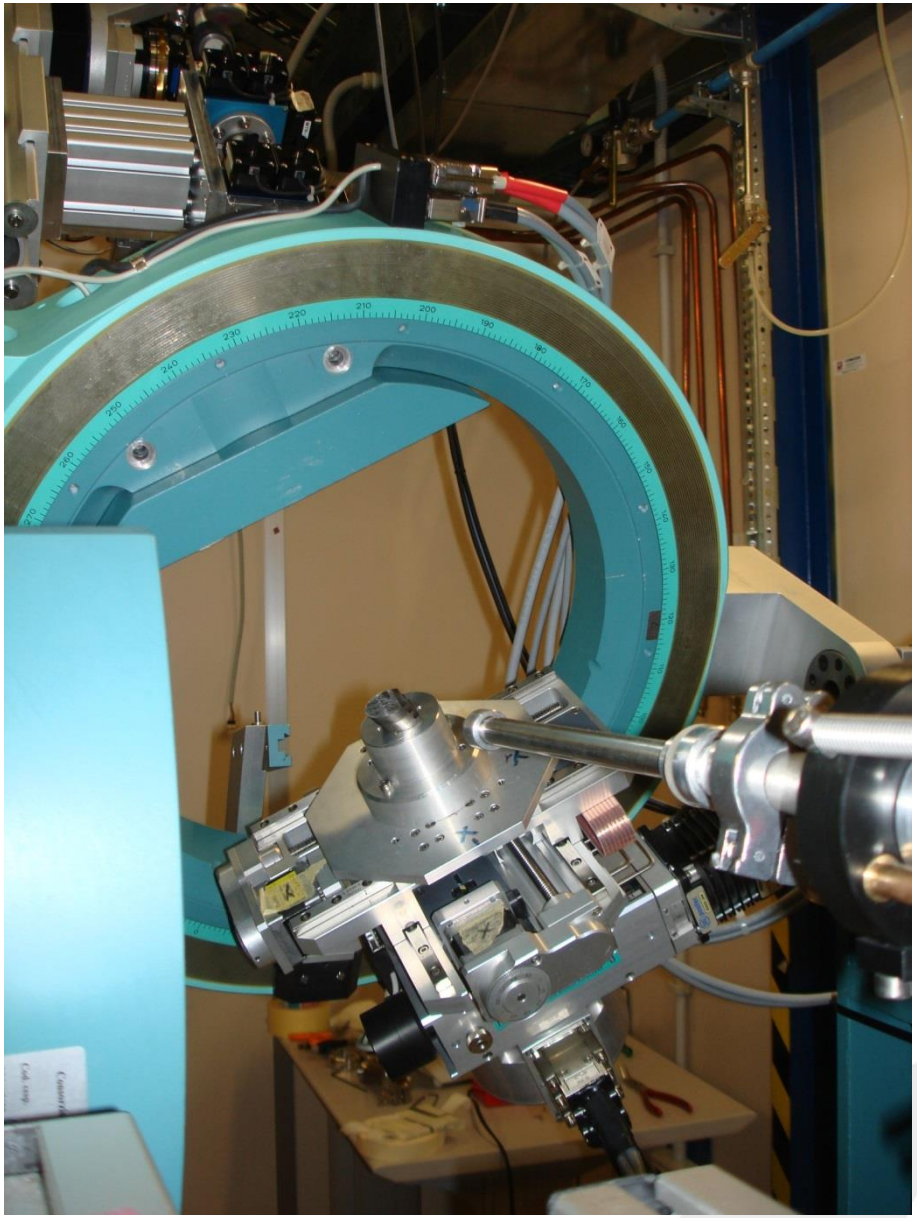

Diffraction for stress analysis

- The posiitionon of the diffraction peak is determiined dor each orientation (d)

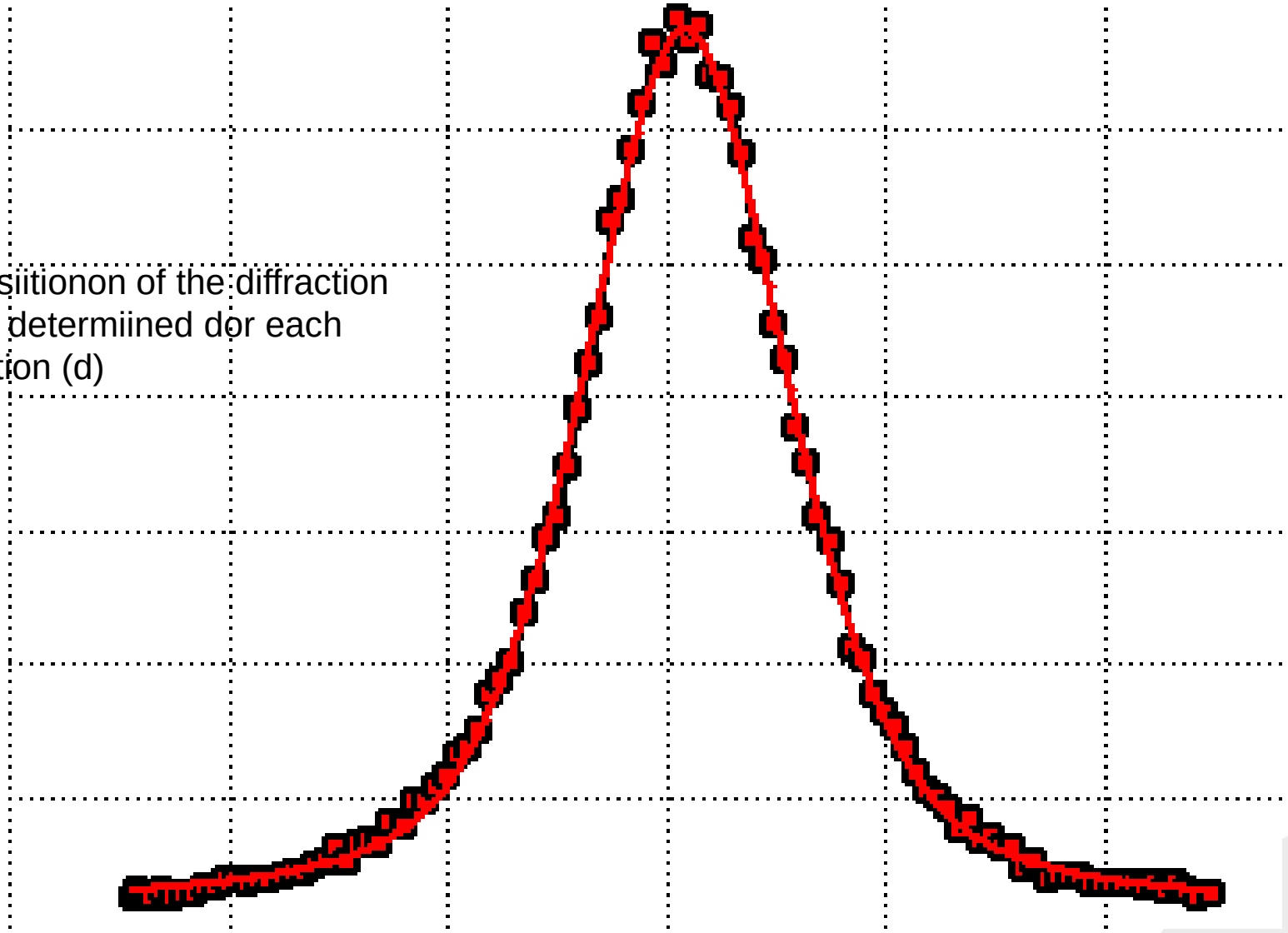

Diffraction for stress analysis

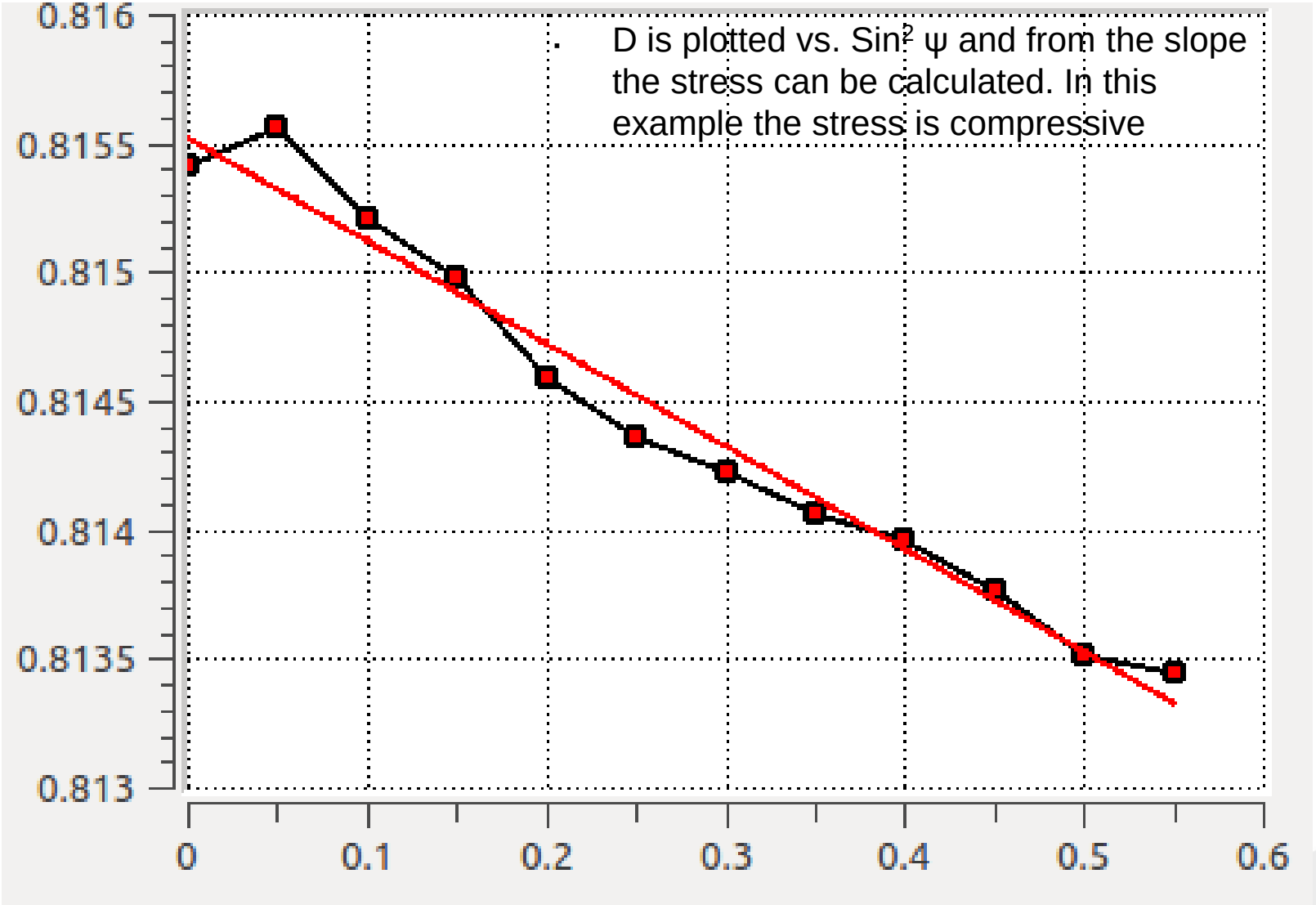

Diffraction for stress analysis

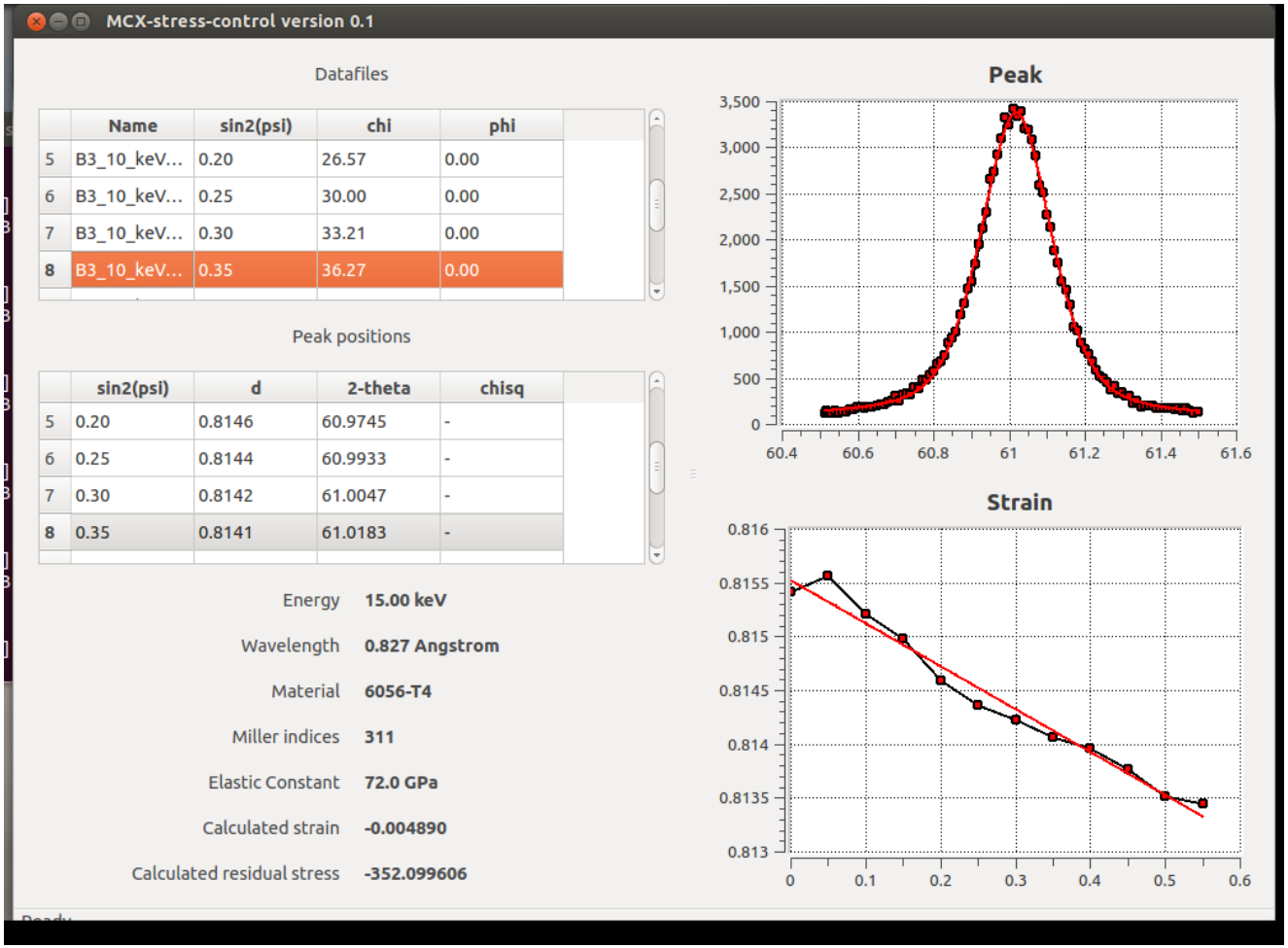

- The result showed that laser peening after drilling the hole acutually weakens tha material, whereas first applying laser peening ad subsequently drilling th hole results in a stringer material

Operando battery studies

- Li batteries

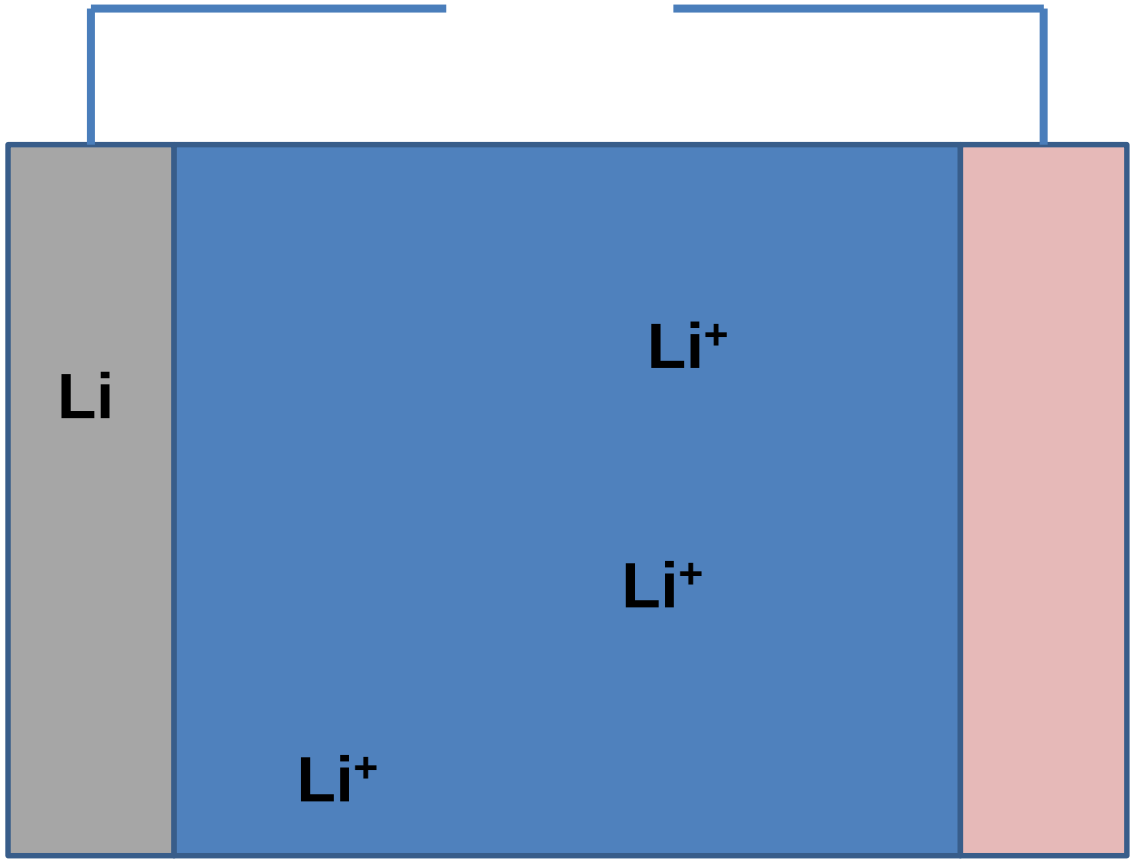

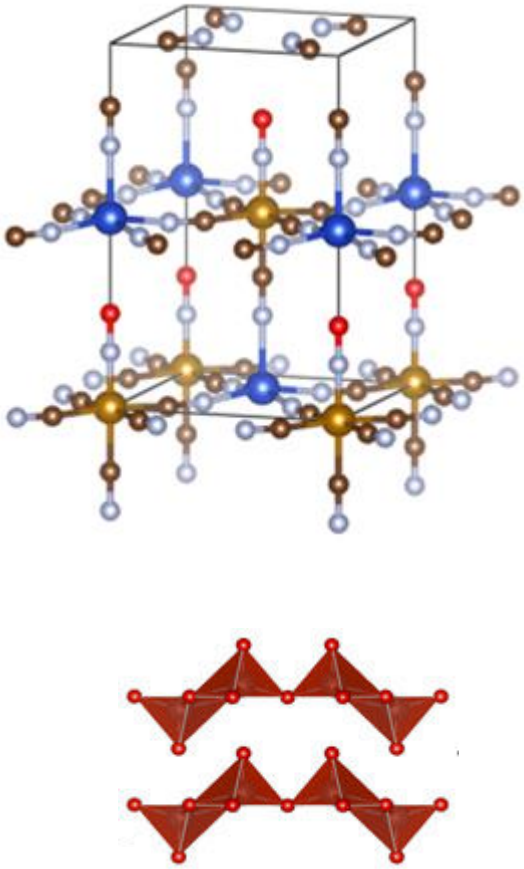

Operando battery studies

- Li batteries

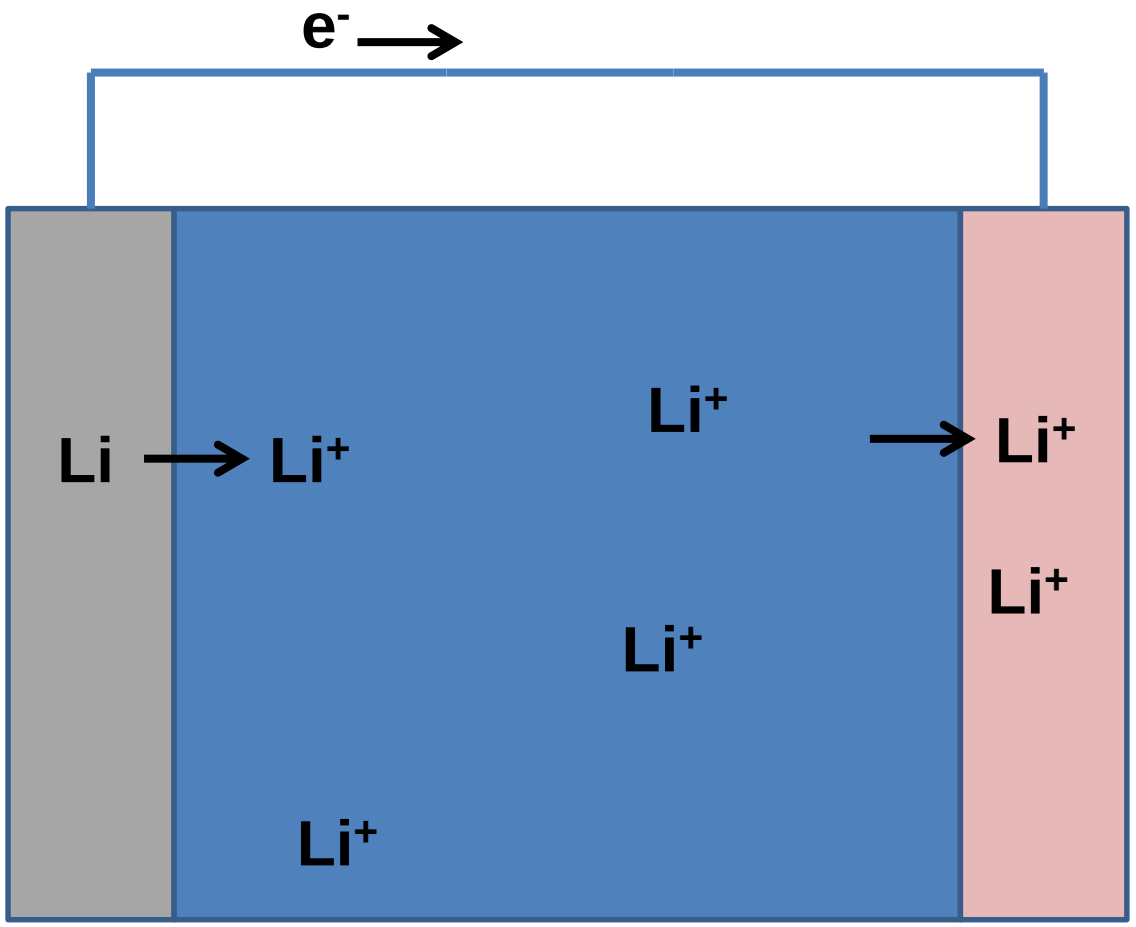

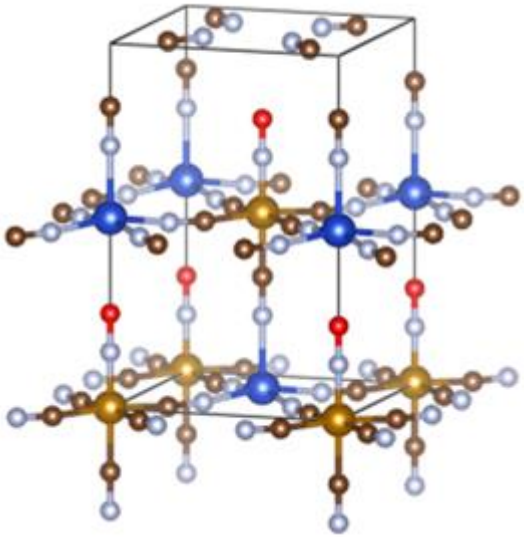

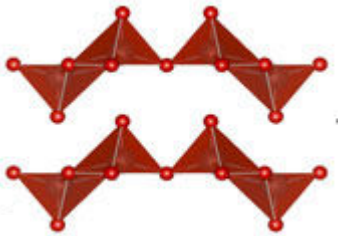

Operando battery studies

- Li batteries

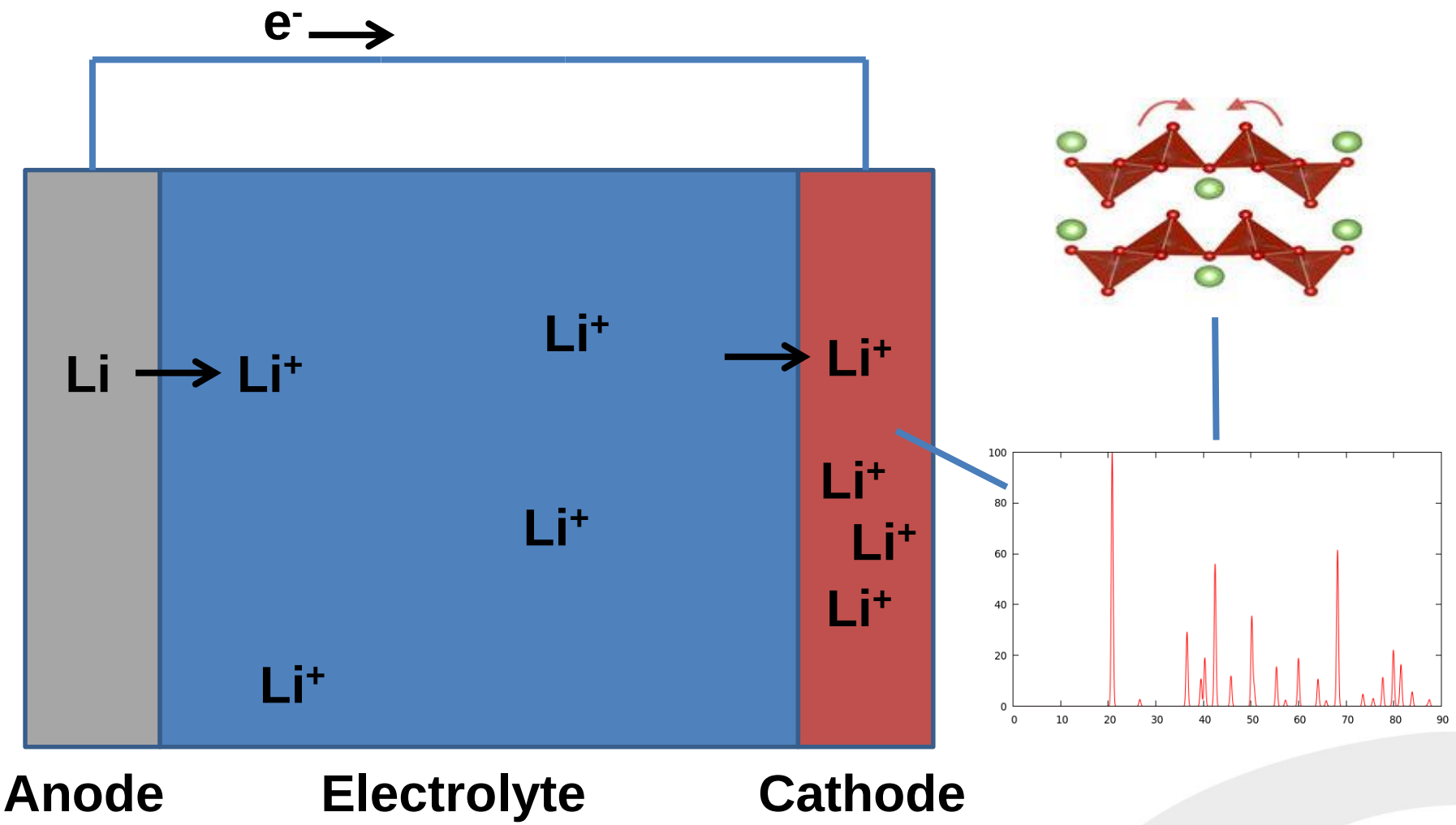

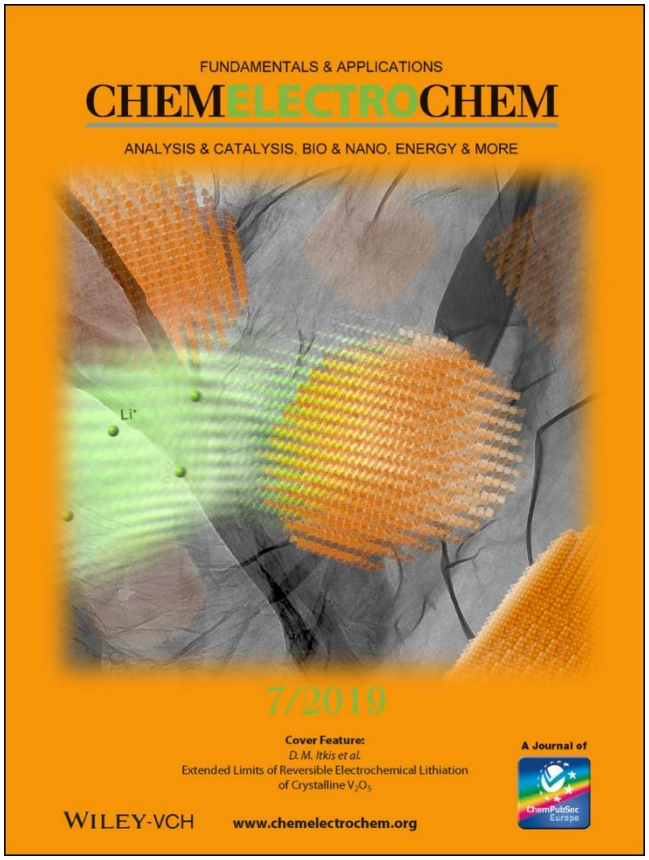

Extended Limits of Reversible Electrochemical Lithiation of Crystalline V2O5

Daniil M. Itkis, Victor A. Krivchenko, Anna Ya. Kozmenkova, Margarita S. Pakhotina, Filipp S. Napolskiy, Lara Gigli, Jasper Plaisier, Nellie R. Khasanova and Evgeny V. Antipov

Elettra
Sincrotrone
Trieste

Lithiation of Crystalline V_2O_5/RGO

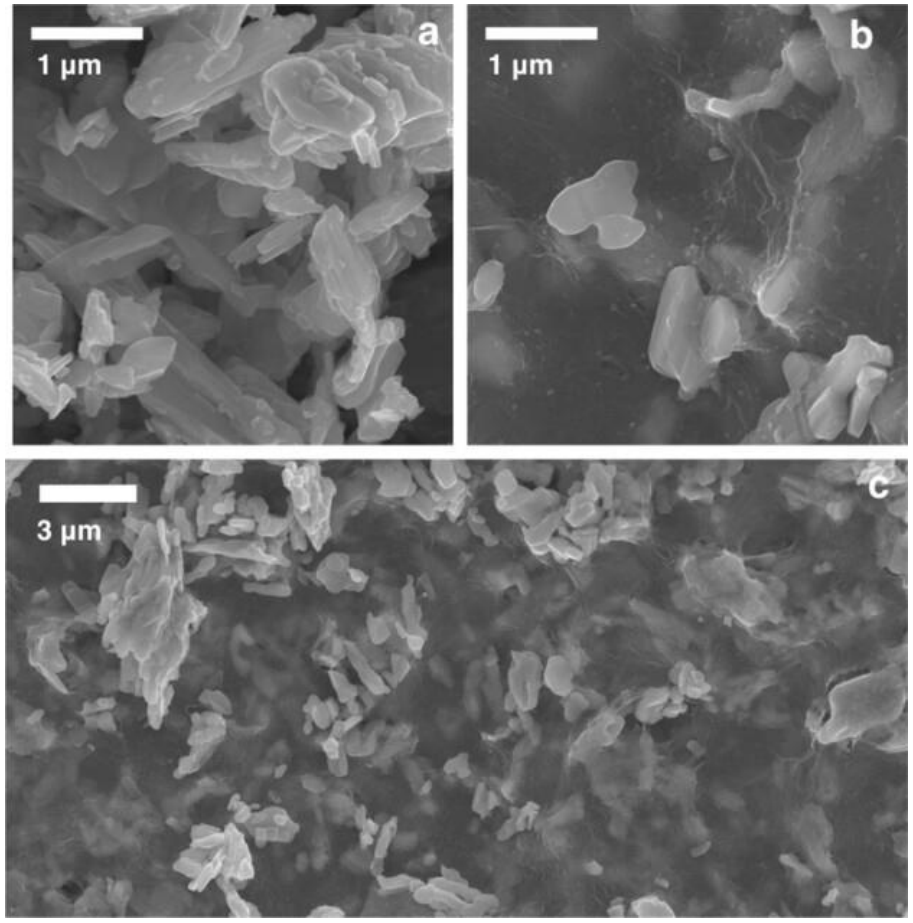

- Vanadium (V) oxide was suggested as an attractive host for electrochemical lithium yet in 1970s due to ability of multielectron redox in layered V_2O_5
- Insertion of extremely high amounts of lithium (up to 3 moles per mole of oxide) is possible, however, it is believed that insertion/extraction of about 1.8 moles of Li^+ can enable sustainable cycling.

Elettra
Sincrotrone
Trieste

Lithiation of Crystalline V_2O_5/RGO

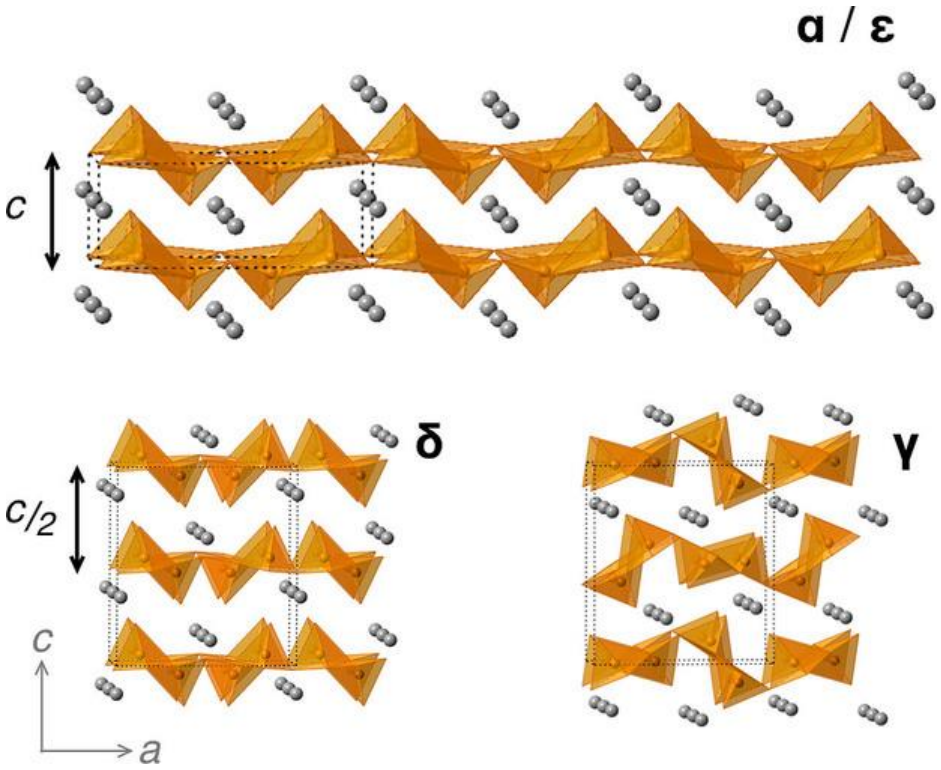

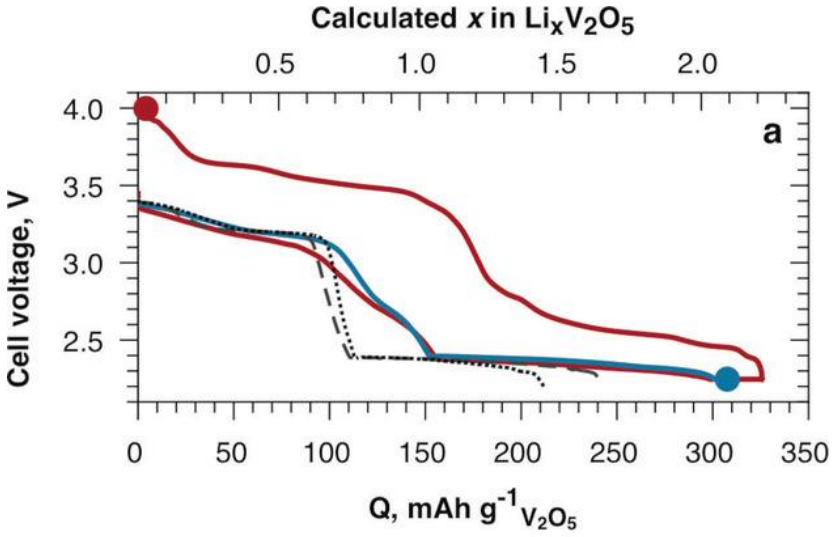

$V_2O_5 + xLi^+ + xe^- \leftrightarrows Li_xV_2O_5$ (0 < x < 3)

Elettra
Sincrotrone
Trieste

Lithiation of Crystalline V_2O_5/RGO

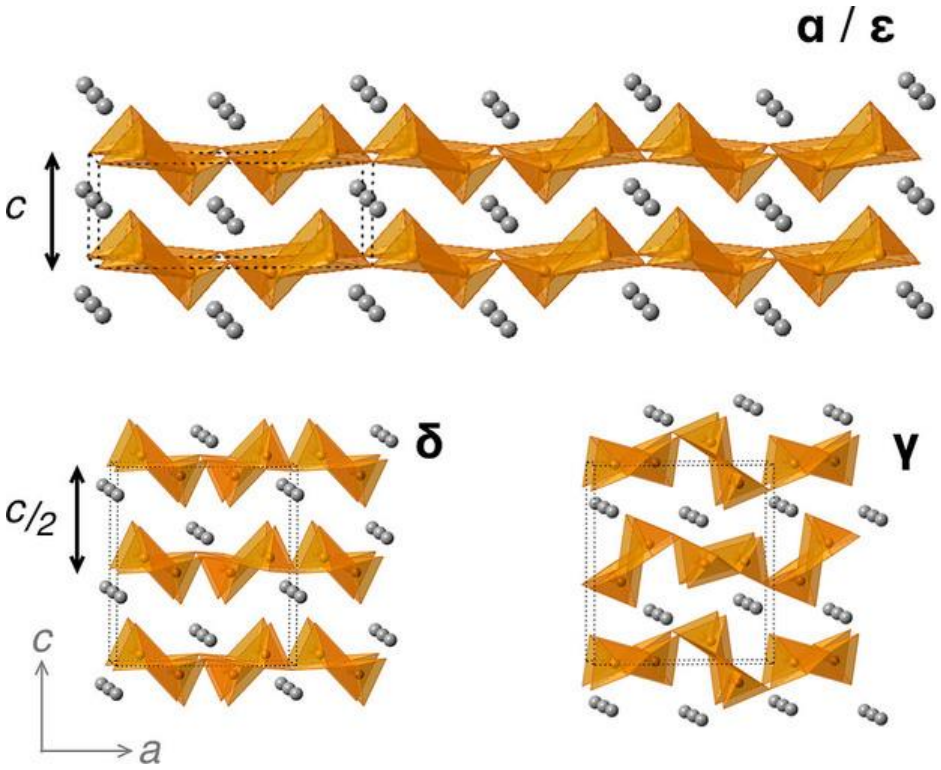

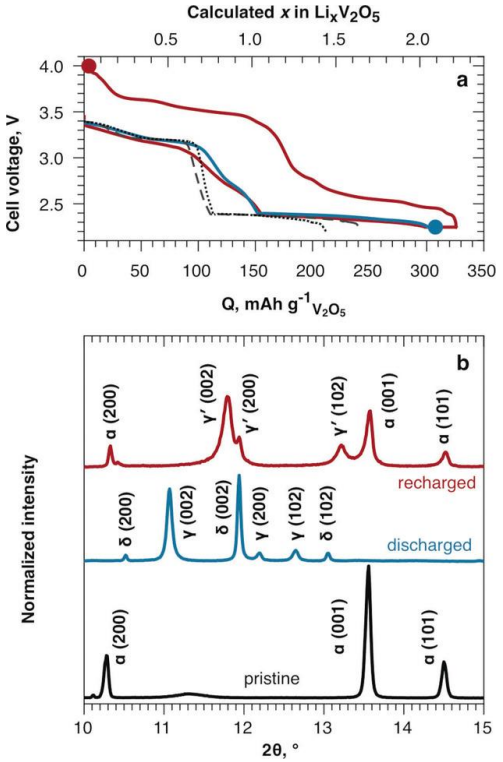

$V_2O_5 + xLi^+ + xe^- \leftrightarrows Li_xV_2O_5$ (0 < x < 3)

Elettra
Sincrotrone
Trieste

Operando battery studies on V_2O_5/RGO

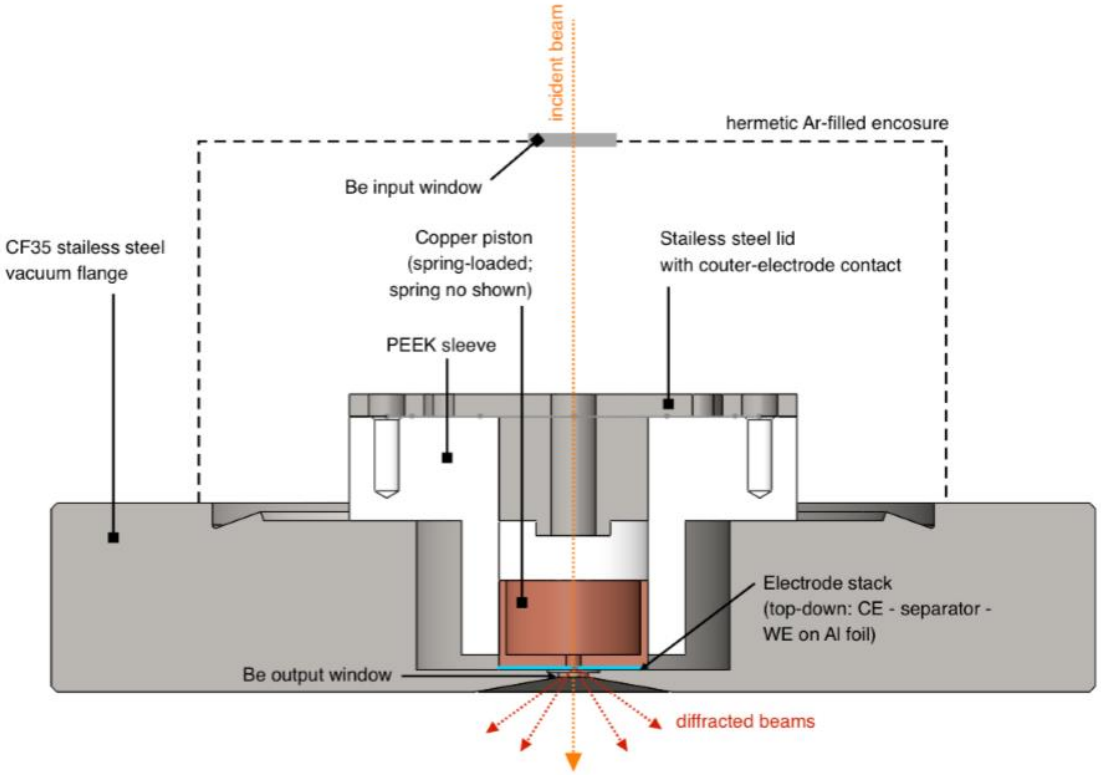

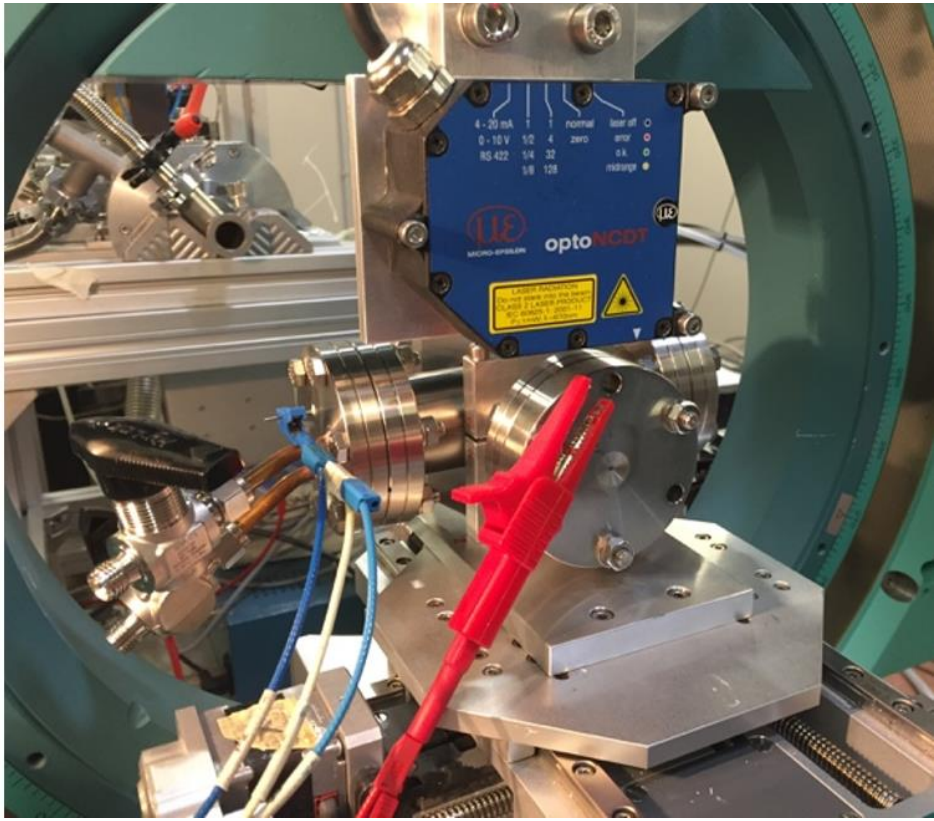

Elettra
Sincrotrone
Trieste

Operando battery studies on V_2O_5/RGO

The experiment:

- Cathode: Airbrushed slurry of V_2O_5 (85%), RGO (10%) and PVDF (5%) on Al
- Anode: Lithium
- Electrolyte: 1 M $LiClO_4$ in PC/DME

- Wavelength 1.033 Angstrom
- 2θ range 8° to 35° with a 0.01° step
- 0.5 s/point acquisition

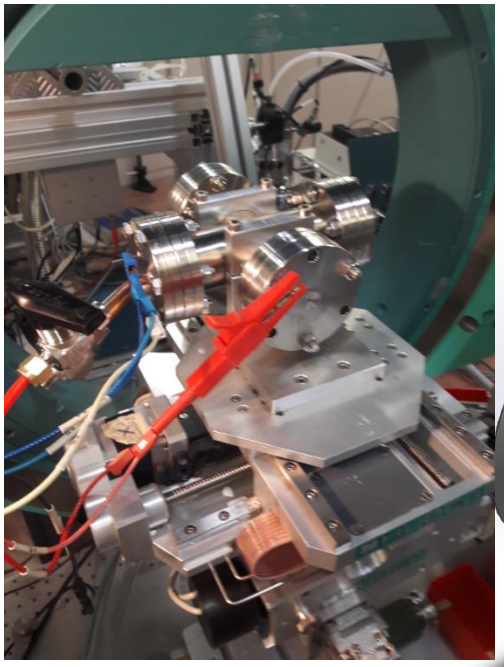

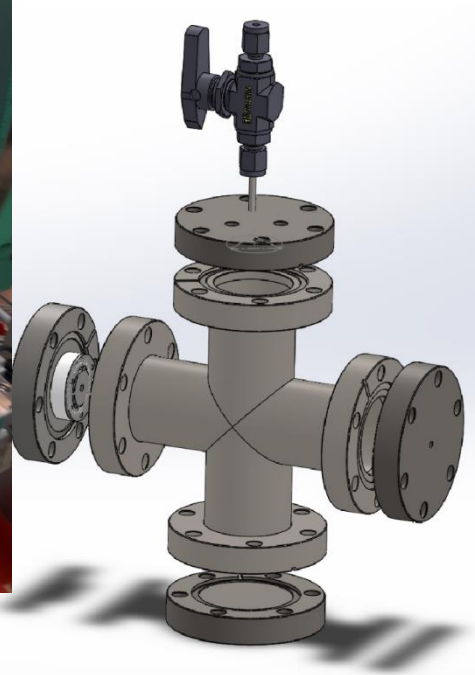

Elettra
Sincrotrone
Trieste

Operando battery studies on V_2O_5/RGO

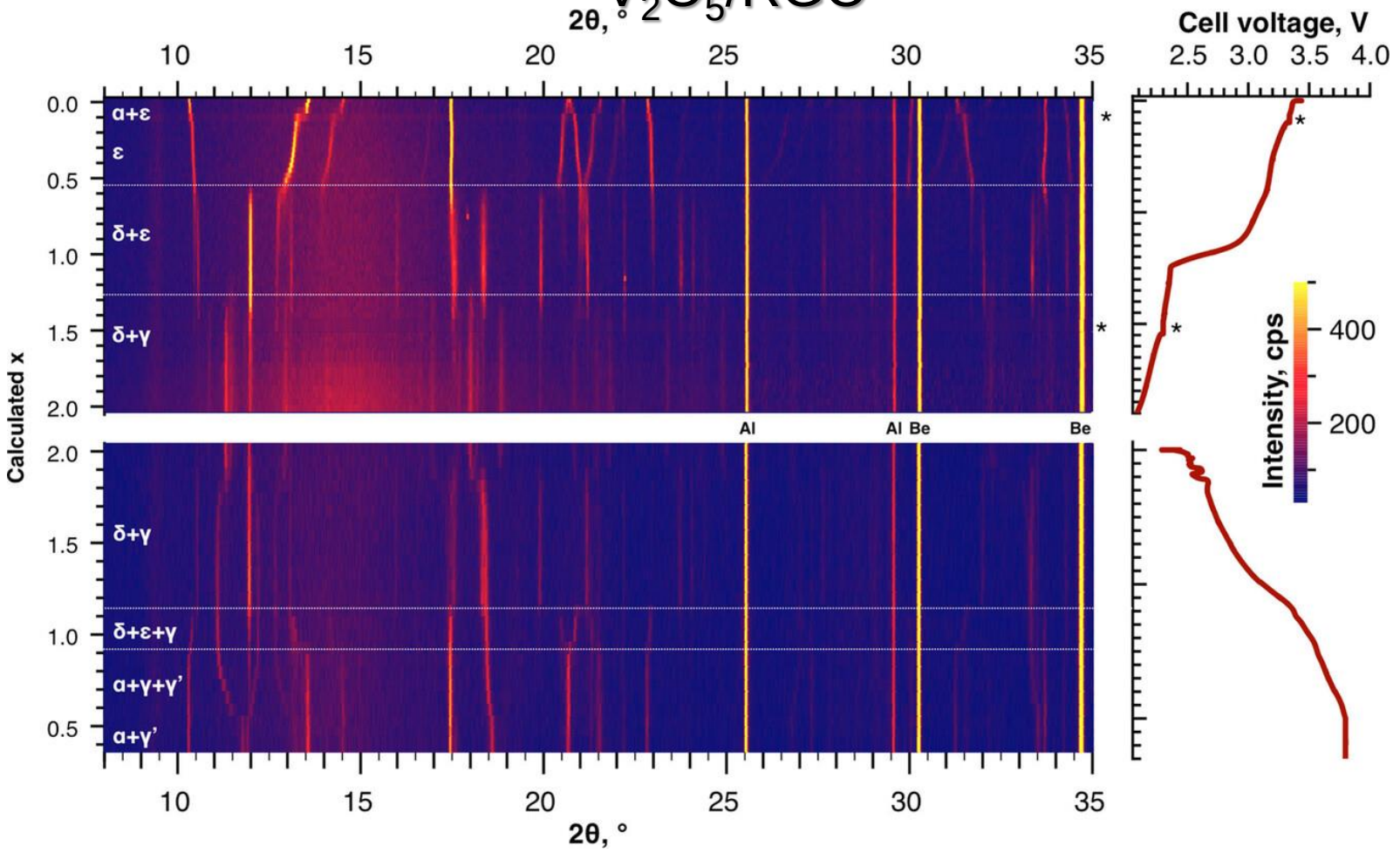

Elettra
Sincrotrone
Trieste

Operando battery studies on V_2O_5/RGO

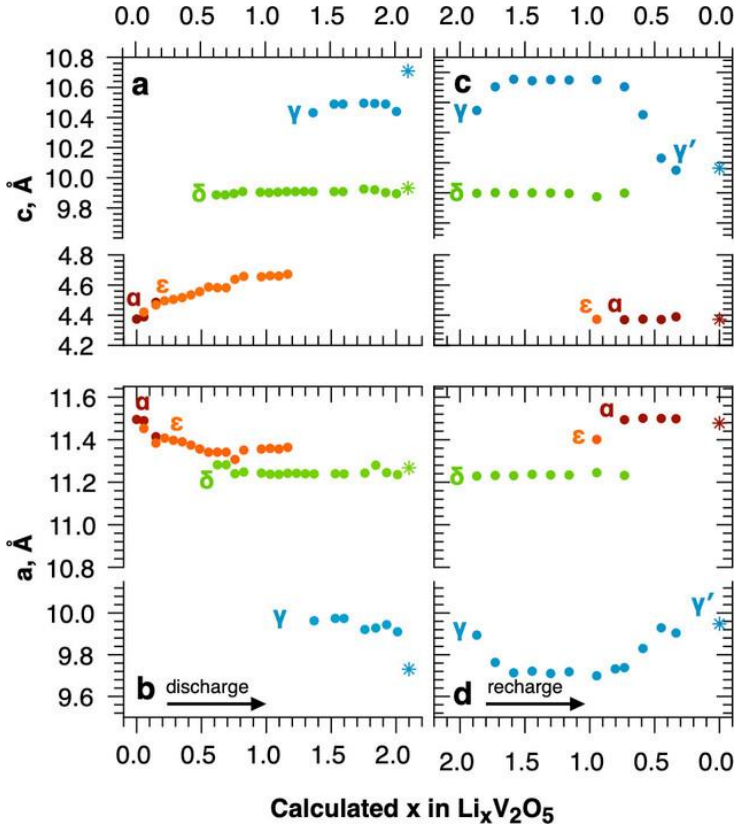

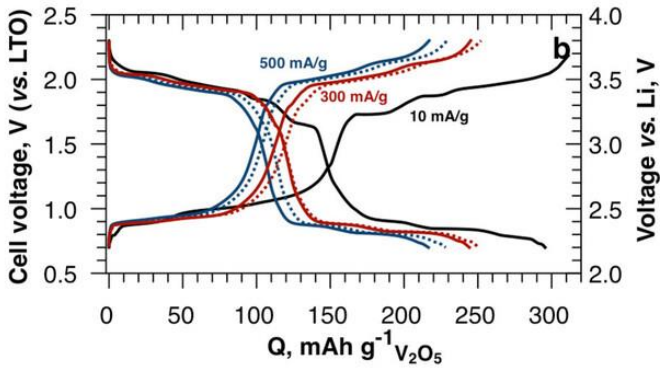

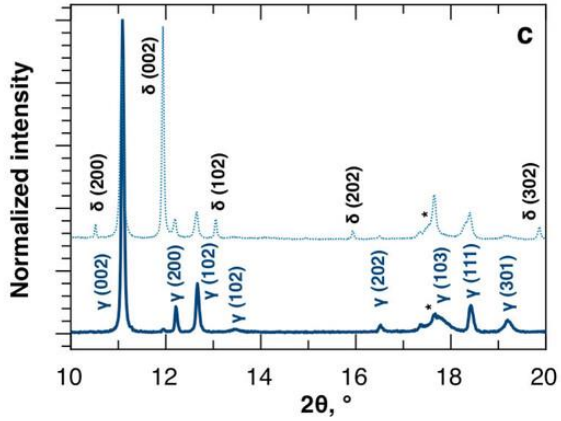

Elettra
Sincrotrone
Trieste

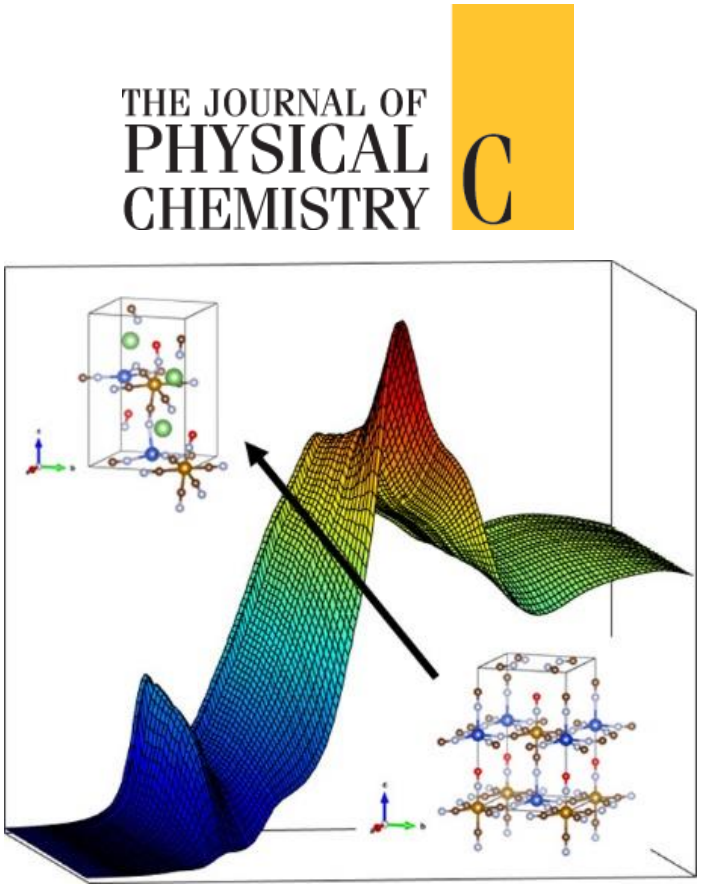

Beyond the Oxygen Redox Strategy in Designing Cathode Material for Batteries: Dynamics of a Prussian Blue-like Cathode Revealed by Operando X-ray Diffraction and X-ray Absorption Fine Structure and by a Theoretical Approach

Angelo Mullaliu, Giuliana Aquilanti, Lorenzo Stievano, Paolo Conti, Jasper Plaisier, Sylvain Cristol, Marco Giorgetti

Elettra
Sincrotrone
Trieste

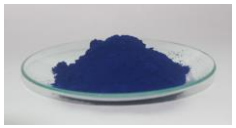

Prussian Blue Analogues: CuNP

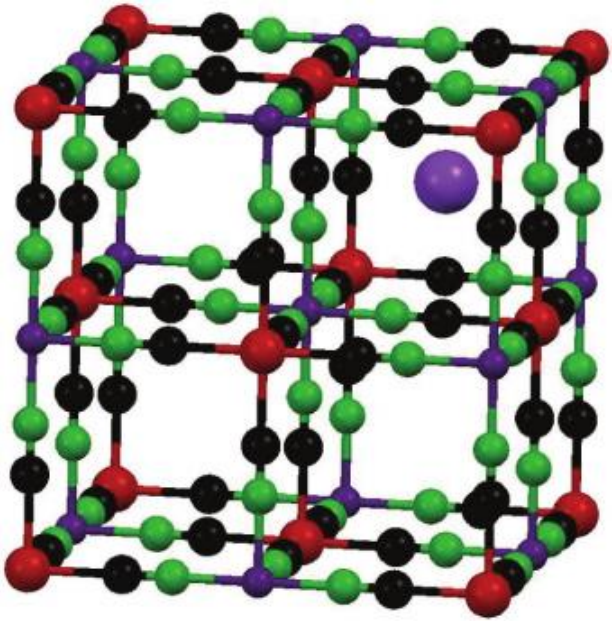

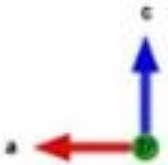

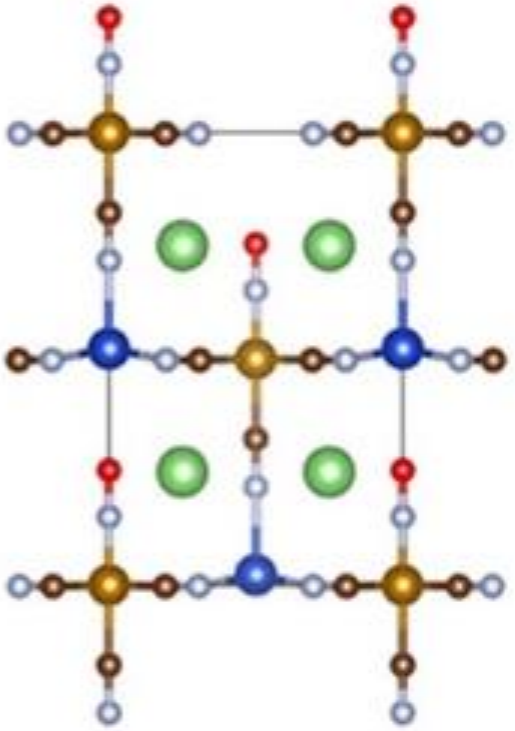

Copper nitroprusside (CuNP), $Cu[Fe(CN)_5(NO)]$

Elettra
Sincrotrone
Trieste

Prussian Blue Analogues: XAS

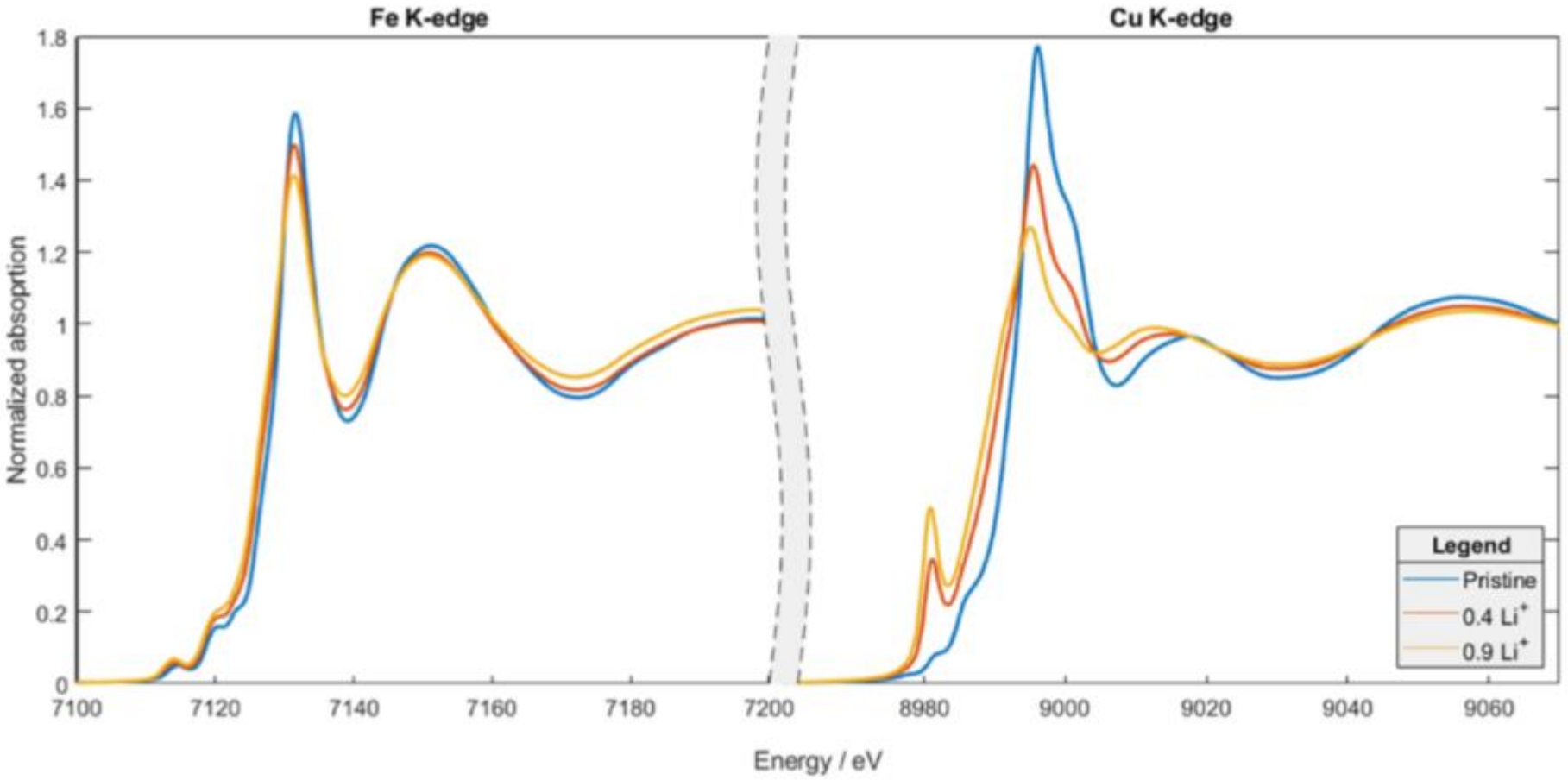

•123

Elettra
Sincrotrone
Trieste

Operando battery studies: CuNP

The experiment:

- Cathode: CuNP (70%), carbon black (10%), vapor-grown carbon fibers-high density (10%) and PTFE (10%)
- Anode: Lithium
- Electrolyte: 1 M $LiPF_6$ in EC/DC

- Wavelength 1 Angstrom
- 2θ range 10° to 30° with a 0.01° step
- 0.5 s/point acquisition

- Discharge to 1.8 V versus Li^+/Li and subsequent charge to 3.5 V versus Li^+/Li at C/22 current rate

Elettra
Sincrotrone
Trieste

Operando battery studies: CuNP

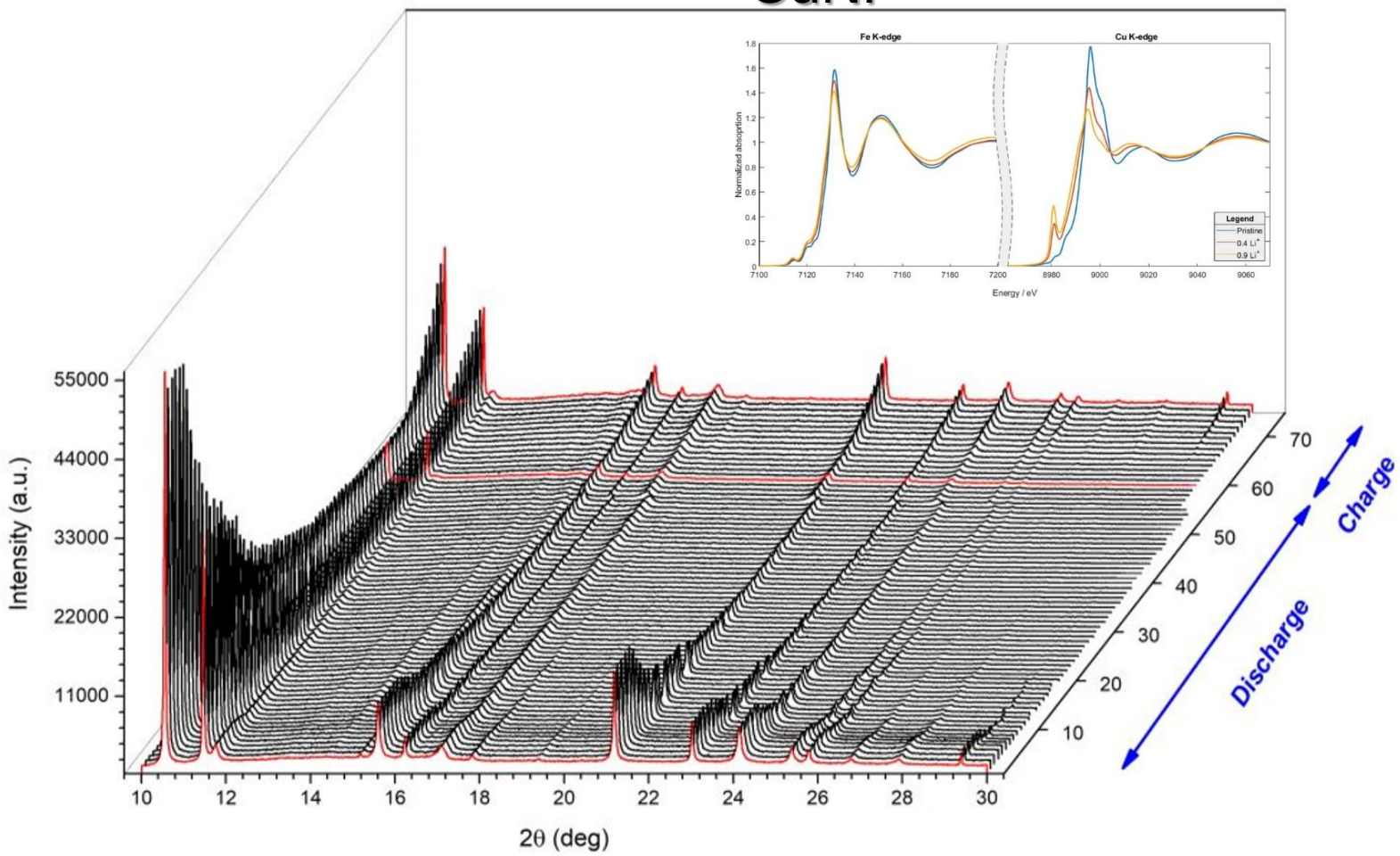

Elettra
Sincrotrone
Trieste

Operando battery studies: CuNP

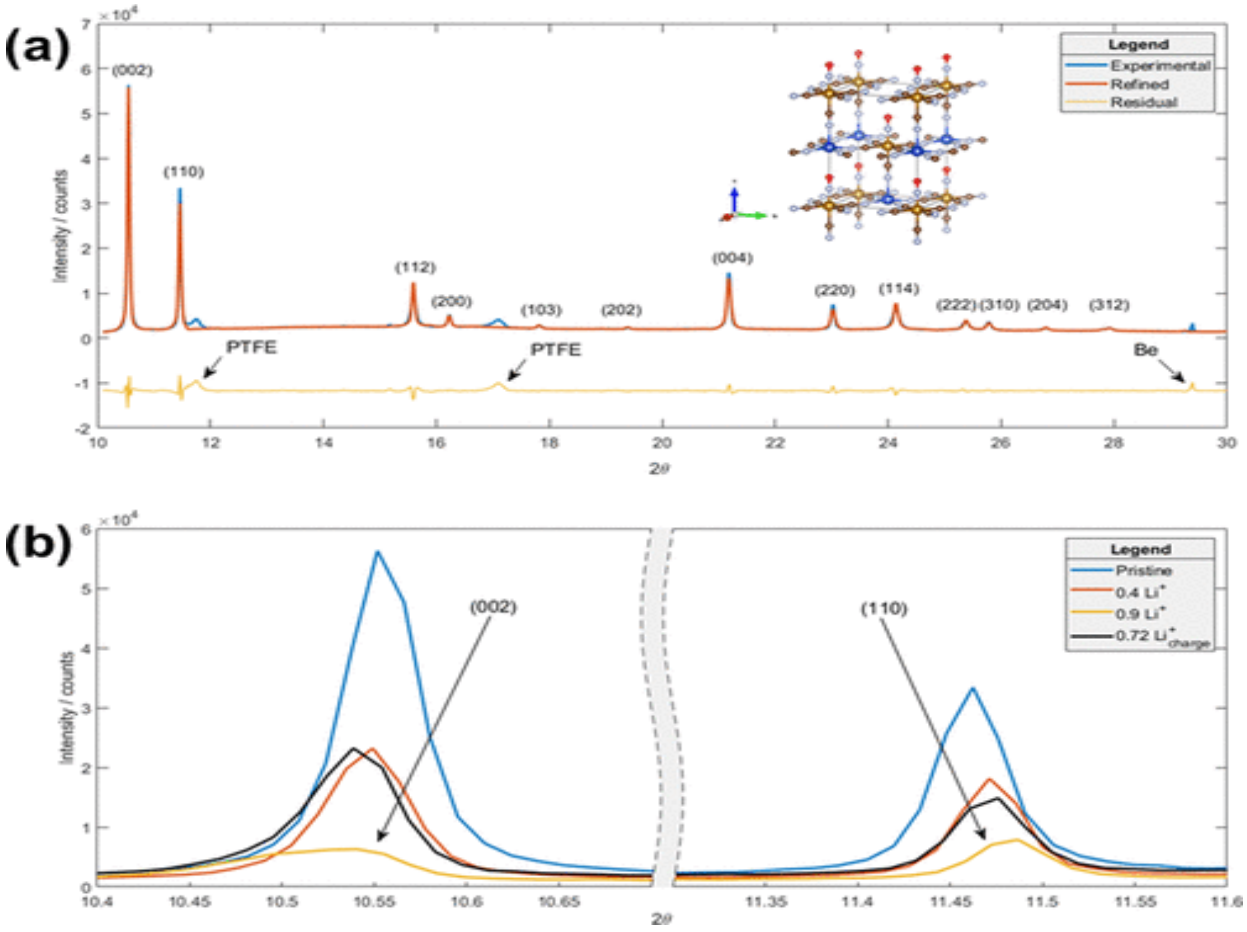

Elettra
Sincrotrone
Trieste

Operando battery studies: CuNP

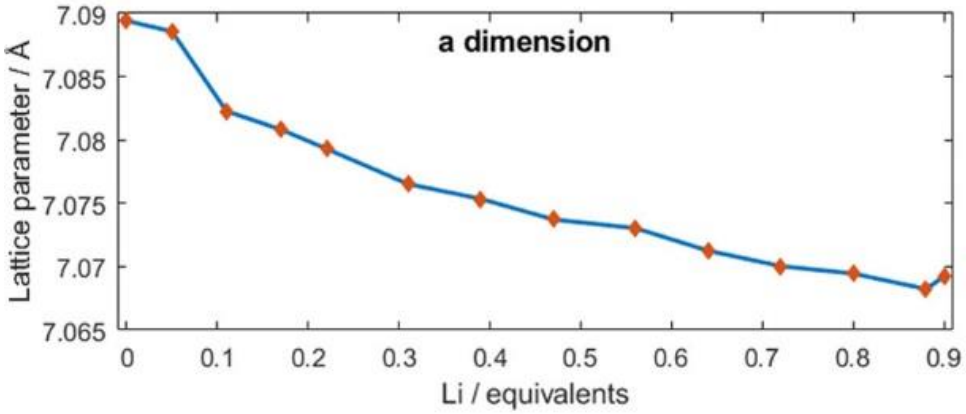

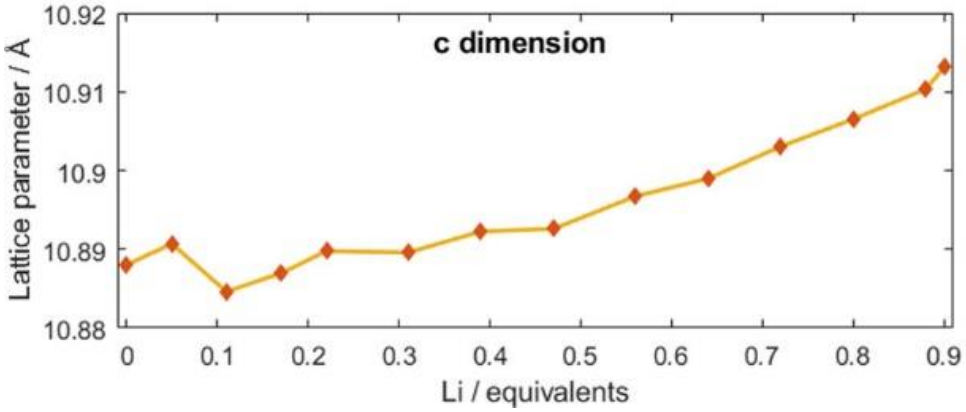

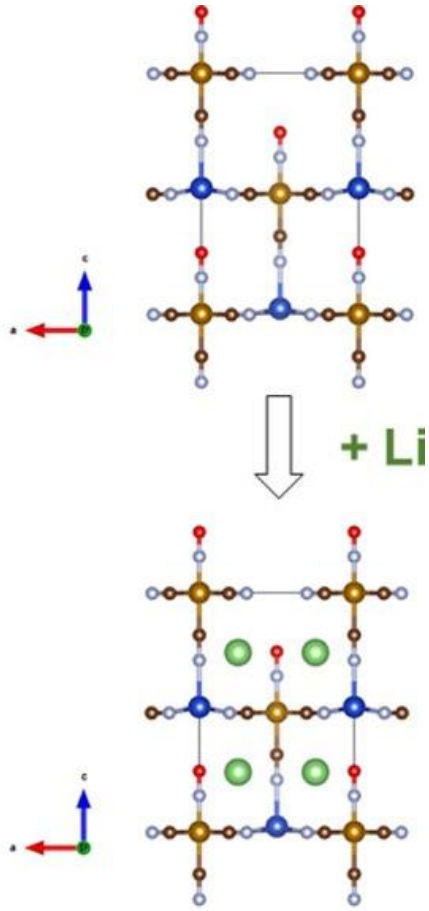

Line profile analsis - example

- Correlation between microstructure and bioequivalence in Anti-HIV Drug Efavirenz, C. Fandaruff *et al.*, **European Journal of Pharmaceutics and Biopharmaceutics** 91, 52-58 (2015)

Elettra Sincrotrone Trieste

Line profile analsis - example

- Polymorphism and particle size distribution can impact the dissolution behaviour and, as a consequence, bioavailability and bioequivalence of poorly soluble drugs, such as Efavirenz (EFV).
- The aim of this work was to study microstructure, a solid-state property of current interest in the pharmaceutical area, in order to find an explanation for the dissolution and bioequivalence behaviour.
- The microstructure of EFV raw materials was studied by Whole Powder Pattern Modelling (WPPM) of X-ray powder diffraction data.

Line profile analysis - example

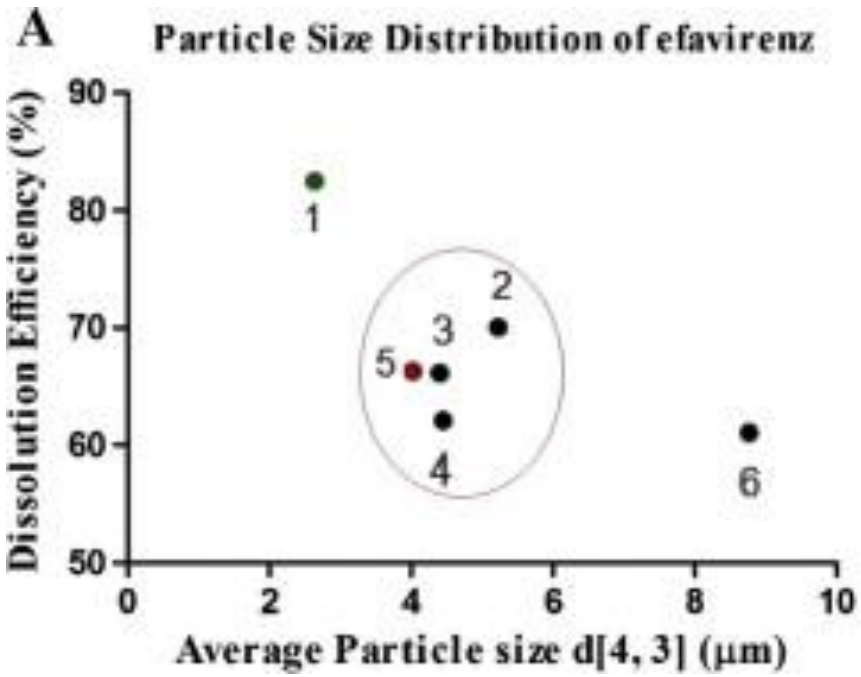

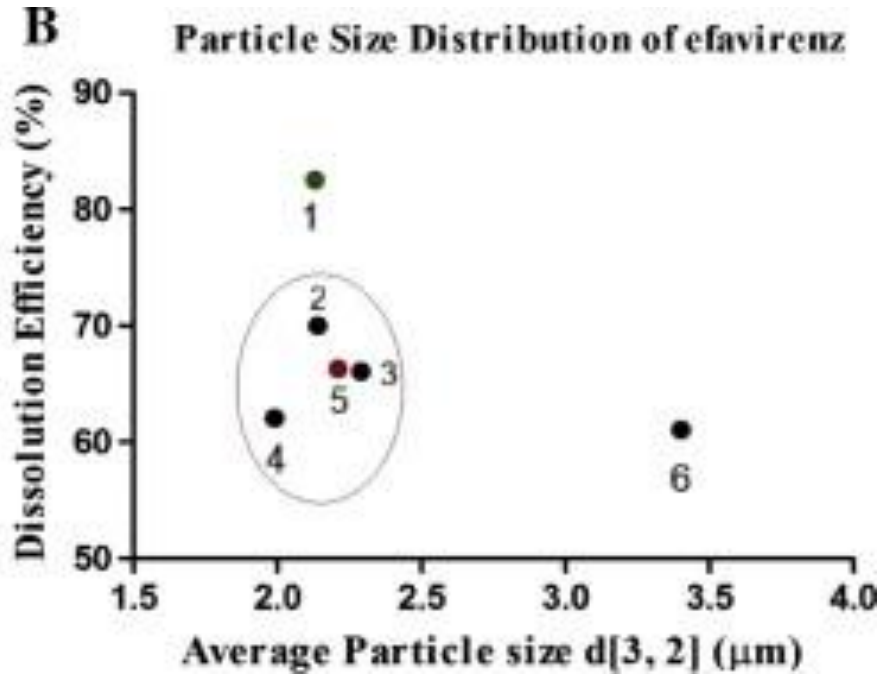

Line profile analysis - example

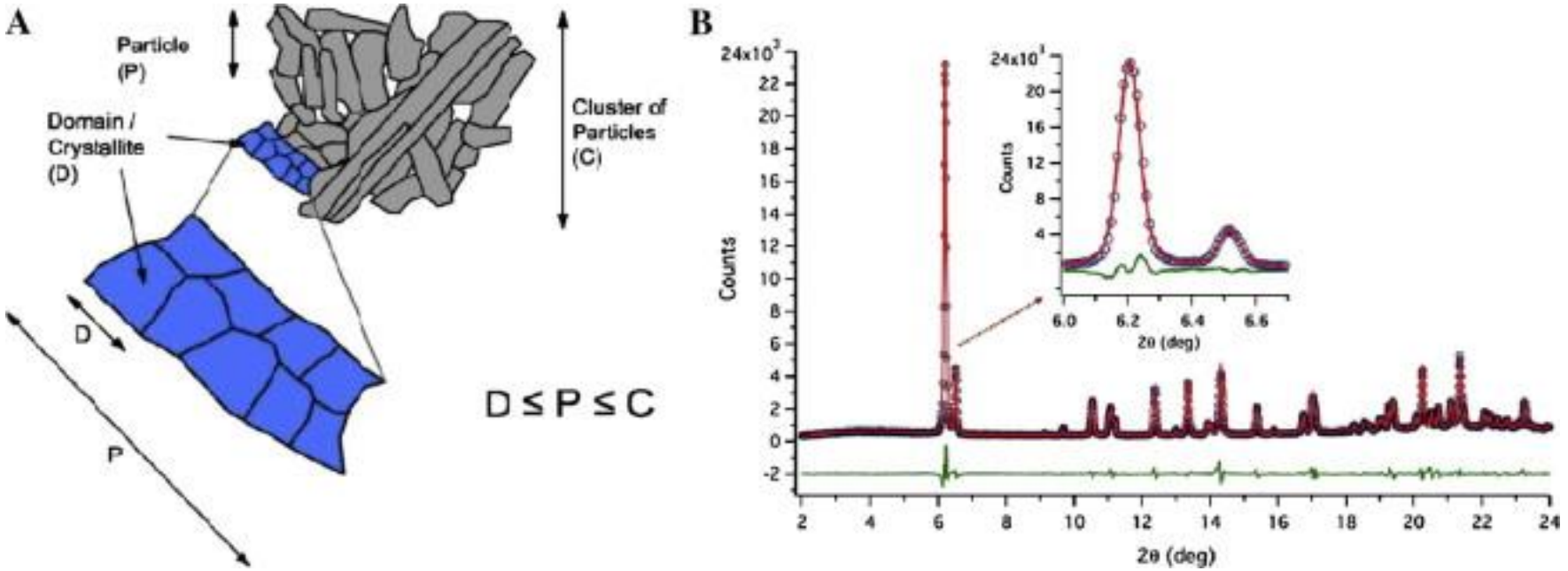

Elettra
Sincrotrone
Trieste

Line profile analysis - example

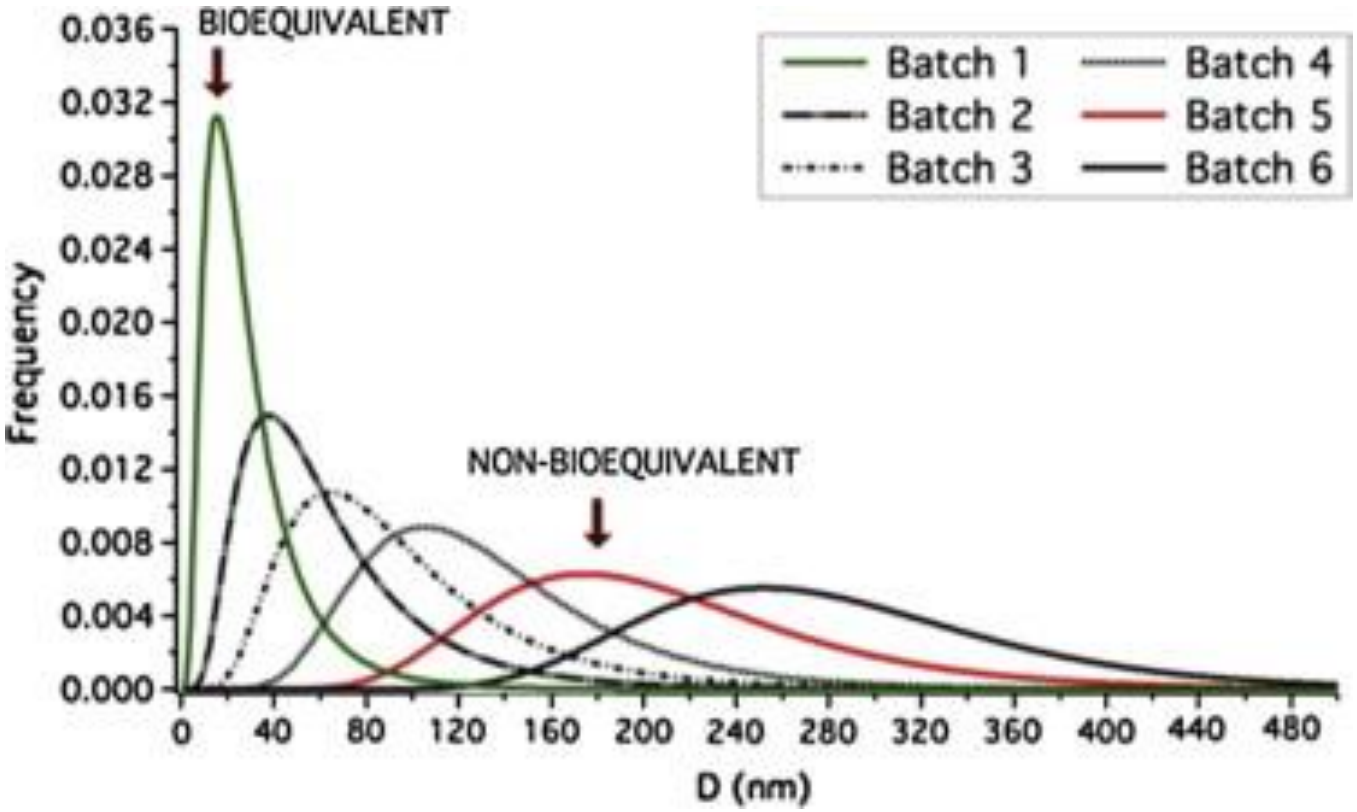

Elettra
Sincrotrone
Trieste

Line profile analysis - example

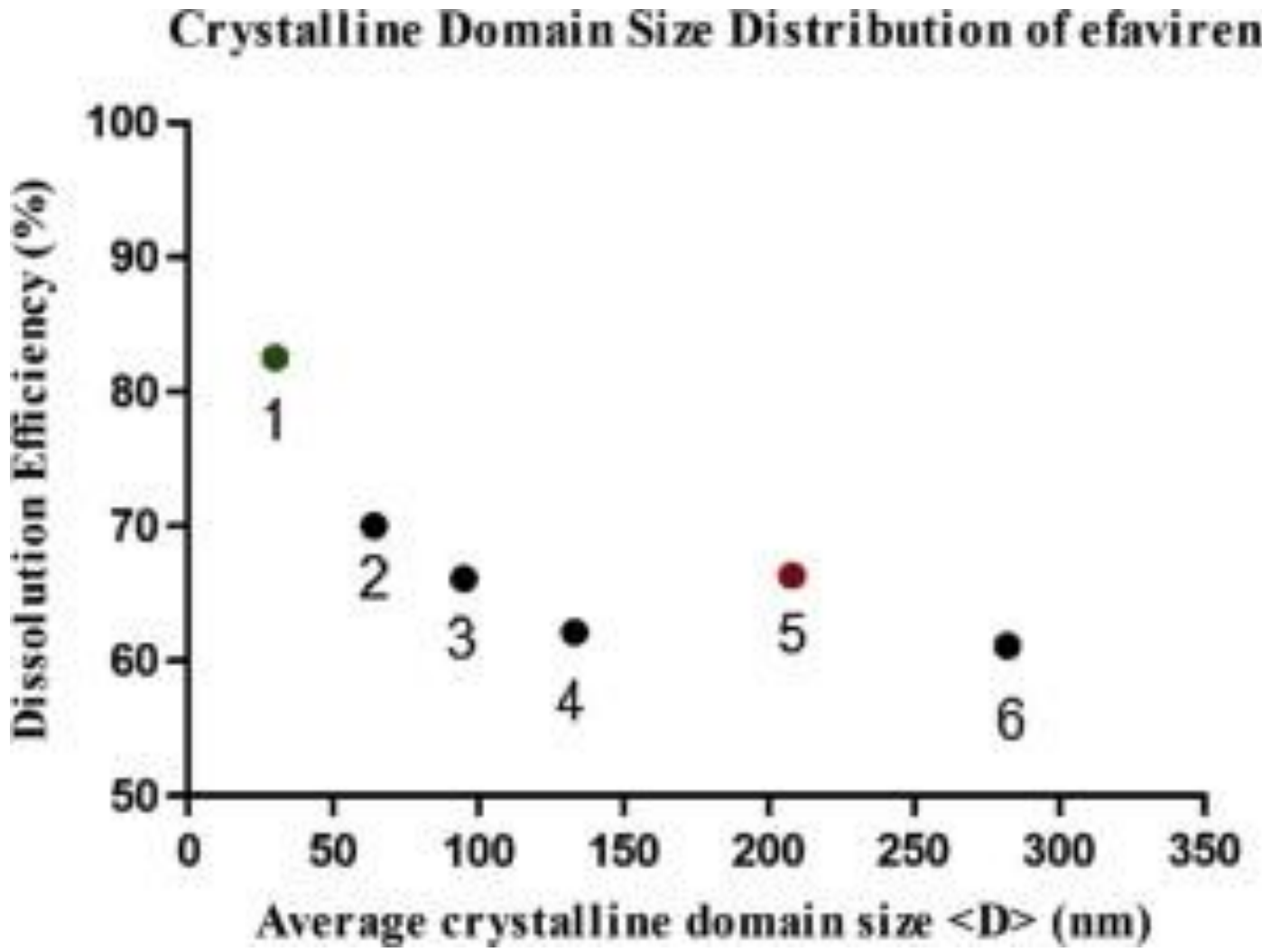

Elettra
Sincrotrone
Trieste

Structure determination

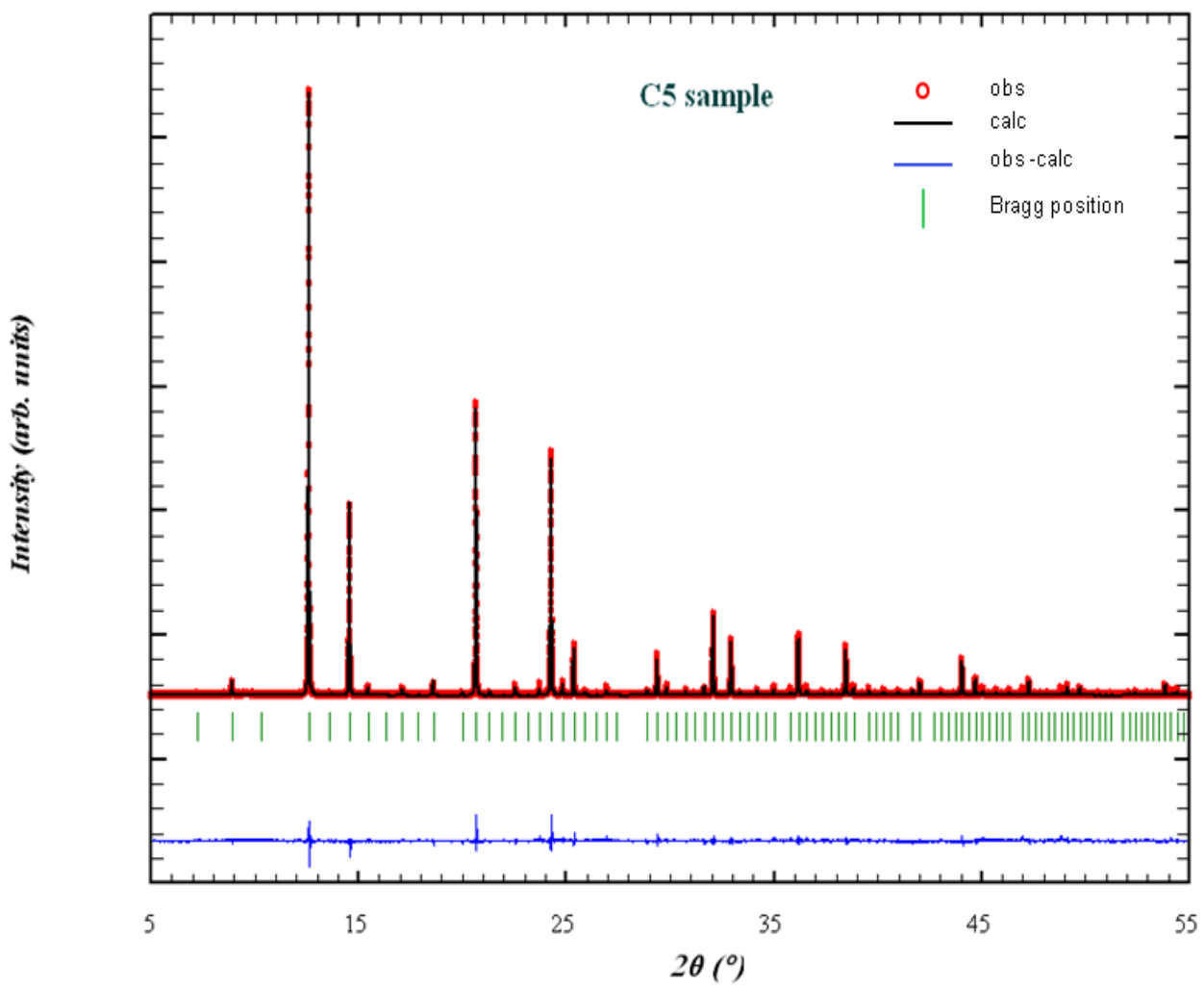

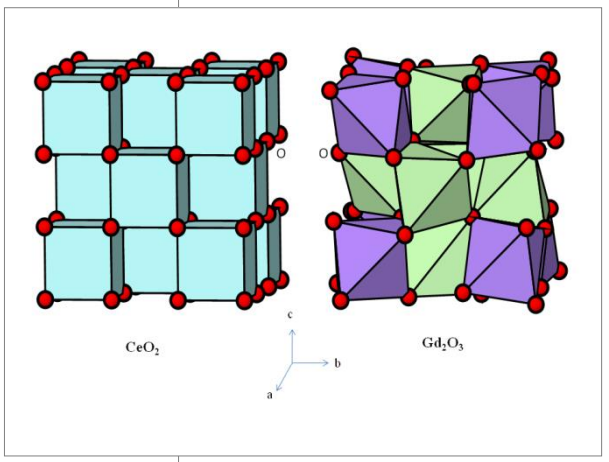

Structure determination - example

- Direct localzation of atoms in mixed-occupancy powders by resonant contrast diffraction, M.K. Panda *et al*., H. Palancher *et al.*, *Angew. Chem. Int. Ed*., **44**, 1725-1729 (2005)

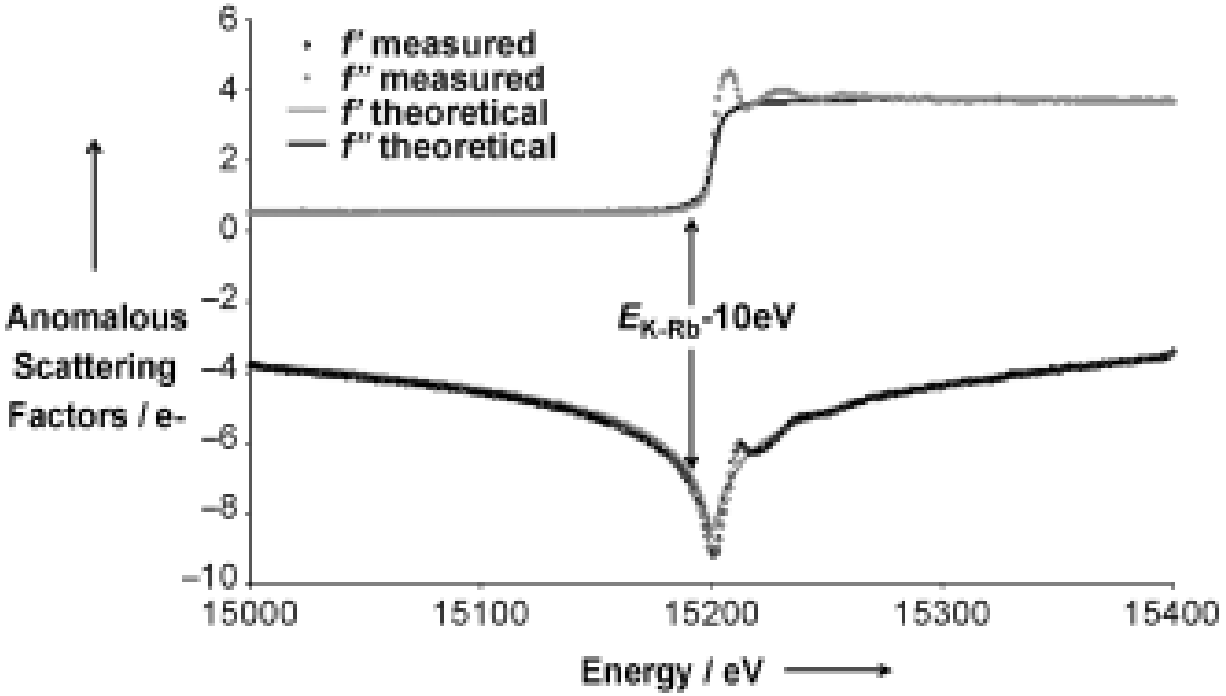

$f = f_o + \Delta f' + i.\Delta f''$

Elettra Sincrotrone Trieste

Structure determination - example

- Resonant scattering variations near an absorption edge provide chemical sensitivity and are used to extract the contribution of a single element to each crystallographic site.

- The method was demonstrated for highly-crystalline solids of industrial interest: bicationic X zeolites to determine Sr^{2+} and Rb^{+} cation distributions in SrRbX

- Since Sr^{2+} and Rb^{+} have the same number of electrons and similar neutron scattering lengths (b_{Sr} = 0.702 x 10^{-12} cm; b_{Rb} = 0.709 x 10^{-12} cm) this is a particularly difficult case for conventional X-ray or neutron diffraction

Elettra
Sincrotrone
Trieste

Structure determination - example

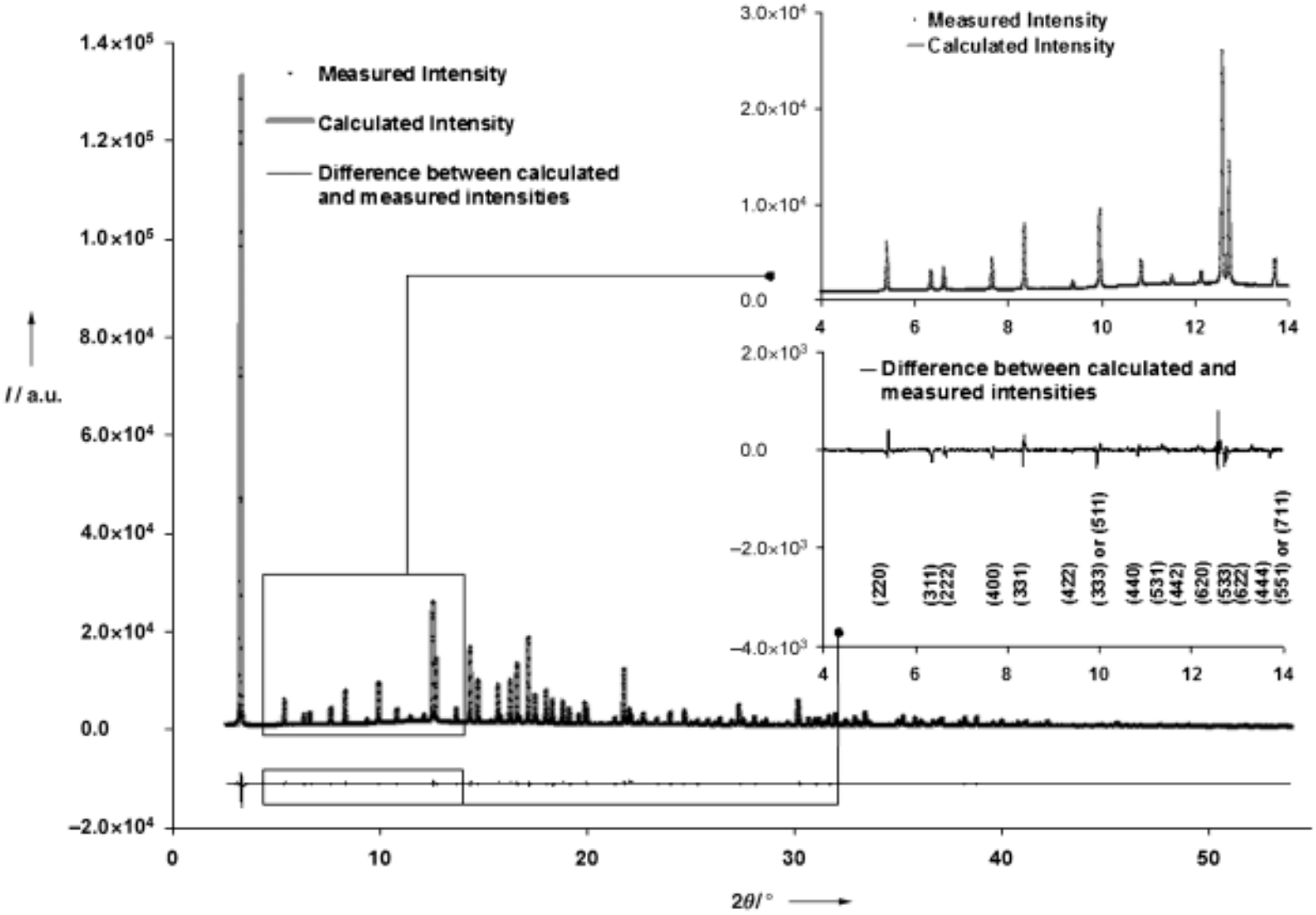

Structure determination - example

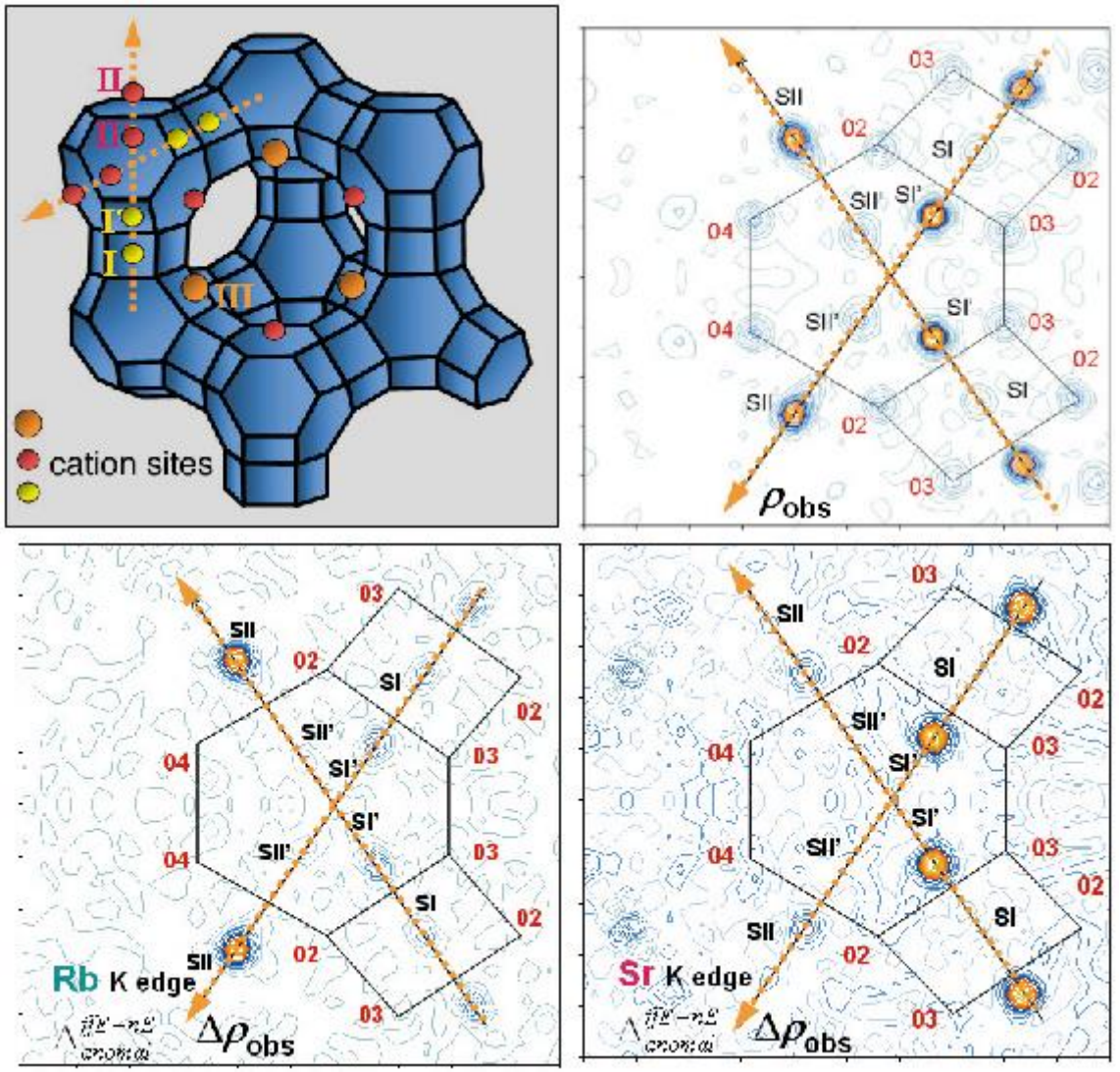

Structure determination - example

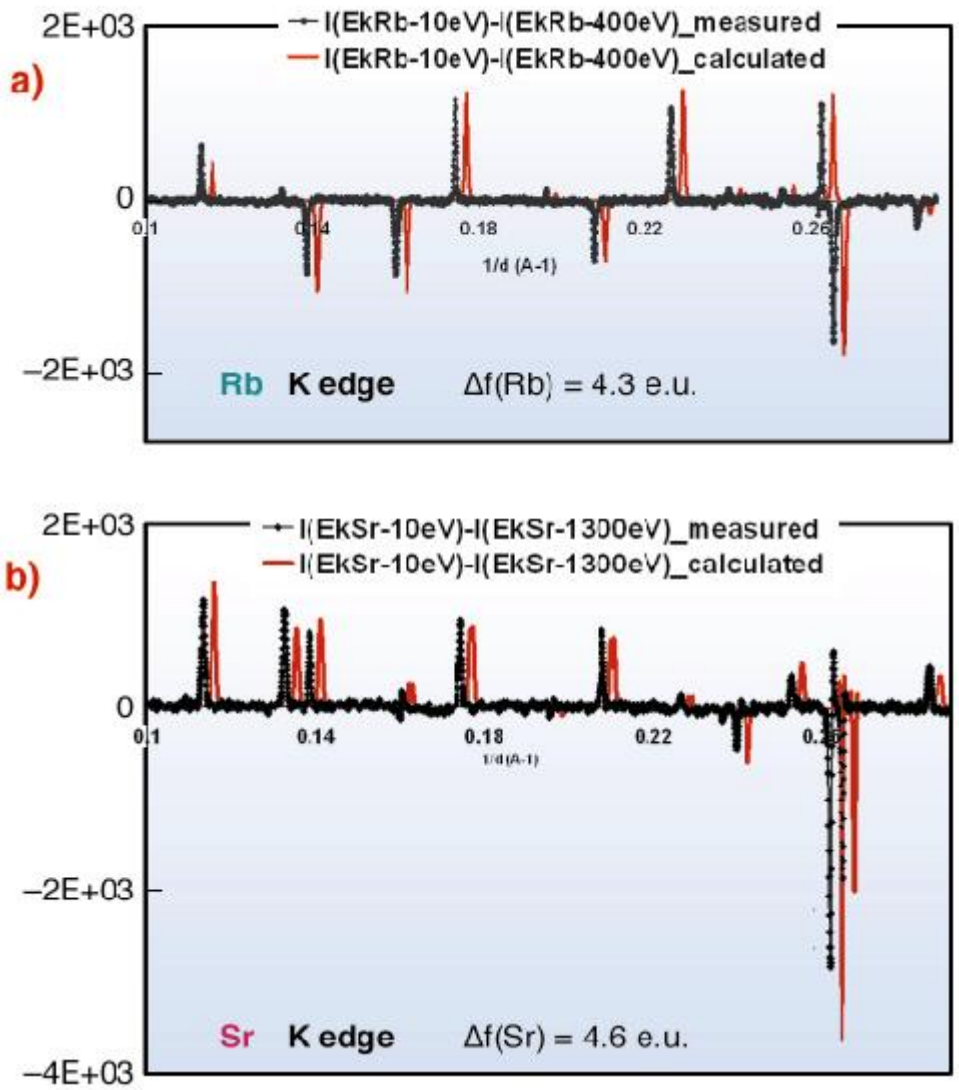

Elettra
Sincrotrone
Trieste

Thank you!

Elettra
Sincrotrone
Trieste

www.elettra.eu